

ALMA MATER STUDIORUM · UNIVERSITÀ DI
BOLOGNA

Scuola di Scienze
Corso di Laurea Magistrale in Fisica

**ONE DIMENSIONAL EXTENDED
HUBBARD MODEL:
TWO-PARTICLE BOUND STATES
AND RESONANCES**

Relatore:

Prof. Loris Ferrari

Presentata da:

Serena Fazzini

Correlatore:

Prof.ssa Elisa Ercolessi

**Sessione II
Anno Accademico 2013/2014**

Sommario

In questo lavoro di tesi è stato svolto uno studio analitico sul modello di Hubbard esteso unidimensionale al fine di osservare la presenza di eventuali risonanze che possano dare origine alla formazione di stati legati di due particelle. L'esistenza di uno stato legato stabile ha suscitato grande interesse negli ultimi anni, sia in ambito teorico che sperimentale, poichè è alla base di molti fenomeni che vengono osservati nei sistemi a molti corpi a basse temperature, come il BCS-BEC crossover. Pertanto si è ritenuto utile studiare il problema a due corpi nel modello di Hubbard esteso, che in generale non è integrabile. Il modello considerato contiene interazioni a primi e secondi vicini, in aggiunta all'interazione di contatto presente nel modello di Hubbard.

Il problema è stato indagato analiticamente attraverso il Bethe ansatz, che consente di trovare tutti gli autovalori e le autofunzioni dell'Hamiltoniana. L'ansatz di Bethe sulla funzione d'onda è stato generalizzato per poter tener conto dei termini di interazione a più lungo raggio rispetto all'interazione di contatto.

Si trova che, in questo modello, nel limite termodinamico, possono avvenire delle risonanze (o *quasi*-risonanze) in cui la lunghezza di scattering diverge, contrariamente a quanto avviene nel modello di Hubbard. Tale fenomeno si verifica quando il livello energetico discreto degli stati legati "tocca" la banda di scattering. Inoltre, con l'aggiunta di nuovi termini di interazione emergono nuovi stati legati. Nel caso in esame, si osservano due famiglie di stati legati, se lo spin totale delle due particelle è 1, e tre famiglie di stati legati, se lo spin totale è 0.

Contents

Introduction	V
1 The Hubbard Model	1
1.1 Introduction to the Hubbard model	1
1.1.1 Some particular cases	5
1.2 Symmetries of the Hubbard model	6
1.3 On the physics of the model	16
1.3.1 Some more recent results	20
2 Bethe Ansatz	23
2.1 The basic idea of the Bethe ansatz: the Heisenberg chain . . .	24
2.2 Bethe Ansatz solutions for the Hubbard model	26
2.2.1 The two-particle case	26
2.2.2 Bound states in the thermodynamic limit	33
2.2.3 The many-particle case	35
3 Two-body solutions for the extended Hubbard model	39
3.1 First-neighbor interaction	39
3.1.1 Periodic boundary conditions	45
3.2 Second-neighbor interaction	46
3.3 Bound states in the thermodynamic limit	49
4 Scattering resonances	51
4.1 Basic scattering theory	51
4.1.1 Identical particles	53
4.2 Scattering process on a lattice	54
5 Our results	57
5.1 Scattering states and bound states	57
5.2 Resonances	66

6	The role of resonances and future perspectives	71
6.1	3D Feshbach resonance and BCS-BEC crossover	72
6.2	Two-particle scattering and confinement-induced resonances in <i>quasi</i> -1D systems	74
6.3	One-channel and two-channel Feshbach physics on a 1D lattice	76
	Conclusions	81
	A Number of states	81
	Bibliography	82

Introduction

Both the development of techniques for cooling atoms to very low temperatures and the realization of optical lattices have opened a thriving field of research in condensed matter physics. The great impact of ultracold gases on current physics is linked to the extraordinary degree of control on physical parameters that is obtained in such systems. This has opened the way to the investigation of phases of matter previously inaccessible - such as the superfluid one - and related quantum phase transitions [1, 2, 3].

In recent times a crossover between a Bardeen-Cooper-Schrieffer (BCS) superfluid of Cooper pairs, with spatially overlapping wave functions, to a Bose-Einstein Condensate (BEC) of molecules of two tightly bound fermions has been realized [4].

Many interesting results have been obtained also in low dimensions. Indeed optical lattices not only allow to tune the interaction strength, but also provide a waveguide which makes possible to confine the system along one or two spatial directions.

Parallel to the experimental results, many works have been made in the theoretical field to search for models capable of predicting the behaviour of atomic and molecular systems in these new regimes.

Among them, the Hubbard model [5, 6] is one of the most studied. In fact, despite its simplicity, it has a very rich phenomenology. In particular, the one-dimensional Hubbard model is integrable [7], thus offering the possibility to get much information through exact analytical calculations. A powerful technique usually used to solve this model is the *Bethe ansatz* which allows to reduce the solution of the stationary Schrödinger equation to a set of algebraic equations.

The Hubbard Hamiltonian depicts the hopping of particles from one site to neighbouring one and takes into account for the two-body interactions through an effective contact potential.

In this work a more general model which retains also the first- and second-neighbour interactions has been considered. Extensions of the Hubbard model are in general not integrable and the many-body problem is difficult

to solve. Several approximate or numerical techniques (e.g. *density matrix renormalization group*) exist for one-dimensional systems. However, having an exact analytical solution in a simpler case - such as a few-body problem - is useful to get some hint about the N -particle case. Thus, here the focus is on underlying two-body physics.

In particular, the Bethe ansatz is generalized to solve the two-particle problem in the extended Hubbard model with interactions truncated at second neighbors. The method allows to obtain all eigenvalues and eigenfunctions of the Hamiltonian. Particular attention is devoted to the bound states and the resonances that produce them. Indeed the formation of a stable two-particle bound state is of great interest in both experimental and theoretical physics for two fundamental reasons. The first is the crucial role it plays in the many N -particle problems, such as the BCS-BEC crossover previously mentioned. The second is the possibility to study its expansion dynamics (see, for example, [8]).

The thesis is organized as follows.

Chapter 1 is devoted to the Hubbard model. Its main properties are described and some interesting results are briefly reported.

In Chapter 2 the Bethe ansatz method for the Hubbard model is introduced. The two-body problem is explicitly solved and an overview on the N -particle case is given.

In Chapter 3 the method is generalized to solve the extended Hubbard model and new results are shown. A fermionic model has been studied. Hence the spin degrees of freedom must have been taken into account. The whole study has been conducted separating the problem into one for the triplet state and one for the singlet state.

In Chapter 4 some basic concepts about scattering theory are recalled, such as the *scattering length* and the *scattering resonances*. Then the same parameters are defined for a one-dimensional scattering problem on a lattice.

An accurate analysis of our results is made in Chapter 5, in which the existence of resonances that give rise to the bound states is underlying. This is a fundamental question that emerges when a non-zero range interaction is introduced.

Finally, Chapter 6 is a description of the role of resonances in current experimental physics and an interpretation of our results in the context of cold atomic gases.

Chapter 1

The Hubbard Model

1.1 Introduction to the Hubbard model

The Hubbard model [5, 9] is one of the most successful models in describing the physics of the microscopic world. It is of great use in theoretical condensed matter physics thanks to its capability of accounting for many phenomena, despite its simplicity. It was introduced in 1963 by John Hubbard [10, 11, 12, 13, 14, 15] to model electronic correlations in narrow energy bands. It provides an approximate description of the electrons in a solid: the model depicts the hopping of the electrons in a lattice from one site to neighboring one and takes into account for the Coulomb interaction through an effective short range potential that acts only if two electrons are on the same site. Nowadays it is applied to many cases, in particular it is used to model fermionic and also bosonic particles in optical lattices where the interaction can be both repulsive or attractive. It is very useful since, in its standard form or in some derived forms, allows to account for many experimental results.

Here we derive the Hubbard Hamiltonian from an approximate description of interacting electrons in a solid following Hubbard's original work.

A solid consists of ions and electrons in a three-dimensional crystalline structure. Since our aim is to study the dynamics of the electrons in the solid, we can regard the ions as forming a static lattice. Thus they have the only effect of producing a periodic potential. This assumption is justified because the ions are much heavier than the electrons. In this approximation, the electron gas can be described by the following Hamiltonian

$$H = \underbrace{\sum_{i=1}^N h(\mathbf{x}_i, \mathbf{p}_i)}_{H_0} + \underbrace{\sum_{1 \leq i < j \leq N} V_C(\mathbf{x}_i - \mathbf{x}_j)}_V \quad (1.1)$$

where

$$h(\mathbf{x}_i, \mathbf{p}_i) = \frac{\mathbf{p}_i^2}{2m} + V_I(\mathbf{x}_i) \quad (1.2)$$

is the one-particle Hamiltonian, N is the number of electrons, V_I is the periodic potential of the ions and

$$V_C(\mathbf{x}) = \frac{e^2}{\|\mathbf{x}\|} \quad (1.3)$$

is the Coulomb repulsion among the electrons. In spite of the approximation we made neglecting the motion of positive ions, Hamiltonian (1.1) is still too complicated to be solved exactly. A possible simplification may be the mean-field approximation. The first step in doing it is to add an auxiliary potential $V_a(\mathbf{x})$ to one-particle piece H_0 of the Hamiltonian and subtracting it in the two-body part V . We define the new one-body and two-body potentials

$$V(\mathbf{x}) = V_I(\mathbf{x}) + V_a(\mathbf{x}) \quad (1.4)$$

$$U(\mathbf{x}, \mathbf{y}) = V_C(\mathbf{x} - \mathbf{y}) - \frac{1}{N-1} (V_a(\mathbf{x}) - V_a(\mathbf{y})) \quad (1.5)$$

and the new one-particle Hamiltonian

$$\tilde{h}(\mathbf{x}, \mathbf{p}) = \frac{\mathbf{p}^2}{2m} + V(\mathbf{x}) \quad (1.6)$$

so that Hamiltonian (1.1) becomes

$$H = \sum_{i=1}^N \tilde{h}(\mathbf{x}_i, \mathbf{p}_i) + \sum_{1 \leq i < j \leq N} U(\mathbf{x}_i, \mathbf{x}_j). \quad (1.7)$$

The mean-field approximation is just setting $U(\mathbf{x}_i, \mathbf{x}_j) = 0$ for each pair of electrons i and j . This means a single electron does not interact with each of the others by a two-body repulsion but feels only an average interaction

strength $V_a(\mathbf{x})$, generated by them, that screens the attractive interaction of the ions. Thus the auxiliary potential $V_a(\mathbf{x})$ must be chosen in such a way that the matrix elements of the effective two-body potential $U(\mathbf{x}, \mathbf{y})$ between the eigenstates of the one-particle Hamiltonian \tilde{h} are negligibly small. In some cases (e.g. systems that exhibit magnetism or superconductivity) this cannot be achieved since the residual two-body interactions $U(\mathbf{x}, \mathbf{y})$ are crucial. However we can obtain a two-body potential $U(\mathbf{x}, \mathbf{y})$ reduced in range and magnitude compared to the full Coulomb interaction $V_C(\mathbf{x} - \mathbf{y})$ because much of the Coulomb interaction effects are incorporated into the single particle part of H .

In the many-body Hilbert space it is convenient to use second quantized operators. Thus we write Hamiltonian (1.7) in second quantization. To do this we need a suitable basis of states. We may construct it starting from the eigenstates of the one-particle Hamiltonian \tilde{h} ; these are the wave functions $\psi_{\alpha\mathbf{k}}$ that obey eigenvalue equation

$$\tilde{h}(\mathbf{x}, \mathbf{p})\psi_{\alpha\mathbf{k}}(\mathbf{x}) = \epsilon_{\alpha\mathbf{k}}\psi_{\alpha\mathbf{k}}(\mathbf{x}) \quad (1.8)$$

where α is the band index and \mathbf{k} the quasi-momentum, which runs over the first Brillouin zone. Since \tilde{h} contains only a kinetic term and a periodic potential, its eigenfunctions are Bloch states [16]; so they have the following form

$$\psi_{\alpha\mathbf{k}}(\mathbf{x}) = e^{i\mathbf{k}\cdot\mathbf{x}}u_{\alpha\mathbf{k}}(\mathbf{x}) \quad (1.9)$$

with $u_{\alpha\mathbf{k}}(\mathbf{x} + \mathbf{R}) = u_{\alpha\mathbf{k}}(\mathbf{x})$ if \mathbf{R} is a lattice vector; hence u is a periodic function with the same periodicity of the lattice. Bloch functions are localized in \mathbf{k} -space. A complementary one-particle basis is formed by the Wannier states $\phi_{\alpha i}$ which are localized in real space. This two bases relate to each other through the following transformations

$$\begin{aligned} \phi_{\alpha i}(\mathbf{x}) &= \frac{1}{\sqrt{L}} \sum_{\mathbf{k}} \psi_{\alpha\mathbf{k}}(\mathbf{x} - \mathbf{R}_i) = \frac{1}{\sqrt{L}} \sum_{\mathbf{k}} e^{-i\mathbf{k}\cdot\mathbf{R}_i} \psi_{\alpha\mathbf{k}}(\mathbf{x}) \\ \psi_{\alpha\mathbf{k}} &= \frac{1}{\sqrt{L}} \sum_i e^{i\mathbf{k}\cdot\mathbf{R}_i} \phi_{\alpha i}(\mathbf{x}) \end{aligned} \quad (1.10)$$

where L design the number of lattice sites.

Let us introduce creation operators $c_{\alpha\mathbf{k}\sigma}^\dagger$ of electrons of spin σ in Bloch states

$\psi_{\alpha\mathbf{k}}$ and their Fourier transforms

$$c_{\alpha i \sigma}^\dagger = \frac{1}{\sqrt{L}} \sum_{\mathbf{k}} e^{-i\mathbf{k}\cdot\mathbf{R}_i} \tilde{c}_{\alpha\mathbf{k}\sigma}^\dagger \quad (1.11)$$

which create electrons of spin σ in Wannier states. Finally we define the field operator

$$\Psi_\sigma^\dagger(\mathbf{x}) = \sum_{\alpha\mathbf{k}} \psi_{\alpha\mathbf{k}}^*(\mathbf{x}) \tilde{c}_{\alpha\mathbf{k}\sigma}^\dagger = \sum_{\alpha i} \phi_{\alpha i}^*(\mathbf{x}) c_{\alpha i \sigma}^\dagger \quad (1.12)$$

which creates an electron of spin σ at position \mathbf{x} . Hence Hamiltonian (1.7) can be written as

$$\begin{aligned} H = & \sum_{\sigma=\uparrow\downarrow} \int dx^3 \Psi_\sigma^\dagger(\mathbf{x}) \tilde{h}(\mathbf{x}, \mathbf{p}) \Psi_\sigma(\mathbf{x}) \\ & + \frac{1}{2} \sum_{\sigma, \sigma'=\uparrow\downarrow} \int dx^3 \Psi_\sigma^\dagger(\mathbf{x}) \Psi_{\sigma'}^\dagger(\mathbf{y}) U(\mathbf{x}, \mathbf{y}) \Psi_{\sigma'}(\mathbf{y}) \Psi_\sigma(\mathbf{x}) \end{aligned} \quad (1.13)$$

and, substituting the expressions for the field operators, this is equivalent to the following second-quantized form in the Wannier basis

$$H = - \sum_{\alpha} \sum_{i,j} \sum_{\sigma} t_{ij}^{\alpha} c_{\alpha i \sigma}^\dagger c_{\alpha j \sigma} + \frac{1}{2} \sum_{\alpha, \beta, \gamma, \delta} \sum_{i, j, k, l} \sum_{\sigma, \sigma'} U_{ijkl}^{\alpha\beta\gamma\delta} c_{\alpha i \sigma}^\dagger c_{\beta j \sigma'}^\dagger c_{\gamma k \sigma'} c_{\delta l \sigma} \quad (1.14)$$

with the hopping matrix elements given by

$$t_{ij}^{\alpha} = -\langle i | \tilde{h} | j \rangle = - \int dx^3 \phi_{\alpha}^*(\mathbf{x} - \mathbf{R}_i) \tilde{h}(\mathbf{x}, \mathbf{p}) \phi_{\alpha}(\mathbf{x} - \mathbf{R}_j) = \frac{1}{L} \sum_{\mathbf{k}} e^{i\mathbf{k}\cdot(\mathbf{R}_i - \mathbf{R}_j)} \epsilon_{\alpha\mathbf{k}} \quad (1.15)$$

and the interaction parameters given by

$$U_{ijkl}^{\alpha\beta\gamma\delta} = \langle ij | U | kl \rangle = \int dx^3 dy^3 \phi_{\alpha}^*(\mathbf{x} - \mathbf{R}_i) \phi_{\beta}^*(\mathbf{y} - \mathbf{R}_j) U(\mathbf{x}, \mathbf{y}) \phi_{\gamma}(\mathbf{y} - \mathbf{R}_k) \phi_{\delta}(\mathbf{x} - \mathbf{R}_l). \quad (1.16)$$

An optimal choice of Wannier states (through an optimal choice of the auxiliary potential V_a) minimizes the influence of the mutual Coulomb interaction that means the range and magnitude of $U_{ijkl}^{\alpha\beta\gamma\delta}$. When these terms are small compared to the hopping matrix elements, they can be set equal to zero in a first approximation, and can later be taken into account by perturbation

theory (band theory). The Hubbard model takes the interaction parameters no longer negligible but their range is still very small: in the sum only the largest terms are retained and the others are omitted. In particular, it takes the intra-atomic Coulomb interaction $U_{iii}^{\alpha\beta\gamma\delta}$ large compared to the inter-atomic interaction terms and this is the only term that cannot be neglected compared to the hopping matrix elements.

A further simplification occurs when the Fermi surface lies within a single conduction band, say $\alpha = 1$, so that we can ignore matrix elements that couple to other bands, if they are away from the Fermi level. We set $t_{ij}^\alpha = t_{ij}$ and $U_{iii}^{\alpha\beta\gamma\delta} = U$. This is the so-called *one-band Hubbard model* and the corresponding Hamiltonian is

$$H = \sum_{ij} \sum_{\sigma} t_{ij} c_{i\sigma}^\dagger c_{j\sigma} + \frac{U}{2} \sum_i c_{i\sigma}^\dagger c_{i\sigma'}^\dagger c_{i\sigma'} c_{i\sigma}. \quad (1.17)$$

Finally we assume the tight-binding approximation, which consist in retaining only hopping matrix elements between nearest neighbours. Thus, introducing the particle number operator $n_{i\sigma} = c_{i\sigma}^\dagger c_{i\sigma}$, Hamiltonian (1.17) reduces to

$$H = -t \sum_{\langle ij \rangle} \sum_{\sigma} c_{i\sigma}^\dagger c_{j\sigma} + U \sum_i n_{i\uparrow} n_{i\downarrow} \quad (1.18)$$

where the symbol $\langle ij \rangle$ denotes summation over ordered pairs of nearest neighbours. We have assumed isotropic hopping of strength t between nearest neighbours and have suppressed the terms t_{ii} , since they may be absorbed into chemical potential in a grand canonical description of the model.

1.1.1 Some particular cases

Despite its apparent simplicity, the Hubbard model is not exactly soluble in general. Two particular and useful cases are the limits $U/t = 0$ and $U/t \gg 1$, respectively.

In the first case, the Hamiltonian is that of a non-interacting system, so it can be diagonalized choosing a suitable basis. This basis is the Bloch basis. Using transformation (1.11), we get

$$H_{U=0} = \sum_{\mathbf{k}\sigma} \epsilon(\mathbf{k}) \tilde{c}_{\mathbf{k}\sigma}^\dagger \tilde{c}_{\mathbf{k}\sigma} \quad (1.19)$$

with

$$\epsilon(\mathbf{k}) = -t \sum_j e^{-i\mathbf{k}\cdot\mathbf{a}_j}. \quad (1.20)$$

Here index j denotes the first neighbours of a given site and \mathbf{a}_j is the distance vector. So, for example, in three dimension the coordination number of a simple cubic cell is 6 and the sum in equation (1.20) consists of six exponentials: $\epsilon(\mathbf{k}) = -2t(\cos(k_x a) + \cos(k_y a) + \cos(k_z a))$; whereas in one dimension the lattice is a chain of length L and $\epsilon(k) = -2t \cos ka = -2t \cos k$ if we set $a = 1$.

In the large- U limit, the hopping term can be neglected in a zeroth-order approximation, that means we may set $t = 0$. This is called the atomic limit because the Hamiltonian is diagonal in the so-called Wannier basis which describes electrons localized at the lattice sites, identified with the atomic orbitals. We will see the specific case of one dimensional Hamiltonian in the following section. In a higher order approximation the hopping term is considered as a perturbation. In this way we get an effective Hamiltonian that can be mapped in an antiferromagnetic Heisenberg Hamiltonian if the system is near half-filling ($N \simeq L$). [9]

These special cases may be useful to study some particular features of electron systems, like magnetic behaviour. Going back to the full Hamiltonian (1.18), this can be exactly solved in two particular cases, namely the extremes of lattice coordination numbers two and infinity. In the following we will concentrate on the first case, which corresponds to a one dimensional lattice. In fact the 1D Hubbard model has the particular feature of being integrable.

1.2 Symmetries of the Hubbard model

The Hubbard model has many symmetries. Here we show them explicitly in the one dimensional case; however the results generalize to bipartite lattices of arbitrary dimension. The Hamiltonian we consider is (1.18) that in 1D can be written as

$$H = -t \sum_{j=1}^L \sum_{\sigma=\uparrow\downarrow} \left(c_{j\sigma}^\dagger c_{j+1\sigma} + c_{j+1\sigma}^\dagger c_{j\sigma} \right) + U \sum_{j=1}^L n_{j\uparrow} n_{j\downarrow}. \quad (1.21)$$

We are dealing with a chain of finite size, so we have to consider the problem of the boundary conditions. We choose to impose periodic boundary conditions on the operators, $c_{L+1\sigma} = c_{1\sigma}$. In this way the Hamiltonian is invariant under cyclic permutations of the lattice sites, or, equivalently, under lattice translations of a ring of L sites.

Creation and annihilation operators $c_{j\sigma}^\dagger$ and $c_{j\sigma}$ are canonical Fermi operators. They satisfy the following anticommutation rules

$$\{c_{j\sigma}, c_{i\sigma'}\} = \{c_{j\sigma}^\dagger, c_{i\sigma'}^\dagger\} = 0$$

$$\{c_{j\sigma}, c_{i\sigma'}^\dagger\} = \delta_{ji}\delta_{\sigma\sigma'}$$
(1.22)

for $i, j = 1, \dots, L$ and $\sigma, \sigma' = \uparrow, \downarrow$.

We have to define the Hilbert space $\mathcal{H}^{(L)}$ of the Hubbard model through a suitable basis of states. We begin by defining the vacuum state $|0\rangle$, which corresponds to the empty lattice, as that annihilated by operators $c_{j\sigma}$:

$$c_{j\sigma}|0\rangle = 0, \quad j = 1, \dots, L, \quad \sigma = \uparrow, \downarrow.$$
(1.23)

The space of states $\mathcal{H}^{(L)}$ of the Hubbard model is spanned by all linear combinations of the so-called Wannier states

$$|\mathbf{x}, \sigma\rangle = c_{x_N\sigma_N}^\dagger \dots c_{x_1\sigma_1}^\dagger |0\rangle$$
(1.24)

where we have introduced row vectors of electron and spin coordinates, $\mathbf{x} = (x_1, \dots, x_N)$ and $\sigma = (\sigma_1, \dots, \sigma_N)$, with $x_j \in \{1, \dots, L\}$ and $\sigma_j = \uparrow, \downarrow$. Hence we regard the state (1.24) as a state of N electrons where electron j -th has spin σ_j and is located at lattice site x_j . In the Hubbard model the electrons can hop from one site to another, that is to say, each variable x_j can change its value in the range $1, \dots, L$ under the action of Hamiltonian (1.21) due to the kinetic term; whereas the spin coordinate vector σ doesn't change since the Hamiltonian doesn't incorporate spin flip operators.

According to (1.22), creation operators at different sites or with different spin indices anticommute, hence $(c_{j\sigma}^\dagger)^2 = 0$. This makes the number of linearly independent Wannier states necessarily finite. A basis of the Hilbert space $\mathcal{H}^{(L)}$ is obtained by ordering the Fermi operators in (1.24). We may choose for instance

$$\mathcal{B} = \{|\mathbf{x}, \sigma\rangle \in \mathcal{H}^{(L)} | N = 0, \dots, 2L \quad \& \quad x_{j+1} \geq x_j, \quad \sigma_{j+1} > \sigma_j \quad \text{if} \quad x_{j+1} = x_j\} \quad (1.25)$$

where by convention $\uparrow > \downarrow$. The number of all linearly independent vectors of the form (1.24) for a fixed number of particle N is equal to $\binom{2L}{N}$. Thus the dimension of the Hilbert space is

$$\dim \mathcal{H}^{(L)} = \sum_{N=0}^{2L} \binom{2L}{N} = 4^L. \quad (1.26)$$

The same result can be obtained from the following considerations. A site can be empty, singly occupied by one electron with up or down spin, doubly occupied by two electrons of opposite spins. Thus there are four possible states associated with every lattice site

$$|0\rangle, \quad c_{j\uparrow}^\dagger |0\rangle, \quad c_{j\downarrow}^\dagger |0\rangle, \quad c_{j\uparrow}^\dagger c_{j\downarrow}^\dagger |0\rangle \quad (1.27)$$

and, since the chain has L sites, the dimension of the space of states is 4^L . We have shown the properties of operators $c_{j\sigma}^\dagger$ and their Hermitian conjugate $c_{j\sigma}$ which are included in the hopping term of the Hamiltonian. Now we focus our attention on the local particle number operators $n_{j\sigma} = c_{j\sigma}^\dagger c_{j\sigma}$ that appear in the interaction term. From relations (1.22) we get the following commutation rule

$$[n_{j\sigma}, c_{i\sigma'}^\dagger] = \delta_{ji} \delta_{\sigma\sigma'} c_{i\sigma'}^\dagger \quad \text{with} \quad n_{j\sigma} |0\rangle = 0 \quad (1.28)$$

and therefore

$$n_{j\sigma} |\mathbf{x}, \sigma\rangle = \sum_{i=1}^N \delta_{jx_i} \delta_{\sigma\sigma_i} |\mathbf{x}, \sigma\rangle. \quad (1.29)$$

Thus, $n_{j\sigma} |\mathbf{x}, \sigma\rangle = |\mathbf{x}, \sigma\rangle$ if site j is occupied by an electron of spin σ , and zero otherwise. So it counts the number of electron of spin σ on site j . Another important operator is the total number particle operator

$$\hat{N} = \sum_{j=1}^L (n_{j\uparrow} + n_{j\downarrow}) = \hat{N}_\uparrow + \hat{N}_\downarrow \quad (1.30)$$

where \hat{N}_\uparrow and \hat{N}_\downarrow are the particle number operators for up- and down-spin electrons, respectively. Each of them commutes with the Hubbard Hamiltonian:

$$[H, \hat{N}_\uparrow] = [H, \hat{N}_\downarrow] = [H, \hat{N}] = 0. \quad (1.31)$$

Thus this Hamiltonian preserves the total number of particles and the number of up and down spins.

As mentioned in the preceding section, some information about the Hubbard model can be obtained by considering separately the two contributions that make up the Hamiltonian (1.21), that are obtained for $U/t = 0$ and $U/t \rightarrow \infty$, respectively. In fact, in these simple cases the Hamiltonian can be diagonalized and understood by elementary means.

We have already seen that for $U/t = 0$ the Hamiltonian is diagonal in the Bloch states, defined by transformation (1.11) with $\alpha = 1$. In the one dimensional case, imposing periodic boundary conditions, the possible values of the momentum k are a set of discrete values parameterized by the integer n :

$$k = \frac{2\pi n}{L}, \quad n = 1, 2, \dots, L \quad \text{or, equivalently} \quad n = 0, 1, \dots, L - 1. \quad (1.32)$$

The Fourier transformation (1.11) is a canonical transformation, since operators $\tilde{c}_{k\sigma}^\dagger$ and $\tilde{c}_{k\sigma}$ also satisfy the canonical anticommutation relations (1.22). For $t = 0$ the Hamiltonian reduces to

$$H_{t=0} \equiv H_{U=\infty} = U\hat{D} = U \sum_{j=1}^L n_{j\uparrow} n_{j\downarrow} \quad (1.33)$$

where \hat{D} counts the number of doubly occupied sites. As mentioned before, this Hamiltonian is diagonal in the Wannier basis:

$$\begin{aligned} \hat{D}|\mathbf{x}, \sigma\rangle &= \sum_{k,l}^N \delta_{x_k, x_l} \delta_{\sigma_k, \uparrow} \delta_{\sigma_l, \downarrow} |\mathbf{x}, \sigma\rangle \\ &\quad \sum_{1 \leq k < l \leq N} \delta_{x_k, x_l} (\delta_{\sigma_k, \uparrow} \delta_{\sigma_l, \downarrow} + \delta_{\sigma_k, \downarrow} \delta_{\sigma_l, \uparrow}) |\mathbf{x}, \sigma\rangle \\ &\quad \sum_{1 \leq k < l \leq N} \delta_{x_k, x_l} (\delta_{\sigma_k, \uparrow} + \delta_{\sigma_k, \downarrow}) (\delta_{\sigma_l, \uparrow} + \delta_{\sigma_l, \downarrow}) |\mathbf{x}, \sigma\rangle \\ &\quad \sum_{1 \leq k < l \leq N} \delta_{x_k, x_l} |\mathbf{x}, \sigma\rangle. \end{aligned} \quad (1.34)$$

$H_{U=0}$ and \hat{D} do not commute. Hence the Hubbard Hamiltonian can neither be diagonal in the Bloch basis nor in the Wannier basis. In the next chapter we will construct eigenfunctions of the full Hamiltonian (1.21) through not a trivial method, the so-called *Bethe ansatz*. The physics of the Hubbard model depends on the competition between the two contribution $H_{U=0}$ and $H_{t=0}$ (or \hat{D}) to the Hamiltonian. The first prefers to delocalize the electrons, whereas the latter favours localization. The ratio U/t is a measure for the relative contribution of both terms and is the intrinsic, dimensionless coupling constant of the Hubbard model.

In order to study the symmetries of the Hamiltonian it is useful to add a chemical potential term $(U/t)(-\hat{N}/2 + L)$ which, because of the particle number conservation, does not affect the eigenstates. Dividing the Hamiltonian by t , the resulting expression is

$$H = - \sum_{j=1}^L \sum_{\sigma=\uparrow\downarrow} (c_{j\sigma}^\dagger c_{j+1\sigma} + c_{j+1\sigma}^\dagger c_{j\sigma}) + \frac{U}{t} \sum_{j=1}^L \left(\frac{1}{2} - n_{j\uparrow}\right) \left(\frac{1}{2} - n_{j\downarrow}\right). \quad (1.35)$$

Symmetries play a fundamental role in theoretical physics since they are related to conservation laws and have some important consequences. For example, the symmetry properties under the exchange of identical particles lead to a classification of all elementary particles as either bosons or fermions, whose quantum statistics is different, with profound implications for their behaviour.

Thus, here we illustrate some important symmetries of the model under examination [5, 17]. Apart from the obvious symmetries, like the translational symmetry or the symmetry under spin flip, there are many others. Some of them depend on the coupling constant U/t and are related to the fact that the one-dimensional Hubbard model is integrable. We concentrate on the U/t -independent symmetries, which can be extended to arbitrary dimensions. All the symmetry operators will be written in terms of creation and annihilation operators and will turn out to have relatively simple representations in this notation. Since the Hubbard model is defined on a lattice, there are symmetries related to the lattice in addition to those connected to the spin.

Thus we introduce the symmetric group \mathcal{G}^L formed by all permutations of site indices. In order to construct a representation of \mathcal{G}^L , we construct the elementary permutation operator in terms of Fermi operators:

$$\Pi_\ell^{i\sigma,j\sigma'} = 1 - (c_{i\sigma}^\dagger - c_{j\sigma'}^\dagger)(c_{i\sigma} - c_{j\sigma'}) \quad (1.36)$$

This is the operator that interchanges fermions at sites i and j (in both coordinate and spin variables). It should not be confused with an operator that interchanges electrons i and j . Subscript ℓ indicate that it is an operator acting on lattice sites and not on electrons; hence i and j refer to lattice sites and not to electrons.

The following relations hold on

$$\Pi_\ell^{i\sigma,j\sigma'} = (\Pi_\ell^{i\sigma,j\sigma'})^\dagger, \quad \Pi_\ell^{i\sigma,j\sigma'} = \Pi_\ell^{j\sigma',i\sigma} \quad (1.37)$$

$$\Pi_\ell^{i\sigma,j\sigma'} c_{j\sigma'} = c_{i\sigma} \Pi_\ell^{i\sigma,j\sigma'}, \quad \Pi_\ell^{i\sigma,j\sigma'} c_{i\sigma}^\dagger = c_{j\sigma'}^\dagger \Pi_\ell^{i\sigma,j\sigma'}, \quad \Pi_\ell^{i\sigma,j\sigma'} c_{j\sigma'}^\dagger = c_{i\sigma}^\dagger \Pi_\ell^{i\sigma,j\sigma'} \quad (1.38)$$

$$\Pi_\ell^{i\sigma,j\sigma'} \Pi_\ell^{j\sigma',k\sigma''} = \Pi_\ell^{i\sigma,k\sigma''} \Pi_\ell^{i\sigma,j\sigma'} = \Pi_\ell^{j\sigma',k\sigma''} \Pi_\ell^{i\sigma,k\sigma''}, \quad i \neq j \neq k \neq i \quad (1.39)$$

$$\Pi_\ell^{i\sigma,j\sigma'} \Pi_\ell^{i\sigma,j\sigma'} = 1 \quad (1.40)$$

$$[\Pi_\ell^{i\sigma,j\sigma'}, \Pi_\ell^{k\sigma''l\sigma'''}] = 0 \quad \text{if } i, j \neq k, l \quad (1.41)$$

and operators $\Pi_\ell^{i\sigma,j\sigma'}$ generate a representation of the symmetric group.

Operators related to the spacial symmetries of the Hubbard model can be obtained by imagining the L sites as forming a regular polygon with L edges and corners and considering the symmetries of this polygon. They are generated by a rotation through $2\pi/L$ and by an arbitrary reflection which maps the polygon onto itself. The corresponding symmetry operators are the shift operator and the parity operator. They are defined as

$$\hat{O}_S = \hat{O}_{L\uparrow} \hat{O}_{L\downarrow}, \quad \hat{O}_{n\sigma} = \Pi_\ell^{n-1\sigma,n\sigma} \dots \Pi_\ell^{2\sigma,3\sigma} \Pi_\ell^{1\sigma,2\sigma} \quad (1.42)$$

and

$$\hat{R} = \hat{R}_{L\uparrow} \hat{R}_{L\downarrow}, \quad \hat{R}_{L\sigma} = \prod_{j=1}^{L/2} \Pi_\ell^{j\sigma, L-j+1\sigma} \quad (1.43)$$

respectively. Here \hat{O}_S is the left shift operator, that makes a cyclic permutation over the electrons on the L sites of the chain and generates a shift to the left by one lattice site. Its Hermitian conjugate \hat{O}_S^\dagger is the right shift operator.

Two more important symmetries are the spin flip and the Shiba transformation, which are useful to restrict the ranges of the number of electrons N

and down spins M . The Hubbard Hamiltonian is invariant under the reversal of all spin, obtained through the operator

$$\hat{J} = \prod_{j=1}^L \Pi_{\ell}^{j\uparrow, j\downarrow} = \prod_{j=1}^L (1 - n_j + S_j^+ + S_j^-) \quad (1.44)$$

where $n_j = n_{j\uparrow} + n_{j\downarrow}$ counts the particle number on site j , whereas $S_j^+ = c_{j\uparrow}^\dagger c_{j\downarrow}$ and $S_j^- = c_{j\downarrow}^\dagger c_{j\uparrow}$ are the spin-flip operators on site j .

This transformation maps the eigenstates with M down-spin electrons and $N - M$ up-spin electrons one-to-one onto the eigenstates with M up-spin electrons and $N - M$ down-spin electrons. Thus the z -component S^z of the total spin changes its sign. This allow to restrict to non-negative values of S^z when we diagonalize the Hamiltonian.

The other useful transformation that allow to simplify the diagonalization of the Hamiltonian is the Shiba transformation, which is obtained by applying the operators

$$\hat{J}_\sigma^{\text{Shiba}} = (c_{L\sigma}^\dagger \mp c_{L\sigma})(c_{L-1\sigma}^\dagger \pm c_{L-1\sigma}) \dots (c_{2\sigma}^\dagger - c_{2\sigma})(c_{1\sigma}^\dagger + c_{1\sigma}) \quad (1.45)$$

with $\sigma = \uparrow, \downarrow$. Here the upper sign in the right hand side applies to a chain with an even number of sites L , while the lower sign applies to an odd L . We have $[\hat{J}_\sigma^{\text{Shiba}}, c_{j\sigma}] = 0$ and

$$\hat{J}_\sigma^{\text{Shiba}} c_{j\sigma} \left(\hat{J}_\sigma^{\text{Shiba}} \right)^\dagger = (-1)^j c_{j\sigma}^\dagger. \quad (1.46)$$

Hence the Shiba transformation on bipartite lattices acts in the following manner

$$\begin{aligned} c_{j\sigma} &\longrightarrow (-1)^j c_{j\sigma}^\dagger & c_{j\bar{\sigma}} &\longrightarrow c_{j\bar{\sigma}} \\ c_{j\sigma}^\dagger &\longrightarrow (-1)^j c_{j\sigma} & c_{j\bar{\sigma}}^\dagger &\longrightarrow c_{j\bar{\sigma}}^\dagger \end{aligned} \quad (1.47)$$

where $\bar{\sigma} = \uparrow$ if $\sigma = \downarrow$ and vice versa. Clearly, for an even number of lattice sites, the tight-binding part of the Hubbard Hamiltonian (1.35) is invariant under this transformation, while the interaction part changes its sign:

$$H_U \longrightarrow H_{-U}. \quad (1.48)$$

The empty lattice is mapped to

$$\hat{J}_\sigma^{\text{Shiba}}|0\rangle = c_{L\sigma}^\dagger \dots c_{1\sigma}^\dagger |0\rangle \quad (1.49)$$

which is the fully spin polarized half-filled band state.

Of course, we can also apply the Shiba transformation to a lattice with an odd number of sites; in that case, however, the kinetic term of the Hubbard Hamiltonian is not invariant.

Let us consider an even number of lattice site L . If we perform Shiba transformations for both up and down spins, the Hamiltonian is not altered, since the sign of U is switched twice, but the empty lattice state is mapped onto a state with all sites doubly occupied. Thus, all eigenstates of the Hubbard Hamiltonian (1.35) with N electrons are mapped onto eigenstates with $2L - N$ electrons. Hence we may restrict ourselves to $N \leq L$ (*below half filling*) when we diagonalize the Hamiltonian, since we can extend the result to the case *above half filling* through a Shiba transformation.

An important symmetry related to the Shiba transformation is the so-called η -pairing symmetry. This is an $SU(2)$ symmetry. An other $SU(2)$ symmetry is that of rotations in spin space. The full symmetry realized for the Hubbard Hamiltonian (1.35) is

$$SO(4) = SU(2) \times SU(2)/\mathbb{Z}_2. \quad (1.50)$$

We present some details. Let us define the spin operators:

$$S^\alpha = \sum_{j=1}^L S_j^\alpha = \frac{1}{2} \sum_{j=1}^L \sum_{\sigma, \sigma'} c_{j\sigma}^\dagger (\sigma^\alpha)_{\sigma\sigma'} c_{j\sigma'} \quad (1.51)$$

where $\alpha = x, y, z$ indicates a component and the matrices σ^α are the Pauli matrices

$$\sigma^x = \begin{pmatrix} 0 & 1 \\ 1 & 0 \end{pmatrix}, \quad \sigma^y = \begin{pmatrix} 0 & -i \\ i & 0 \end{pmatrix}, \quad \sigma^z = \begin{pmatrix} 1 & 0 \\ 0 & -1 \end{pmatrix}. \quad (1.52)$$

Hence, for each site j , we have a total spin S_j with components

$$\begin{aligned}
S_j^x &= \frac{1}{2}[c_{j\uparrow}^\dagger c_{j\downarrow} + c_{j\downarrow} c_{j\uparrow}] \\
S_j^y &= \frac{1}{2i}[c_{j\uparrow}^\dagger c_{j\downarrow} - c_{j\downarrow} c_{j\uparrow}]
\end{aligned} \tag{1.53}$$

$$S_j^z = \frac{1}{2}[c_{j\uparrow}^\dagger c_{j\uparrow} - c_{j\downarrow}^\dagger c_{j\downarrow}] = \frac{1}{2}[n_{j\uparrow} - n_{j\downarrow}].$$

In general the Hubbard Hamiltonian doesn't commute with a spin component at a site j

$$[H, S_j^\alpha] \neq 0 \tag{1.54}$$

but it commutes with each component of the total spin:

$$[H, S^\alpha] \equiv \sum_j [H, S_j^\alpha] = 0 \tag{1.55}$$

and thus is fully rotationally invariant.

The Pauli matrices form a basis of the fundamental representation of the SU(2) algebra and satisfy the commutation relations

$$[\sigma^\alpha, \sigma^\beta] = 2i\epsilon_{\alpha\beta\gamma}\sigma^\gamma \tag{1.56}$$

where $\epsilon_{\alpha\beta\gamma}$ is the totally antisymmetric tensor. Hence, as was claimed above, the spin operators generate a representation of SU(2):

$$[S^\alpha, S^\beta] = i\epsilon_{\alpha\beta\gamma}S^\gamma. \tag{1.57}$$

We shall usually use the ladder operators

$$S^\pm = S^x \pm iS^y \tag{1.58}$$

instead of S^x and S^y . They have the explicit form

$$\begin{aligned}
S^+ &= \sum_{j=1}^L c_{j\uparrow}^\dagger c_{j\downarrow} \\
S^- &= \sum_{j=1}^L c_{j\downarrow}^\dagger c_{j\uparrow}
\end{aligned} \tag{1.59}$$

and obey the commutation relations

$$\begin{aligned}
[S^z, S^\pm] &= \pm S^\pm \\
[S^+, S^-] &= 2S^z.
\end{aligned}
\tag{1.60}$$

Let us now consider the η -pairing symmetry. It has its origin in the behaviour of the Hubbard Hamiltonian under the Shiba transformation.

If we apply the Shiba transformation to the spin operators S^\pm, S^z , we get

$$\begin{aligned}
\hat{J}_\downarrow^{Shiba} S^+ \left(\hat{J}_\downarrow^{Shiba} \right)^\dagger &= \sum_{j=1}^L (-1)^j c_{j\uparrow}^\dagger c_{j\downarrow}^\dagger = \eta^+ \\
\hat{J}_\downarrow^{Shiba} S^- \left(\hat{J}_\downarrow^{Shiba} \right)^\dagger &= \sum_{j=1}^L (-1)^j c_{j\downarrow}^\dagger c_{j\uparrow}^\dagger = \eta^- \\
\hat{J}_\downarrow^{Shiba} S^z \left(\hat{J}_\downarrow^{Shiba} \right)^\dagger &= \frac{1}{2} \sum_{j=1}^L (-1)^j (n_{j\uparrow} + n_{j\downarrow} - 1) = \frac{1}{2} (\hat{N} - L) = \eta^z.
\end{aligned}
\tag{1.61}$$

Hence

$$\begin{aligned}
S^+ &\longrightarrow \eta^+ \\
S^- &\longrightarrow \eta^- \\
S^z &\longrightarrow \eta^z.
\end{aligned}
\tag{1.62}$$

The η operators are called the pairing operators or the pseudo-spin operators and satisfy the following commutation relations

$$\begin{aligned}
[\eta^\pm, \eta^z] &= \pm \eta^\pm \\
[\eta^+, \eta^-] &= 2\eta^z.
\end{aligned}
\tag{1.63}$$

This can easily be verified by applying the Shiba transformation to (1.60). Hence they also obey an SU(2) algebra. We may define the analogues of S^x and S^y :

$$\begin{aligned}
\eta^x &= \frac{1}{2}(\eta^+ + \eta^-) \\
\eta^y &= -\frac{i}{2}(\eta^+ - \eta^-)
\end{aligned}
\tag{1.64}$$

which satisfy

$$[\eta^\alpha, \eta^\beta] = i\epsilon_{\alpha\beta\gamma} \eta^\gamma
\tag{1.65}$$

with $\alpha, \beta = x, y, z$.

The invariance of the Hubbard Hamiltonian (1.35) under the η -pairing symmetry follows from the application of the Shiba transformation to $[H_{-U}, S^\alpha] = 0$:

$$[H, \eta^\alpha] = 0. \quad (1.66)$$

In conclusion, Hamiltonian (1.35) commutes with two $SU(2)$ algebras, that of spin and that of pseudo-spin. Thus we may be tempted to claim that it obeys an $SU(2) \times SU(2)$ algebra. It is not true. In fact equation (1.66) holds only for an even number of lattice sites L . This fact imposes restrictions on joint irreducible representations of spin and η -spin realised on eigenstates of the Hubbard Hamiltonian. We can easily verify that

$$S^z + \eta^z = \hat{N}_\uparrow - \frac{L}{2}. \quad (1.67)$$

For an even L , this quantity is an integer and the symmetry is that expressed in (1.50)

$$SU(2) + SU(2)/\mathbb{Z}_2 = SO(4). \quad (1.68)$$

1.3 On the physics of the model

Before continuing with our discussion and showing some explicit results in the one-dimensional case, we try to give an overview on the phenomena that the model is able to account for. It was introduced as a simple effective model for the study of correlation effects of d -electrons in transition metals [18, 10]. It is believed to provide a qualitative description of the magnetic properties of these materials and the Mott metal-insulator transition [19]. As mentioned before, the dimension of the lattice underling the system is a crucial parameter and, despite its simplicity, the model is exactly soluble only in one-dimension. However it has long been studied and a variety of approximate analytical and numerical results are known also in higher dimensions. Here we illustrate some general properties of the Hubbard model in two and three dimensions.

A first step toward understanding a quantum Hamiltonian is to search for its ground state. In absence of an exact solution, a variational approach can be tempted. It consists of two fundamental steps. The first consists in making a judicious choice of a family of states (the so-called *variational states*)

to describe the model. These states depend on some variational parameters γ . Hence the second step consists in calculating the energy as the expectation value of the Hamiltonian on the variational states Ψ^γ and minimizing it respect to the γ parameters, since the variational theorem states that

$$\frac{\langle \Psi^\gamma | H | \Psi^\gamma \rangle}{\langle \Psi^\gamma | \Psi^\gamma \rangle} = E^\gamma \geq E_0 \quad (1.69)$$

where E_0 is the exact ground state energy.

A possible choice for the variational states is that of the so-called *magnetic states*, which allow to observe the emergence of a magnetic behaviour in the Hubbard model. In the Hartree-Fock approximation the two-body operator in Hamiltonian (1.18) factorizes in a sum of one-body operators as

$$\langle \Psi^\gamma | n_{j\uparrow} n_{j\downarrow} | \Psi^\gamma \rangle = \langle n_{j\uparrow} n_{j\downarrow} \rangle = \langle n_{j\uparrow} \rangle \langle n_{j\downarrow} \rangle - \langle S_j^+ \rangle \langle S_j^- \rangle. \quad (1.70)$$

Thus we can easily make a Fourier transform and write the Hamiltonian in \mathbb{K} space. Then we define the magnetic states through the creation and annihilation operators $a_{\mathbf{k}\sigma}^\dagger$, $a_{\mathbf{k}\sigma}$, which are related to the c -operators through the following linear transformation

$$\begin{pmatrix} a_{\mathbf{k}\uparrow}^\dagger \\ a_{\mathbf{k}\downarrow}^\dagger \end{pmatrix} = \begin{pmatrix} \cos \theta_{\mathbf{k}} & \sin \theta_{\mathbf{k}} \\ -\sin \theta_{\mathbf{k}} & \cos \theta_{\mathbf{k}} \end{pmatrix} \begin{pmatrix} c_{\mathbf{k}\uparrow}^\dagger \\ c_{\mathbf{k}+\mathbf{q}\downarrow}^\dagger \end{pmatrix} \quad (1.71)$$

where q and $\theta_{\mathbf{k}}$ are the variational parameters. Thus the variational magnetic states are

$$|\Psi^{q, \theta_{\mathbf{k}}}\rangle = \prod_{\sigma=\uparrow, \downarrow, \mathbf{k}} a_{\mathbf{k}\sigma}^\dagger |0\rangle. \quad (1.72)$$

With this ansatz we get the following results

$$\left. \begin{aligned} \langle S_i^x \rangle &= \cos(\mathbf{q}R_i) m_{\mathbf{q}} \\ \langle S_i^y \rangle &= -\sin(\mathbf{q}R_i) m_{\mathbf{q}} \end{aligned} \right\} \longrightarrow \langle S_i^+ \rangle = e^{-i\mathbf{q}R_i} m_{\mathbf{q}} \quad (1.73)$$

$$\langle S_i^z \rangle = m_z \quad (1.74)$$

with $m_{\mathbf{q}}$ and m_z some parameters. For explicit calculation we remand to reference [9, chap 4]. Here we are interested only on the results. From the preceding equations we can see that there are spin density waves in the xy plane and a constant magnetisation along the z -axis.

Another important result that can be derived is the Stoner's criterion for a ferromagnetic instability

$$2U\chi(0) = 1 \quad (1.75)$$

where $\chi(0)$ is the uniform magnetic susceptibility for noninteracting electrons

$$\chi(0) = \frac{1}{2} \sum_{\mathbf{k}} \frac{dn(\epsilon_{\mathbf{k}})}{d\epsilon_{\mathbf{k}}} = \frac{1}{2} \rho_{\uparrow}(0) \quad (1.76)$$

with

$$n(\epsilon) = \frac{1}{e^{\epsilon/T} + 1} \quad (1.77)$$

the Fermi function and $\rho_{\uparrow}(0)$ the noninteracting, single spin density of states at the Fermi energy. We may also obtain a Stoner's criterion for the spin density wave instability at wave vector \mathbf{q} :

$$2U\chi(\mathbf{q}) = 1 \quad (1.78)$$

where

$$\chi(\mathbf{q}) = \frac{1}{2} \sum_{\mathbf{k}} \frac{n(\epsilon_{\mathbf{k}+\mathbf{q}}) - n(\epsilon_{\mathbf{k}})}{\epsilon_{\mathbf{k}} - \epsilon_{\mathbf{k}+\mathbf{q}}}. \quad (1.79)$$

Maximizing $\chi(\mathbf{q})$ therefore determines the ordering wave vector at which the magnetic instability first occurs as we increase the magnitude of U . We see that while $\chi(0)$ is determined only by the Fermi surface density of states, $\chi(\mathbf{q})$ is sensitive to the Fermi surface geometry. In particular it depends on the existence of parallel sections on the Fermi surface which are separated by the wave vector \mathbf{q}_{nest} . Here the label *nest* stays for *nesting* which is how this phenomenon is called. The nesting yields a large number of small energy denominators $|\epsilon(\mathbf{k}) - \epsilon(\mathbf{k} + \mathbf{q})|$ in the sum (1.79). The divergence of $\chi(\mathbf{q}_{nest})$ may produce a magnetic ground state also for small values of U/t . The nesting is most relevant in one dimension and for the two-dimensional square lattice near half-filling ($N \approx L$) (see figure 1.1).

The Stoner's criterion is known to overestimate the magnetic ordering and underestimate quantum disordering effect due to spin fluctuations. However we can assert that in the Hubbard model there is at least short-range magnetic ordering when the Stoner criterion is satisfied.

We have seen that the Hubbard model allows to observe the emergence of spin density waves and ferromagnetic behaviour. Thus, with the variational magnetic states (1.72), it may be used to describe spin density wave systems (e.g. chromium) and metallic ferromagnets (e.g. iron). The model admits other orderings, such as charge density waves and superconductivity. These can be observed with different variational Fock states, obtained by

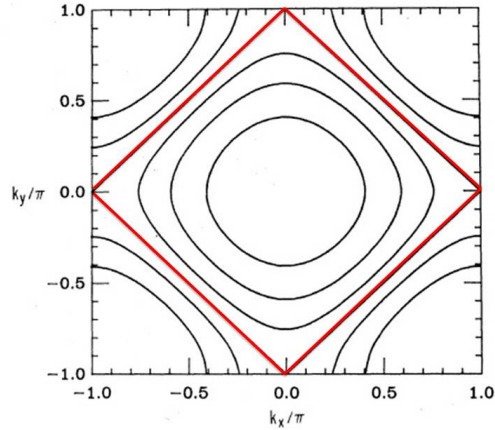


Figure 1.1: The figure shows Fermi surfaces for electrons on a two-dimensional square lattice with nearest-neighbor hopping only. Different curves refer to different band filling, which enhances from the inner surface to the outer surface. The red surface is that for half-filling $N/L = 1$ and is nested. (Figure from [20])

performing other canonical transformations on the electron creation operators, similar to (1.71).

Therefore in the Hubbard Hamiltonian interactions between electrons can lead to fluctuation in charge density and fluctuations in spin density. Several studies have been made that take into account only the latter, in order to describe the Mott transition. This is a metal-insulator transition in which the insulator phase is due to electron correlation and presents a magnetic behaviour. The Hubbard model presents a very rich physics also at zero temperature, since we observe a transition phase from a non magnetic metal to an antiferromagnetic metal and then from this one to an antiferromagnetic insulator, as the ratio U/W is enhanced (where W is the band width). At finite temperature, the ground state remains antiferromagnetic for large values of U/W and only at high temperature it becomes paramagnetic. These results are summarized in the phase diagram in figure 1.2 [21]. Even in the two-dimensional case, the Hubbard model shows magnetic ordering. The phase diagram at zero temperature according to the Hartree-Fock mean field theory is shown in figure 1.3. Hence the ground state can have a paramagnetic phase, a ferromagnetic phase or an antiferromagnetic phase as the interaction parameter U/t and the band filling N/L are varied. However the mean field theory works better and better as the dimension of the lattice increases and in $D = 2$ its results are not accurate. Hirsch [20] showed through numerical Monte Carlo simulation that the ground state is antiferromagnetic

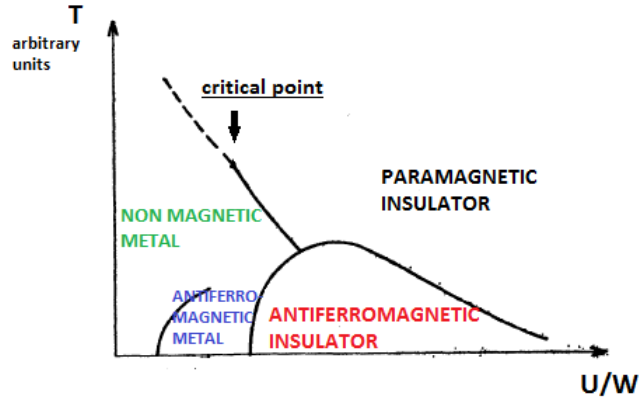


Figure 1.2: Schematic phase diagram for the 3D Hubbard model. Figure from [21]

at half filling for each value of the interaction and paramagnetic for $N/L \neq 1$. The phase diagram is shown in figure 1.4.

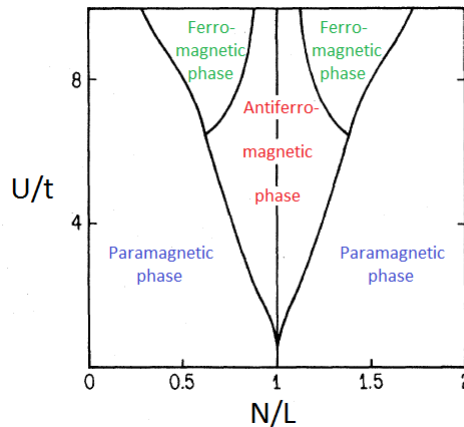


Figure 1.3: Schematic Hartree-Fock phase diagram for the 2D Hubbard model. Figure from [20].

1.3.1 Some more recent results

Even though the Hubbard model is a rather simple model, it continues to attract attention and to yield surprise such as new phases and quantum phase transitions.

In particular, study of the Hubbard model and its extensions has intensified with the experimental investigation on cold bosonic and fermionic atoms subject to an optical lattice. In fact, the remarkable controllability of cold atom systems has opened the possibility of studying strongly correlated systems in

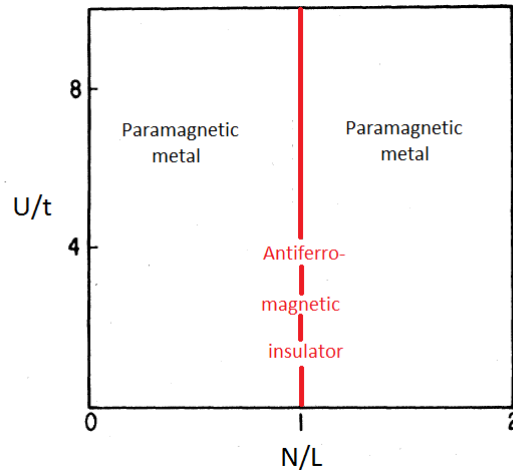


Figure 1.4: Schematic phase diagram for the 2D Hubbard model from numerical calculations. Figure from [20].

regimes inaccessible to solid state materials.

A good synergy between experimental efforts and theoretical investigations is crucial. Among all model Hamiltonians, the Hubbard model and its extensions - in one, two and three dimensions - are the simplest models with highly tunable parameters and in many cases they provide concrete Hamiltonians in which the physics can be examined with powerful numerical methods.

Several works have been made in this direction since some important experimental results have been reached, such as the realization of the Mott metal-insulator transition in ultracold atoms confined in an optical lattice [22].

It is also believed that the Hubbard model physics is relevant to high-temperature superconductivity, a phenomenon related to the Mott insulating phase and still not understood.

Theoretical models use the simple Hubbard or Bose-Hubbard Hamiltonian with contact interaction (U) only or with the extension to near neighbor interactions (V). Some interesting results for the one-dimensional extended Bose-Hubbard model have been achieved in [23], where different phases have been observed as U and V are varied, among them Mott insulating, Haldane insulating and superfluid.

Some more realistic models, which take into account the trapping potential, have also been studied. In the temperature regime that is of interest for current experiments, different phases are observed as the on-site interaction U and the particle number N are varied (see figure 1.5) [24]. For low interaction strength the system is a Fermi liquid everywhere in the trap. However,

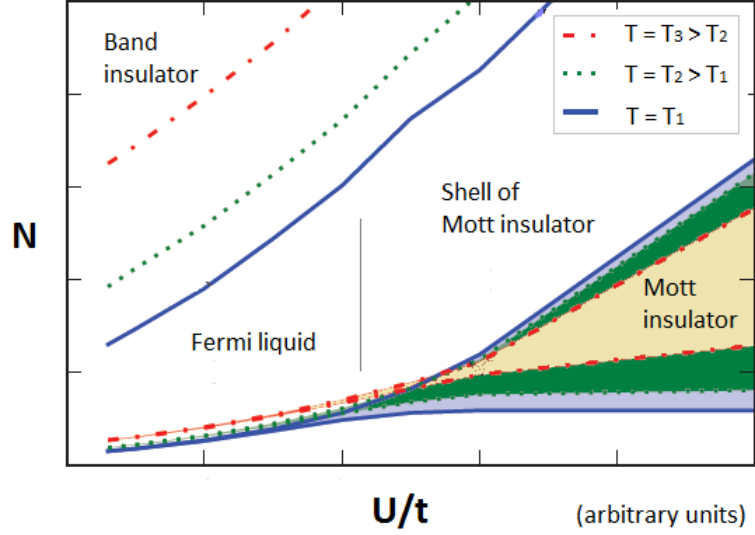


Figure 1.5: State diagram of the gas in a 3D optical lattice with parabolic trapping potential. Figure from [24]

as the particle number is increased to very large values, a band insulator with double occupancy ($n = 2$) forms in the center of the trap. For larger interaction strength a Mott insulating region appears, in which the density is pinned to one particle per site ($n = 1$). This region is surrounded by a liquid region close to the boundary of the trap. Increasing the number of atoms in the trap at large U/t can increase the pressure on the atoms and can cause the occurrence of a liquid region with filling larger than one in the center, surrounded by a shell of Mott insulator with $n = 1$.

At lower temperatures an antiferromagnetic transition is observed [25]. For further information about Hubbard model investigation, refer to [6].

Chapter 2

Bethe Ansatz

The Bethe ansatz is an exact method for obtaining eigenvalues and eigenvectors of certain one-dimensional quantum many-body models. It was introduced by Hans Bethe in 1931 to find the exact solutions of the one-dimensional spin-1/2 Heisenberg model, a linear chain of electrons with uniform exchange interaction between nearest neighbors. Bethe constructed the many-body wave functions and reduced the problem of calculating the spectrum of the Hamiltonian to solving a set of N coupled algebraic equations, where N is the number of overturned spins. The Bethe ansatz is a powerful tool because it reduces a problem of exponential complexity to one of polynomial complexity. Bethe's work marked the beginning of the theory of exactly solvable quantum systems: since then the method has been extended to other models in one dimension and has become influential to an extent not imagined at the time. During the 1960's E. H. Lieb and W. Liniger applied the Bethe ansatz on the Bose gas with delta-function potential [26] and then E. H. Lieb extended it to problems in statistical mechanics solving three archetypal cases of the six-vertex model [27, 28, 29]. The generalization of Bethe's ansatz to models with internal degrees of freedom like spin proved to be very hard, because scattering involves changes of the internal states of the scatterers. The solution of this problem was found by C. N. Yang [30] and M. Gaudin [31] with the so-called *nested Bethe ansatz*. Today, a lot of quantum many-body systems are known to be solvable by some variant of the Bethe ansatz. The Hubbard model is included here. If the system is finite, the eigenvalues and eigenvectors can be obtained by a brute force numerical diagonalization with not too much effort. However the Bethe ansatz is advantageous because it provides a set of quantum numbers associated to the eigenstates which allow to distinguish them according to specific physical properties. Moreover in many cases the results can be extended to the thermodynamic limit.

We are interested in studying the Hubbard model, so we will not discuss the Heisenberg chain in full detail. However we give a brief overview on this topic to introduce the basic idea of the Bethe ansatz [32, 33, 34].

2.1 The basic idea of the Bethe ansatz: a brief overview on the Heisenberg chain

The Hamiltonian of the 1D-Heisenberg model is

$$\begin{aligned} H &= -J \sum_{j=1}^L \mathbf{S}_j \cdot \mathbf{S}_{j+1} = \\ &= -J \sum_{j=1}^L \left\{ \frac{1}{2} (S_j^+ S_{j+1}^- + S_j^- S_{j+1}^+) + S_j^z S_{j+1}^z \right\} \end{aligned} \quad (2.1)$$

where L is the chain length, \mathbf{S}_j the spin operator (with periodic boundary condition $\mathbf{S}_{L+1} = \mathbf{S}_1$) and $S_j^\pm = S_j^x \pm iS_j^y$ are spin flip operators introduced in the preceding chapter. We want to solve the eigenvalue problem

$$H|\psi\rangle = E|\psi\rangle. \quad (2.2)$$

H acts on a Hilbert space of dimension 2^L spanned by the orthogonal basis vectors $|\sigma_1 \dots \sigma_L\rangle$, where $\sigma_j = \uparrow, \downarrow$ represents an up or down spin at site j . The spin operators act on this vector in the following way

$$\begin{aligned} S_j^+ |\dots \uparrow \dots\rangle &= 0 & S_j^+ |\dots \downarrow \dots\rangle &= |\dots \uparrow \dots\rangle \\ S_j^- |\dots \uparrow \dots\rangle &= |\dots \downarrow \dots\rangle & S_j^- |\dots \downarrow \dots\rangle &= 0 \\ S_j^z |\dots \uparrow \dots\rangle &= \frac{1}{2} |\dots \uparrow \dots\rangle & S_j^z |\dots \downarrow \dots\rangle &= -\frac{1}{2} |\dots \downarrow \dots\rangle \end{aligned} \quad (2.3)$$

so that the application of H on $|\sigma_1 \dots \sigma_L\rangle$ yields a linear combination of basis vectors, each of them has the same number of down spins. In order to solve the problem, we can fix the number N of down spins, because $[H, S^z] = 0$, where S^z is the total spin along the z -axis. If $N = 0$, we have all up spins and the only eigenvector is $|\uparrow \dots \uparrow\rangle$, with eigenvalue $E_0 = -JL/4$. In the subspace with one down spin ($N = 1$), any eigenvector is a superposition of

the basis vectors and can be written as

$$|\Psi\rangle = \sum_{x=1}^L \psi(x)|x\rangle \quad (2.4)$$

with $|x\rangle = S_x^- |\uparrow \dots \uparrow\rangle$. The eigenvector $|\Psi\rangle$ is a solution of the eigenvalue equation $H|\Psi\rangle = E|\Psi\rangle$ if the coefficients $\psi(x)$ satisfy the linear equations

$$2[E - E_0]\psi(x) = J[2\psi(x) - \psi(x-1) - \psi(x+1)] \quad (2.5)$$

for $x = 1, 2, \dots, L$ and with $\psi(x+L) = \psi(x)$. So we have passed from a second-quantized form to a first-quantized form of the eigenvalue equation, which has L linearly independent solutions. These solutions are plane waves

$$\psi(x) = e^{ikx}, \quad k = \frac{2\pi}{L}n, \quad n = 1, \dots, L \quad (2.6)$$

and the corresponding eigenvalues are

$$E - E_0 = J(1 - \cos k). \quad (2.7)$$

The peculiarity of the Bethe ansatz begin to emerge when we consider the case $N = 2$. Now we can write the state as

$$|\Psi\rangle = \sum_{1 \leq x_1 < x_2 \leq L} \psi(x_1, x_2)|x_1, x_2\rangle \quad (2.8)$$

where $|x_1, x_2\rangle = S_{x_1}^- S_{x_2}^- |\uparrow \dots \uparrow\rangle$ are the basis vectors of this subspace. The problem is always to determine the coefficients $\psi(x_1, x_2)$ and the eigenvalues. Bethe's basic idea was to suppose that the wave functions $\psi(x_1, x_2)$ are superpositions of plane waves of the form

$$\psi(x_1, x_2) = A_1 e^{i(k_1 x_1 + k_2 x_2)} + A_2 e^{i(k_1 x_2 + k_2 x_1)}. \quad (2.9)$$

Now this expression has to be inserted into eigenvalue equation. For $x_2 \neq x_1 + 1$ this gives the energy eigenvalues, which are the sum of the energy of the two single-particle states: $E - E_0 = J \sum_{j=1,2} (1 - \cos k_j)$. If we substitute this expression into eigenvalue equation for $x_2 = x_1 + 1$, we get the amplitude ratio A_1/A_2 . Finally we determine the possible values of the momenta k_1, k_2 from the requirement that the wave function be translationally invariant:

$\psi(x_1, x_2) = \psi(x_2, x_1 + L)$. The equations for k_1 and k_2 are known as the Bethe equations. Hence the problem has been reduced to a set of algebraic equations that can be solved by analytical or numerical methods.

2.2 Bethe Ansatz solutions for the Hubbard model

We now discuss the Bethe ansatz solutions for the one-dimensional Hubbard model:

$$H = -t \sum_{i=1}^L \sum_{\sigma=\uparrow,\downarrow} (c_{i\sigma}^\dagger c_{i+1\sigma} + c_{i+1\sigma}^\dagger c_{i\sigma}) + U \sum_{i=1}^L (n_{i\uparrow} n_{i\downarrow}). \quad (2.10)$$

As for the Heisenberg chain, the stationary Schrödinger equation (2.2) for the Hamiltonian (2.10) can be reduced to a set of algebraic equations, which is tractable in the thermodynamic limit. These equations are known as the Lieb-Wu equations to honour E. H. Lieb and F. Y. Wu, who first obtained them [35]. The roots of the Lieb-Wu equations parameterize the eigenvalues and eigenstates of the Hamiltonian (2.10). They encode all information about the model but are not explicitly known in the general N -particle case. So we begin with the exact solution of the two-particle problem. This can be done because Hamiltonian (2.10) preserve the number of particles: $[H, \hat{N}] = 0$, with $\hat{N} = \sum_i c_i^\dagger c_i$. Hence we may consider the eigenvalue problem (2.2) in the sectors of fixed numbers of particles $N = 0, 1, \dots, 2L$, where L is the number of sites. This corresponds to switching from second to first quantization.

2.2.1 The two-particle case

In order to pass from the second quantization to the first quantization representation, we write the two-particle state $|\Psi\rangle$ as

$$|\Psi\rangle = \frac{1}{2} \sum_{x_1, x_2=1}^L \sum_{\sigma_1, \sigma_2=\uparrow,\downarrow} \psi_{\sigma_1\sigma_2}(x_1, x_2) |x_1\sigma_1, x_2\sigma_2\rangle \quad (2.11)$$

where

$$|x_1\sigma_1, x_2\sigma_2\rangle = c_{x_2\sigma_2}^\dagger c_{x_1\sigma_1}^\dagger |0\rangle \quad (2.12)$$

so that

$$\langle x'_1\sigma'_1, x'_2\sigma'_2 | x_1\sigma_1, x_2\sigma_2 \rangle = \delta_{x'_1, x_1} \delta_{x'_2, x_2} \delta_{\sigma'_1, \sigma_1} \delta_{\sigma'_2, \sigma_2} - \delta_{x'_1, x_2} \delta_{x'_2, x_1} \delta_{\sigma'_1, \sigma_2} \delta_{\sigma'_2, \sigma_1} \quad (2.13)$$

and

$$\langle x'_1\sigma'_1, x'_2\sigma'_2 | \Psi \rangle = \psi_{\sigma'_1\sigma'_2}(x'_1, x'_2). \quad (2.14)$$

We notice that these formulae allow us to easily switch from second to first quantization and vice versa. If we insert expression (2.11) into eigenvalue equation (2.2), this reduces to

$$\begin{aligned} & -t[\psi_{\sigma_1\sigma_2}(x_1+1, x_2) + \psi_{\sigma_1\sigma_2}(x_1-1, x_2) + \psi_{\sigma_1\sigma_2}(x_1, x_2+1) \\ & + \psi_{\sigma_1\sigma_2}(x_1, x_2-1)] + U\delta_{x_1, x_2}\psi_{\sigma_1\sigma_2}(x_1, x_2) = E\psi_{\sigma_1\sigma_2}(x_1, x_2) \end{aligned} \quad (2.15)$$

which indeed is an eigenvalue equation for the wave function $\psi_{\sigma_1\sigma_2}$ in first quantization. The problem we want to solve is to find this wave function and the corresponding energy eigenvalue E . In order to achieve this purpose we make an ansatz on the wave function (the so called *Bethe ansatz*), in which some unknown coefficients appear, and insert it into the preceding equation. This gives the energies E and the conditions that determine the coefficients of the wave functions. The problem is similar to that of a system with a delta-function potential [36, Chap. 2] in the continuum. We need four functions to represent an eigenstate of the two $S = 1/2$ particles system:

$$\psi_{\uparrow\uparrow}(x_1, x_2), \psi_{\uparrow\downarrow}(x_1, x_2), \psi_{\downarrow\uparrow}(x_1, x_2), \psi_{\downarrow\downarrow}(x_1, x_2). \quad (2.16)$$

In order to find the explicit form of the wave function, we distinguish between two different cases: the first in which $\sigma_1 = \sigma_2$ and the second in which $\sigma_1 = \bar{\sigma}_2$ and we make two different ansatz for the corresponding wave functions.

We begin by remembering that the fermion's wave function must be anti-symmetric so that the following relations must be true:

$$\psi_{\uparrow\uparrow}(x_1, x_2) = -\psi_{\uparrow\uparrow}(x_2, x_1) \quad (2.17)$$

$$\psi_{\uparrow\downarrow}(x_1, x_2) = -\psi_{\downarrow\uparrow}(x_2, x_1) \quad (2.18)$$

$$\psi_{\downarrow\downarrow}(x_1, x_2) = -\psi_{\downarrow\downarrow}(x_2, x_1) \quad (2.19)$$

Thus we obtain $\psi_{\uparrow\uparrow}(x_1, x_1) = 0$ and $\psi_{\downarrow\downarrow}(x_1, x_1) = 0$. This means in this

case the Hubbard interaction has no physical effect. The wave function is represented by a determinant:

$$\begin{aligned}\psi_{\uparrow\uparrow}(x_1, x_2) &= C \det \begin{pmatrix} e^{ik_1 x_1} & e^{ik_1 x_2} \\ e^{ik_2 x_1} & e^{ik_2 x_2} \end{pmatrix} = C [e^{i(k_1 x_1 + k_2 x_2)} - e^{i(k_1 x_2 + k_2 x_1)}] \\ &= C e^{iKR} \cdot 2i \sin \left(\frac{k}{2} r \right)\end{aligned}\quad (2.20)$$

where we have introduced the centre of mass $R = \frac{x_1 + x_2}{2}$ and relative $r = x_1 - x_2$ coordinates and the momenta $K = k_1 + k_2$, $k = k_1 - k_2$, k_1 and k_2 being the momenta of the two particles; while C is a normalization coefficient. In the case in which the two particles have opposite spin, we make the following ansatz

$$\begin{aligned}\psi_{\downarrow\uparrow}(x_1, x_2) &= \sum_P [P, Q] e^{i(k_{P_1} x_{Q_1} + k_{P_2} x_{Q_2})} \quad \text{with } x_{Q_1} \leq x_{Q_2} \\ &= ([12, 12] e^{i(k_1 x_1 + k_2 x_2)} + [21, 12] e^{i(k_2 x_1 + k_1 x_2)}) \Theta(x_2 - x_1) + \\ &+ ([12, 21] e^{i(k_1 x_2 + k_2 x_1)} + [21, 21] e^{i(k_2 x_2 + k_1 x_1)}) \Theta(x_1 - x_2) = (2.21) \\ &= e^{iKR} \left\{ ([12, 12] e^{ikr/2} + [21, 12] e^{-ikr/2}) \Theta(-r) + \right. \\ &\quad \left. + ([12, 21] e^{-ikr/2} + [21, 21] e^{ikr/2}) \Theta(r) \right\}\end{aligned}$$

where $\Theta(r)$ is the Heaviside function, defined as

$$\Theta(r) = \begin{cases} 0 & \text{if } r < 0 \\ \frac{1}{2} & \text{if } r = 0 \\ 1 & \text{if } r > 0 \end{cases} \quad (2.22)$$

and $[P, Q]$ is the notation we use to indicate the coefficients. We substitute the expression for the wave function into the eigenvalue equation (2.15), with

$$E = -2t(\cos k_1 + \cos k_2) = -4t \cos(K/2) \cos(k/2). \quad (2.23)$$

This energy is the sum of the two free-particle energies and can be obtained from equation (2.15) with $r \neq 0$. After a short calculation we obtain

$$\begin{aligned}
& -2t \cos \frac{K}{2} \cdot \left\{ [12, 12] e^{ikr/2} (e^{ik/2} [\Theta(-r-1) - \Theta(-r)] + e^{-ik/2} [\Theta(-r+1) - \Theta(-r)]) \right. \\
& \quad + [21, 12] e^{-ikr/2} (e^{-ik/2} [\Theta(-r-1) - \Theta(-r)] + e^{ik/2} [\Theta(-r+1) - \Theta(-r)]) \\
& \quad + [12, 21] e^{-ikr/2} (e^{-ik/2} [\Theta(r+1) - \Theta(r)] + e^{ik/2} [\Theta(r-1) - \Theta(r)]) \\
& \quad \left. + [21, 21] e^{ikr/2} (e^{ik/2} [\Theta(r+1) - \Theta(r)] + e^{-ik/2} [\Theta(r-1) - \Theta(r)]) \right\} + \\
& + U \delta_{r,0} \cdot \left\{ ([12, 12] e^{ikr/2} + [21, 12] e^{-ikr/2}) \Theta(-r) + \right. \\
& \quad \left. + ([12, 21] e^{-ikr/2} + [21, 12] e^{ikr/2}) \Theta(r) \right\} = 0.
\end{aligned} \tag{2.24}$$

As we expected for construction, this equation is always true when $x_1 \neq x_2$. In order to find the relations between the coefficients $[P, Q]$, we apply the continuity condition of the wave function at the boundary $r = 0$ and require that equation (2.24) be satisfied at $r = 0$. From (2.21) we get

$$[12, 12] + [21, 12] = [12, 21] + [21, 21] \tag{2.25}$$

and from (2.24) we get

$$\begin{aligned}
& 2it \cos \left(\frac{K}{2} \right) \sin \left(\frac{k}{2} \right) \{ [12, 12] - [21, 12] + [12, 21] - [21, 21] \} + \\
& + \frac{U}{2} \{ [12, 12] + [21, 12] + [12, 21] + [21, 21] \} = 0.
\end{aligned} \tag{2.26}$$

Using these two equations, we have

$$\begin{pmatrix} [12, 12] \\ [12, 21] \end{pmatrix} = \begin{pmatrix} (u^- - 1) & u^- \\ u^- & (u^- - 1) \end{pmatrix} \begin{pmatrix} [21, 12] \\ [21, 21] \end{pmatrix} \tag{2.27}$$

and

$$\begin{pmatrix} [21, 12] \\ [21, 21] \end{pmatrix} = \begin{pmatrix} (u^+ - 1) & u^+ \\ u^+ & (u^+ - 1) \end{pmatrix} \begin{pmatrix} [12, 12] \\ [12, 21] \end{pmatrix} \tag{2.28}$$

with

$$u^\pm = \frac{2 \cos(K/2) \sin(k/2)}{2 \cos(K/2) \sin(k/2) \pm iU/(2t)}. \tag{2.29}$$

If we define the vector

$$\xi(P) = \begin{pmatrix} [P, Q] \\ [P, Q'] \end{pmatrix} \quad (2.30)$$

indicate with Π_x the permutation operator that interchanges the coordinates of the two particles and introduce the operator

$$Y^\pm = (u^\pm - 1)I + u^\pm \Pi_x \quad (2.31)$$

we can write equation (2.27) and (2.28) as

$$\xi(12) = Y^- \xi(21) \quad (2.32)$$

$$\xi(21) = Y^+ \xi(12). \quad (2.33)$$

We see by the Yang-Baxter relation $Y^+ Y^- = I$ that these two equations are mutually consistent. Using the latter and considering that $\Pi_x [P, Q] = [P, Q']$, we can express all amplitudes $[P, Q]$ in (2.21) in terms of $[12, 12]$ and the wave function $\Psi_{\downarrow\uparrow}(x_1, x_2)$ takes the following form

$$\begin{aligned} \Psi_{\downarrow\uparrow}(R, r) = e^{iKR} \left\{ ([12, 12] e^{ikr/2} + Y^+ [12, 12] e^{-ikr/2}) \Theta(-r) + \right. \\ \left. + (Y^+ \Pi_x [12, 12] e^{ikr/2} + \Pi_x [12, 12] e^{-ikr/2}) \Theta(r) \right\}. \end{aligned} \quad (2.34)$$

2.2.1.1 Singlet and triplet wave functions

The wave function (2.34) has been obtained in the ipotesys that $S^z = 0$, hence the two-particle state could be both a singlet or a triplet state.

Singlet state

A singlet state has total spin $S = 0$ and $S^z = 0$. It has an antisymmetric wave function $\phi_a = (\delta_{\sigma_1\uparrow} \delta_{\sigma_2\downarrow} - \delta_{\sigma_1\downarrow} \delta_{\sigma_2\uparrow}) / \sqrt{2}$:

$$\Pi_\sigma \phi_a = -\phi_a \quad (2.35)$$

where the permutation operator Π_σ interchanges the spin variables. Thus the spatial wave function must be symmetric:

$$\Pi_x \Psi_{\downarrow\uparrow}(R, r) = \Psi_{\downarrow\uparrow}(R, -r) = \Psi_{\downarrow\uparrow}(R, r). \quad (2.36)$$

This implies that $\Pi_x[12, 12] = [12, 12]$ and the singlet wave function has the following form

$$\Psi_{\downarrow\uparrow}(R, r) = [12, 12]e^{iKR} \begin{cases} e^{ikr/2} + (2u^+ - 1)e^{-ikr/2} & r \leq 0 \\ (2u^+ - 1)e^{ikr/2} + e^{-ikr/2} & r \geq 0 \end{cases} \quad (2.37)$$

This can be also rearranged in the following manner

$$\begin{aligned} \Psi_{\downarrow\uparrow}(R, r) &= [12, 12]e^{iKR} \left\{ (2u^+ - 1)e^{ik|r|/2} + e^{-ik|r|/2} \right\} = \\ &= [12, 12]e^{iKR} \left\{ (2u^+ - 1)e^{ik|r|/2} + e^{-ik|r|/2} \right\} = \\ &= [12, 12]e^{iKR} \left\{ 2u^+ \cos\left(\frac{k}{2}r\right) + 2(u^+ - 1)i \sin\left(\frac{k}{2}|r|\right) \right\} = \\ &= \underbrace{[12, 12]e^{iKR} 2u^+}_C \left\{ \cos\left(\frac{k}{2}r\right) + \frac{(u^+ - 1)}{u^+} i \sin\left(\frac{k}{2}|r|\right) \right\} = \\ &= C \left\{ \cos\left(\frac{k}{2}r\right) + \frac{U \csc(k/2)}{2J_K} \sin\left(\frac{k}{2}|r|\right) \right\} \end{aligned} \quad (2.38)$$

with $J_K = 2t \cos(K/2)$.

This wave function is the same obtained by Valiente and Petrosyan in [37] for a state of two bosonic particles in the Hubbard model. Indeed we observe a singlet-state is composed of two fermions with opposite spin and has a symmetric spacial wave function, thus we expect it to behave like a two-boson state.

Triplet state

A triplet state has total spin $S = 1$ and $S^z = 0, \pm 1$. Its wave function ϕ_s has the form

$$\phi_s = \begin{cases} \delta_{\sigma_1\uparrow}\delta_{\sigma_2\uparrow} \\ (\delta_{\sigma_1\uparrow}\delta_{\sigma_2\downarrow} + \delta_{\sigma_1\downarrow}\delta_{\sigma_2\uparrow})/\sqrt{2} \\ \delta_{\sigma_1\downarrow}\delta_{\sigma_2\downarrow} \end{cases} \quad (2.39)$$

and is symmetric:

$$\Pi_\sigma \phi_s = \phi_s. \quad (2.40)$$

Thus the spatial wave function must be antisymmetric. Considering the special case of two electron with opposite spin, we have

$$\Pi_x \Psi_{\downarrow\uparrow}(R, r) = \Psi_{\downarrow\uparrow}(R, -r) = -\Psi_{\downarrow\uparrow}(R, r) \quad (2.41)$$

This yields $\Pi_x[12, 12] = -[12, 12]$ and inserting it into (2.34) we get

$$\Psi_{\downarrow\uparrow}(R, r) = [12, 12]e^{iKR} \{e^{ikr/2} - e^{-ikr/2}\} \quad (2.42)$$

and recover the form (2.20). Since the triplet state is antisymmetric in the electron coordinates, two electrons (and in general two fermions) never sit at the same site and therefore never feel the local interaction. This makes the triplet wave function look like the wave functions of free spinless fermions.

2.2.1.2 Periodic boundary conditions

We are interested in studying a finite system. In particular, we consider a closed chain. Hence we apply periodic boundary conditions to the wave function $\Psi_{\sigma_1\sigma_2}(R, r)$:

$$\Psi_{\sigma_1\sigma_2}(x_2/2, -x_2) = \Psi_{\sigma_1\sigma_2}((L + x_2)/2, L - x_2) \quad (2.43)$$

$$\Psi_{\sigma_1\sigma_2}(x_1/2, x_1) = \Psi_{\sigma_1\sigma_2}((x_1 + L)/2, x_1 - L) \quad (2.44)$$

Because of the antisymmetry it is sufficient to consider the first condition. Applied to (2.34) it gives

$$\begin{aligned} e^{i\frac{K+k}{2}L} \left(Y^+ \Pi_x - e^{-i\frac{K+k}{2}L} \right) [12, 12] e^{i\frac{K-k}{2}x_2} - \\ e^{i\frac{K-k}{2}L} Y^+ \left(Y^- \Pi_x - e^{-i\frac{K-k}{2}L} \right) [12, 12] e^{i\frac{K+k}{2}x_2} = 0 \end{aligned} \quad (2.45)$$

which is satisfied by the condition

$$Y^+ \Pi_x [12, 12] = e^{ik_1 L} [12, 12] \quad (2.46)$$

$$Y^- \Pi_x [12, 12] = e^{-ik_2 L} [12, 12] \quad (2.47)$$

If we are dealing with the singlet state, for which $\Pi_x [12, 12] = [12, 12]$, the previous equations provide the following quantization conditions for the momenta k_1 and k_2

$$e^{ik_1 L} = (2u^+ - 1)^{-1} = \frac{2 \cos(K/2) \sin(k/2) + iU/2t}{2 \cos(K/2) \sin(k/2) - iU/(2t)} \quad (2.48)$$

$$e^{ik_2 L} = 2u^+ - 1 = (2u^- - 1)^{-1} = \frac{2 \cos(K/2) \sin(k/2) - iU/(2t)}{2 \cos(K/2) \sin(k/2) + iU/(2t)}. \quad (2.49)$$

Similarly, in the spin-triplet state, for which $\Pi_x [12, 12] = -[12, 12]$, we obtain the quantization conditions

$$e^{ik_1 L} = e^{ik_2 L} = 1. \quad (2.50)$$

Obviously the same results can be achieved by the application of boundary conditions (2.43) directly to (2.37) and (2.42) for the singlet state and the

triplet state, respectively.

For further calculations, it is useful to introduce a new quantum number, that we call λ . In general we need a second set of quantum numbers that characterize the spin degrees of freedom. This set is composed of M elements, if M is the number of down spins. Hence, in this case we have only one element. We rewrite equations (2.48) and (2.49) in terms of k_1 and k_2 , substituting the expressions for $K = k_1 + k_2$ and $k = k_1 - k_2$:

$$e^{ik_1L} = (2u_{12} - 1)^{-1} = \frac{\sin k_1 - \sin k_2 + iU/(2t)}{\sin k_1 - \sin k_2 - iU/(2t)} \quad (2.51)$$

$$e^{ik_2L} = 2u_{12} - 1 = (2u_{21} - 1)^{-1} = \frac{\sin k_2 - \sin k_1 + iU/(2t)}{\sin k_2 - \sin k_1 - iU/(2t)}. \quad (2.52)$$

Introducing $\lambda = (\sin k_1 + \sin k_2)/2$ these become

$$e^{ik_1L} = \frac{\lambda - \sin k_1 - iU/(4t)}{\lambda - \sin k_1 + iU/(4t)} \quad (2.53)$$

$$e^{ik_2L} = \frac{\lambda - \sin k_2 - iU/(4t)}{\lambda - \sin k_2 + iU/(4t)} \quad (2.54)$$

and their product satisfies

$$\frac{\lambda - \sin k_1 - iU/(4t)}{\lambda - \sin k_1 + iU/(4t)} \cdot \frac{\lambda - \sin k_2 - iU/(4t)}{\lambda - \sin k_2 + iU/(4t)} = 1. \quad (2.55)$$

2.2.2 Bound states in the thermodynamic limit

Here we want to study the bound solutions in the thermodynamic limit, that is to say $L \rightarrow \infty$. Indeed, in this case we may obtain some simplified and more intuitive expressions for the wave functions and the energies.

For the triplet state, the on-site interaction has no physical effect, since the Pauli principle prevents the two particles from occupying the same site. Hence the wave function (2.20) is similar to that of two free fermions. Hence a bound state may not exist. We can easily see this result from the boundary condition (2.50)

$$e^{ik_1L} = e^{ik_2L} = 1. \quad (2.56)$$

A bound state has a relative momentum k with a non-null imaginary part. In particular, for this model, the real part of k is 0 or $\pm\pi$ when the imaginary part is not zero. Thus we may identify the scattering solutions as having a

real momentum k and the bound solutions as having an imaginary momentum $k = -i2\alpha$ or $k = \pm\pi - i2\alpha$, with $\alpha \in \mathbb{R}$. Substituting this value into equation (2.56), we get an equation with no possible solutions.

For the singlet state, the wave function is the (2.37) and can be written as

$$\chi^S(R, r) = e^{iKR} A_1 \left\{ e^{-ik|r|/2} + \frac{A_2}{A_1} e^{ik|r|/2} \right\} \quad (2.57)$$

with

$$\frac{A_2}{A_1} = 2u^+ - 1 = \frac{2J_K \sin(k/2) - iU}{2J_K \sin(k/2) + iU}, \quad J_K = 2t \cos(K/2). \quad (2.58)$$

From the periodic boundary condition (2.49), we get

$$\frac{J_K(e^{ik/2} - e^{-ik/2}) + U}{J_K(e^{ik/2} - e^{-ik/2}) - U} = e^{i\pi n} e^{-ikL/2}. \quad (2.59)$$

Since we are searching for the bound solutions, we set $k/2 = -i\alpha$ or $k/2 = \pm\pi - i\alpha$, with $\alpha \in \mathbb{R}^+$ (it is the same if we take $\alpha \in \mathbb{R}^-$). Hence the previous equation becomes

$$\frac{\pm J_K(e^\alpha - e^{-\alpha}) + U}{\pm J_K(e^\alpha - e^{-\alpha}) - U} = \pm e^{i\pi n} e^{-\alpha L} \xrightarrow{L \rightarrow \infty} 0. \quad (2.60)$$

Thus, imposing that the numerator vanishes, we found a quadratic equation for $\alpha_K = \pm e^{-\alpha}$

$$\alpha_K^2 - \frac{U}{J_K} \alpha_K - 1 = 0 \quad (2.61)$$

which yields

$$\alpha_K = \frac{U}{2J_K} \pm \sqrt{\left(\frac{U}{2J_K}\right)^2 + 1}. \quad (2.62)$$

Since we are assuming $\alpha \in \mathbb{R}^+$, we should have $e^{-\alpha} < 1$ and we should exclude the case $U = 0$. Hence the plus sign in equation (2.62) applies for an attractive interaction $U < 0$ and the minus sign applies for a repulsive interaction $U > 0$.

We may also found the explicit expression for the wave function. Since $k/2 = -i\alpha$ or $k/2 = \pm\pi - i\alpha$ and $A_2/A_1 \rightarrow 0$ in the thermodynamic limit, the (2.57) reduces to a decaying exponential

$$\chi_r^S = \pm C e^{-\alpha|r|} = C \alpha_K^{|r|} \quad (2.63)$$

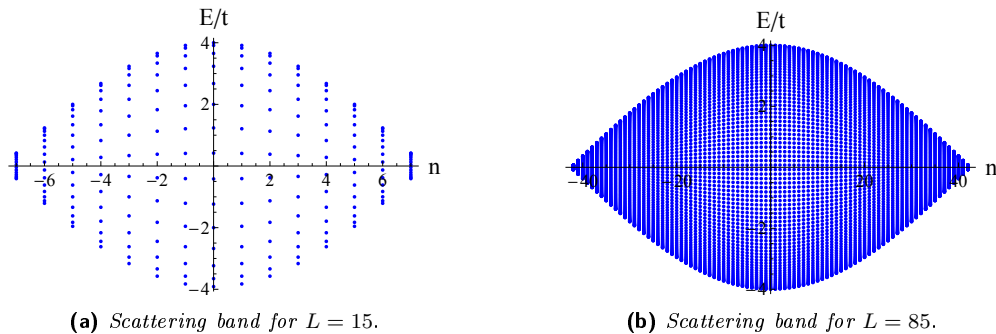


Figure 2.1: Lower energy band for the triplet state in a lattice with $L = 15$ and $L = 85$ sites, respectively. For the triplet state a bound state doesn't exist, since the contact interaction has no physical effect, and only the scattering states appear. The energy is plotted as a function of the integer n that quantizes the centre-of-mass momentum $K = 2\pi n/L$. For each value of n , there are L scattering states, which correspond to different values of the relative momentum $k/2$. In the first Brillouin zone $K \in [-\pi, \pi]$, depicted in the figure, the lower band edge corresponds to $k/2 = 0$ and the upper band edge corresponds to $k/2 = \pi$; in the adjacent region $K \in [\pi, 3\pi]$ it is the opposite.

where C is a normalization constant. We finally calculate the energy

$$E = -2J_K \cos(k/2) = -J_K \left(\alpha_K + \frac{1}{\alpha_K} \right) = \text{sgn}(U) \sqrt{U^2 + (2J_K)^2}. \quad (2.64)$$

In figure 2.1 the lower energy band is plotted for the triplet state in a lattice with $L = 15$ and $L = 85$ sites, respectively. We notice that, obviously, these are all scattering states. In figure 2.2 the energies for a singlet state in the same lattice is plotted, with a contact interaction strength $U/t = 2$. In this case, L bound states appear, one for each permitted value of the centre-of-mass momentum. As L is increased, these dots form a continuum curve, which is that expressed by (2.64). We notice that the bound states exist for a repulsive interaction and that they lie above the scattering band. These states exist for each value of the interaction strength and lie under the scattering band if the interaction is attractive. We finally observe that the density of states is higher at the edges of the band, when $k/2$ approaches 0 or π and at the edges of the first Brillouin zone, when K approaches $\pm\pi$.

2.2.3 The many-particle case

In this section we generalize the previous results to an arbitrary number of fermions. As mentioned before, the first who found the one-dimensional Hubbard model is solvable by the Bethe-ansatz method were Lieb and Wu [35], just after the discovery for spin 1/2 delta-function fermions by Gaudin

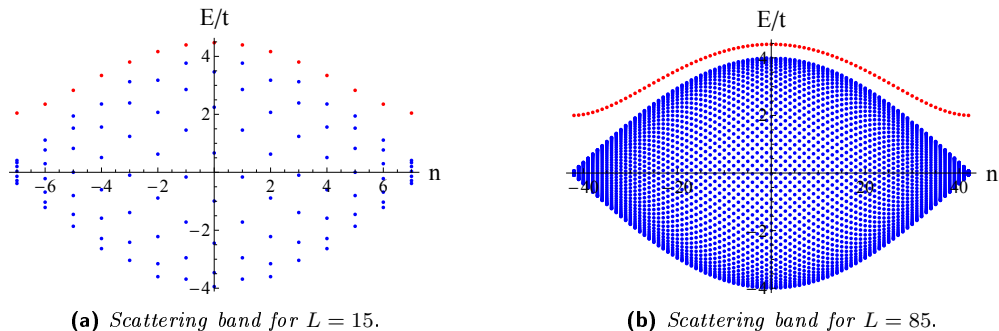


Figure 2.2: Lower energy band for the singlet state in a lattice with $L = 15$ and $L = 85$ sites, respectively, and with a contact interaction strength $U/t = 2$. The blue dots form the scattering states, as in the triplet case; the red dots represent the bound states.

[31] and Yang [30]. Their work is based on the *nested Bethe ansatz* which requires a consistent factorization of multi-particle scattering processes into two-particle ones.

The eigenstates of the Hubbard Hamiltonian (2.10) for a N -particle system can be written as

$$|\Psi\rangle = \frac{1}{N!} \sum_{x_1, \dots, x_N=1}^L \sum_{\sigma_1, \dots, \sigma_N=\uparrow, \downarrow} \psi_\sigma(x_1, \dots, x_N) |x_1 \sigma_1, \dots, x_N \sigma_N\rangle \quad (2.65)$$

and eigenvalue equation (2.15) in the first quantization representation generalizes to

$$-t \sum_{j=1}^N \sum_{n=\pm 1} \psi_\sigma(x_1, x_2, \dots, x_j + n, \dots, x_N) + (U \sum_{j < l} \delta_{jl} - E) \psi_\sigma(x_1, x_2, \dots, x_N) = 0. \quad (2.66)$$

where $\sigma = (\sigma_1, \sigma_2, \dots, \sigma_N)$ indicates the wave function depends on the fermions' spins. If N is the total number of electrons and M is the number of down-spin electrons, we assume $2M \leq N \leq L$ (the other cases are obtained from symmetry arguments). We also assume that the $1, 2, \dots, M$ -th electrons have down spins and that the others have up spins. In the sector $x_{Q_1} \leq x_{Q_2} \leq \dots \leq x_{Q_N}$, the Bethe ansatz imposes the following expression for the wave function

$$\psi_\sigma(x_1, x_2, \dots, x_N) = \sum_P [P, Q] e^{i \sum_{j=1}^N k_{P_j} x_{Q_j}} \quad (2.67)$$

where $P = (P_1, \dots, P_N)$ s and $Q = (Q_1, \dots, Q_N)$ s are permutations of the integers $1, 2, \dots, N$. As for the two-particle case, the energy eigenvalue is the

sum of the energies of the N free particles

$$E = -2t \sum_{j=1}^N \cos k_j \quad (2.68)$$

and so the total momentum

$$K = \sum_{j=1}^N k_j. \quad (2.69)$$

As we treat spin 1/2 fermions on the lattice we only consider two-body scattering by these particles. The procedure is the same as the previous case; the only difference is that we can't define a relative coordinate. From the continuity condition on the boundary of the regions we get some relations between coefficients:

$$[P, Q] = (u_{P_{j+1}P_j} - 1)[P', Q] + u_{P_{j+1}P_j}[P', Q'] \quad (2.70)$$

for $j = 1, 2, \dots, N-1$, where $Q' = (Q_1, \dots, Q_{j+1}, Q_j, \dots, Q_N)$ and $P' = (P_1, \dots, P_{j+1}, P_j, \dots, P_N)$ are permutations of the coordinate indices Q_j, Q_{j+1} and momentum indices P_j, P_{j+1} , respectively; while

$$u_{nm} = \frac{\sin k_n - \sin k_m}{\sin k_n - \sin k_m + iU/(2t)} \quad (2.71)$$

that is the same as (2.29), if we substitute the expressions for K and k : $K = k_1 + k_2$ and $k = k_1 - k_2$. We can regard the coefficients $[Q, P]$ as an elements of an $N! \times N!$ matrix. Then equation (2.70) can be rewritten as

$$\xi_P = Y_{P_{j+1}P_j}^{jj+1} \xi_{P'}, \quad Y_{kl}^{ab} = (u_{kl} - 1)I + u_{kl}\Pi_x^{ab} \quad (2.72)$$

where ξ_P is a column vector for a fixed permutation P of momenta and its elements differ from each other by a permutation Q of coordinates; while Π_x^{ab} is a permutation operator that exchanges elements a and b of the array on which it acts. The label x indicates that it acts only on the coordinates of the particles. For example, if $\tilde{Q} = (\tilde{Q}_1, \tilde{Q}_2, \dots, \tilde{Q}_N) = (5, 7, \dots, N)$, the operator Π_x^{12} acts on $[\tilde{P}, \tilde{Q}]$ in the following way

$$\Pi_x^{12}[\tilde{P}, \tilde{Q}] = [\tilde{P}, \tilde{Q}'], \quad \text{with } \tilde{Q}' = (\tilde{Q}_2, \tilde{Q}_1, \dots, \tilde{Q}_N) = (7, 5, \dots, N) \quad (2.73)$$

and we can write the permutation \tilde{Q}' as $\tilde{Q}' = \tilde{Q}\Pi^{12}$ where we have omitted the label x because there isn't ambiguity. Between Y -operators there exist the so-called Yang-Baxter relations:

$$Y_{ij}^{ab}Y_{ji}^{ab} = I, \quad Y_{jk}^{ab}Y_{ik}^{bc}Y_{ij}^{ab} = Y_{ij}^{bc}Y_{ik}^{ab}Y_{jk}^{bc}. \quad (2.74)$$

Fermionic symmetry requirements imply that the coefficients $[P, Q]$ must be antisymmetric for the exchange of two electrons with the same spin. This reduces the number of coefficients we have to determine. Following the same procedure of the two-particle case, one finally finds the so-called Lieb-Wu equations from the periodic boundary conditions

$$e^{ik_j L} = \prod_{\ell=1}^M \frac{\lambda_\ell - \sin k_j - iU/(4t)}{\lambda_\ell - \sin k_j + iU/(4t)} \quad (2.75)$$

$$\prod_{j=1}^N \frac{\lambda_\ell - \sin k_j - iU/(4t)}{\lambda_\ell - \sin k_j + iU/(4t)} = \prod_{m=1, m \neq \ell}^M \frac{\lambda_\ell - \lambda_m - 2iU/(2t)}{\lambda_\ell - \lambda_m + iU/(2t)}$$

with $j = 1, \dots, N$ and $\ell = 1, \dots, M$.

Solving these equations give the possible values of the quantum numbers k_j and λ_ℓ . For more details see ref. [5, 36, 7].

The reason for which the N -particle problem in the one-dimensional Hubbard model can be exactly solved is that it is an integrable model. Definition of integrability for quantum systems of finite dimensionality with no classical limit, such as a spin chain, is not trivial. For a system that support scattering, such as the Hubbard model, we can identify the concept of *integrability* with that of *non-diffractivity*. This means that the true N -body scattering, which makes the asymptotic wave function deviate from a plane wave, vanishes. Hence, if a system supports scattering and is integrable, the N -body scattering is just a succession of two-body scattering, which is built into the asymptotic Bethe ansatz [7].

Chapter 3

Two-body solutions for the extended Hubbard model

Here we want to find two-body solutions for the extended Hubbard model involving longer range interactions between the particles on the neighbouring lattice sites. In general, this model cannot be handled with the Bethe ansatz in its standard form. However the same procedure can be followed if we adjust the ansatz for the wave function to suit this case. The problem has been solved by Valiente and Petrosyan [38] for two bosonic particles with the first nearest-neighbor interaction, in the thermodynamic limit. We consider the fermionic case in which the problem is made more complicated by the presence of the spin. Moreover we also calculate the solutions of the model with an additional interaction term between the second neighbors. In the next chapter we will show explicit results also for a lattice of finite size.

We start by adding to the Hubbard Hamiltonian (2.10) an interaction term between the first nearest-neighbors. Then we also consider the interaction between the second nearest-neighbors.

3.1 First-neighbor interaction

We consider two fermions in a one-dimensional lattice of size L and assume particles can move from one site to first nearest-neighbors and interact with each other only if they are on the same site or on adjacent sites. The Hamiltonian is

$$H = -t \sum_i \sum_{\sigma} (c_{i\sigma}^{\dagger} c_{i+1\sigma} + c_{i+1\sigma}^{\dagger} c_{i\sigma}) + U \sum_i (n_{i\uparrow} n_{i\downarrow}) + V \sum_i n_i n_{i+1} \quad (3.1)$$

and we want to solve the eigenvalue equation

$$H|\Psi\rangle = E|\Psi\rangle. \quad (3.2)$$

The two-particle state is again of the form (2.11):

$$\begin{aligned} |\Psi\rangle &= \frac{1}{2} \sum_{x_1, x_2=1}^L \sum_{\sigma_1, \sigma_2=\uparrow, \downarrow} \psi_{\sigma_1 \sigma_2}(x_1, x_2) |x_1 \sigma_1, x_2 \sigma_2\rangle = \\ &= \frac{1}{2} \sum_{x_1, x_2=1}^L \sum_{\sigma_1, \sigma_2=\uparrow, \downarrow} \psi_{\sigma_1 \sigma_2}(x_1, x_2) |\sigma_1, \sigma_2\rangle |x_1, x_2\rangle = \\ &= \frac{1}{2} \sum_{x_1, x_2=1}^L \sum_{S, S^z} \chi_{ss^z}(x_1, x_2) |S, S^z\rangle |x_1, x_2\rangle \end{aligned} \quad (3.3)$$

where, passing from the first line to the second we have expressed the same thing in an equivalent notation; while from the second line to the third we have made use of the following change of basis in spin space:

$$|S, S^z\rangle = \sum_{\sigma_1, \sigma_2} \phi^{ss^z}(\sigma_1, \sigma_2) |\sigma_1, \sigma_2\rangle \quad (3.4)$$

so that

$$\psi_{\sigma_1, \sigma_2}(x_1, x_2) = \sum_{S, S^z} \chi_{ss^z}(x_1, x_2) \phi^{ss^z}(\sigma_1, \sigma_2) = \chi(x_1, x_2) \phi(\sigma_1, \sigma_2). \quad (3.5)$$

Here S is the total spin of the two-particle system and S^z is its projection onto the z-axis. $\phi^{ss^z}(\sigma_1, \sigma_2)$ is the spin wave function:

$$\text{triplet state: } \phi_s = \begin{cases} \phi^{11}(\sigma_1, \sigma_2) = \delta_{\sigma_1, \uparrow} \delta_{\sigma_2, \uparrow} \\ \phi^{10}(\sigma_1, \sigma_2) = \frac{1}{\sqrt{2}} (\delta_{\sigma_1, \uparrow} \delta_{\sigma_2, \downarrow} + \delta_{\sigma_1, \downarrow} \delta_{\sigma_2, \uparrow}) \\ \phi^{1-1}(\sigma_1, \sigma_2) = \delta_{\sigma_1, \downarrow} \delta_{\sigma_2, \downarrow} \end{cases} \quad (3.6)$$

$$\text{singlet state: } \phi_a = \phi^{00}(\sigma_1, \sigma_2) = \frac{1}{\sqrt{2}} (\delta_{\sigma_1, \uparrow} \delta_{\sigma_2, \downarrow} - \delta_{\sigma_1, \downarrow} \delta_{\sigma_2, \uparrow}).$$

Transformation (3.5) will be useful when we make the ansatz on the wave function. Now we can proceed in two equivalent ways:

1. we write the Hamiltonian (3.1) in terms of projection operators $|x \sigma, x' \sigma'\rangle\langle x \sigma, x' \sigma'|$

$$\begin{aligned}
H = & -t \sum_{x'_1} \sum_{\sigma'_1} (|x'_1 \sigma'_1\rangle\langle x'_1 + 1 \sigma'_1| + |x'_1 + 1 \sigma'_1\rangle\langle x'_1 \sigma'_1|) + \\
& -t \sum_{x'_2} \sum_{\sigma'_2} (|x'_2 \sigma'_2\rangle\langle x'_2 + 1 \sigma'_2| + |x'_2 + 1 \sigma'_2\rangle\langle x'_2 \sigma'_2|) + \\
& + \frac{U}{2} \sum_{x'_1, x'_2} \sum_{\sigma'_1, \sigma'_2} \delta_{x'_1, x'_2} \delta_{\sigma'_1, \sigma'_2} |x'_1 \sigma'_1, x'_2 \sigma'_2\rangle\langle x'_1 \sigma'_1, x'_2 \sigma'_2| + \\
& + \frac{V}{2} \sum_{x'_1, x'_2} \sum_{\sigma'_1, \sigma'_2} (\delta_{x'_2, x'_1+1} + \delta_{x'_2, x'_1-1}) |x'_1 \sigma'_1, x'_2 \sigma'_2\rangle\langle x'_1 \sigma'_1, x'_2 \sigma'_2|
\end{aligned} \tag{3.7}$$

where

$$\langle x'_1 \sigma'_1, x'_2 \sigma'_2 | x_1 \sigma_1, x_2, \sigma_2 \rangle = \delta_{x'_1, x_1} \delta_{x'_2, x_2} \delta_{\sigma'_1, \sigma_1} \delta_{\sigma'_2, \sigma_2} - \delta_{x'_1, x_2} \delta_{x'_2, x_1} \delta_{\sigma'_1, \sigma_1} \delta_{\sigma'_2, \sigma_2}; \tag{3.8}$$

2. we write the state (3.3) in terms of creation operators $c_{x\sigma}^\dagger$

$$|\Psi\rangle = \frac{1}{2} \sum_{x_1, x_2=1}^L \sum_{\sigma_1, \sigma_2=\uparrow, \downarrow} \psi_{\sigma_1 \sigma_2}(x_1, x_2) c_{x_2 \sigma_2}^\dagger c_{x_1 \sigma_1}^\dagger |0\rangle. \tag{3.9}$$

Then we apply Hamiltonian (3.7) to the state (3.3) or Hamiltonian (3.1) to the state (3.9). In both cases we obtain the following eigenvalue equation

$$\begin{aligned}
& -t[\psi_{\sigma_1 \sigma_2}(x_1 + 1, x_2) + \psi_{\sigma_1 \sigma_2}(x_1 - 1, x_2) + \psi_{\sigma_1 \sigma_2}(x_1, x_2 + 1) + \psi_{\sigma_1 \sigma_2}(x_1, x_2 - 1)] \\
& + [U\delta_{x_1, x_2} + V(\delta_{x_2, x_1+1} + \delta_{x_2, x_1-1}) - E]\psi_{\sigma_1 \sigma_2}(x_1, x_2) = 0.
\end{aligned} \tag{3.10}$$

Introducing the centre of mass $R = \frac{x_1+x_2}{2}$ and relative $r = x_1 - x_2$ coordinates and the momenta $K = k_1 + k_2$ and $k = k_1 - k_2$, it becomes

$$\begin{aligned}
& -t[\psi_{\sigma_1 \sigma_2}\left(R + \frac{1}{2}, r + 1\right) + \psi_{\sigma_1 \sigma_2}\left(R - \frac{1}{2}, r - 1\right) + \psi_{\sigma_1 \sigma_2}\left(R + \frac{1}{2}, r - 1\right) + \\
& \psi_{\sigma_1 \sigma_2}\left(R - \frac{1}{2}, r + 1\right)] + [U\delta_{r,0} + V(\delta_{r,-1} + \delta_{r,1}) - E]\psi_{\sigma_1 \sigma_2}(R, r) = 0.
\end{aligned} \tag{3.11}$$

As in the previous case, we need four function to represent an eigenstate of the two $S = 1/2$ particles system:

$$\psi_{\uparrow\uparrow}(R, r), \psi_{\uparrow\downarrow}(R, r), \psi_{\downarrow\uparrow}(R, r), \psi_{\downarrow\downarrow}(R, r). \tag{3.12}$$

Each of them must satisfy an equation of the form (3.11). In order to find the explicit form of the state (3.3), we pass from $\psi_{\sigma_1\sigma_2}(R, r)$ functions to $\chi_{ssz}(R, r)$ functions through transformation (3.5). Eigenvalue equation for χ_{11} and χ_{1-1} are the same as that for $\psi_{\uparrow\uparrow}$ and $\psi_{\downarrow\downarrow}$, respectively. Summing the eigenvalue equation for $\psi_{\uparrow\downarrow}$ and that for $\psi_{\downarrow\uparrow}$, we get an equation for χ_{10} ; while subtracting them we get an equation for χ_{00} . Each equation is of the form (3.11).

We now distinguish between two different cases: the triplet state and the singlet state. This means that we are working with two different sectors, in which the total spin is $S = 1$ and $S = 0$, respectively. So we make two different ansatz for the wave functions.

We begin by remembering that the fermion's wave function must be antisymmetric. So the spacial wave function must be antisymmetric for the triplet state and symmetric for the singlet state; the following relations must be true:

$$\chi_{11}(R, r) = \chi_{1-1}(R, r) = \chi_{10}(R, r) = \chi^A(R, r) \quad (3.13)$$

$$\chi_{00}(R, r) = \chi^S(R, r) \quad (3.14)$$

with

$$\chi^A(R, -r) = -\chi^A(R, r) \quad (3.15)$$

$$\chi^S(R, -r) = \chi^S(R, r) \quad (3.16)$$

Thus we obtain $\chi^A(R, r) = 0$. This means in this case the on-site interaction has no physical effect.

We make the following ansatz on the wave function:

$$\begin{aligned} \chi^A(R, r) &= \sum_P [P, Q] e^{i(k_{P_1} x_{Q_1} + k_{P_2} x_{Q_2})} \quad \text{with } x_{Q_1} \leq x_{Q_2} \\ &= ([12, 12] e^{i(k_1 x_1 + k_2 x_2)} + [21, 12] e^{i(k_2 x_1 + k_1 x_2)}) \Theta(x_2 - x_1) + \\ &+ ([12, 21] e^{i(k_1 x_2 + k_2 x_1)} + [21, 21] e^{i(k_2 x_2 + k_1 x_1)}) \Theta(x_1 - x_2) = \quad (3.17) \\ &= e^{iKR} \left\{ ([12, 12] e^{ikr/2} + [21, 12] e^{-ikr/2}) \Theta(-r) + \right. \\ &\quad \left. + ([12, 21] e^{-ikr/2} + [21, 21] e^{ikr/2}) \Theta(r) \right\} \end{aligned}$$

that, because of the antisymmetry, becomes

$$\begin{aligned} \chi^A(R, r) &= e^{iKR} \left\{ -([12, 21] e^{ikr/2} + [21, 21] e^{-ikr/2}) \Theta(-r) + \right. \\ &\quad \left. + ([21, 21] e^{ikr/2} + [12, 21] e^{-ikr/2}) \Theta(r) \right\} = \quad (3.18) \\ &= \text{sgn}(r) e^{iKR} ([21, 21] e^{ik|r|/2} + [12, 21] e^{-ik|r|/2}). \end{aligned}$$

where $\Theta(r)$ is the Heaviside function, with $\Theta(r) = 1/2$ at $r = 0$. Inserting it into eigenvalue equation (3.11) and after a little algebra, we get

$$\begin{aligned}
& -4t \cos\left(\frac{K}{2}\right) \cos\left(\frac{k}{2}\right) \left\{ - ([12, 21]e^{ikr/2} + [21, 21]e^{-ikr/2}) \Theta(-r) + \right. \\
& \quad \left. + ([21, 21]e^{ikr/2} + [12, 21]e^{-ikr/2}) \Theta(r) \right\} + \\
& -E \left\{ - ([12, 21]e^{ikr/2} + [21, 21]e^{-ikr/2}) \Theta(-r) + \right. \\
& \quad \left. + ([21, 21]e^{ikr/2} + [12, 21]e^{-ikr/2}) \Theta(r) \right\} + \\
& -2t \cos\left(\frac{K}{2}\right) \left\{ - ([12, 21]e^{ik(r+1)/2} + [21, 21]e^{-ik(r+1)/2}) [\Theta(-r-1) - \Theta(-r)] + \right. \\
& \quad + ([21, 21]e^{ik(r+1)/2} + [12, 21]e^{-ik(r+1)/2}) [\Theta(r+1) - \Theta(r)] + \\
& \quad - ([12, 21]e^{ik(r-1)/2} + [21, 21]e^{-ik(r-1)/2}) [\Theta(-r+1) - \Theta(-r)] + \\
& \quad \left. + ([21, 21]e^{ik(r-1)/2} + [12, 21]e^{-ik(r-1)/2}) [\Theta(r-1) - \Theta(r)] \right\} + \\
& + V(\delta_{r,-1} + \delta_{r,1}) \left\{ - ([12, 21]e^{ikr/2} + [21, 21]e^{-ikr/2}) \Theta(-r) + \right. \\
& \quad \left. + ([21, 21]e^{ikr/2} + [12, 21]e^{-ikr/2}) \Theta(r) \right\} = 0.
\end{aligned} \tag{3.19}$$

Inserting the expression for the energy $E = -4t \cos(K/2) \cos(k/2)$, the first four lines cancel each other out. The remaining equation is always satisfied at $r \neq \pm 1$ and, calculated at $r = \pm 1$, gives a relation between the coefficients:

$$\frac{[21, 21]}{[12, 21]} = -\frac{2t \cos(K/2) + Ve^{-ik/2}}{2t \cos(K/2) + Ve^{ik/2}}. \tag{3.20}$$

In the case in which the two particles have opposite spin, we can't make the same ansatz (3.17) on the wave function because there would be too many restrictions on the coefficients, provided by the symmetry condition and by the requirement for eigenvalue equation (3.11) to be satisfied at $r = 0$ and at $r = \pm 1$. So we use the following form

$$\chi^S(R, r) = e^{iKR} \begin{cases} [12, 12]e^{ikr/2} + [21, 12]e^{-ikr/2} & \text{if } r \leq -1 \\ A_0 & \text{if } r = 0 \\ [12, 21]e^{-ikr/2} + [21, 21]e^{ikr/2} & \text{if } r \geq 1 \end{cases} \tag{3.21}$$

If we require that the wave function be symmetric, we get $[12, 21] = [12, 12]$ and $[21, 21] = [21, 12]$. In order to simplify the notation, we define $[12, 12] =$

A_1 and $[21, 12] = A_2$. Thus the wave function is

$$\chi^S(R, r) = e^{iKR} \begin{cases} A_1 e^{-ik|r|/2} + A_2 e^{ik|r|/2} & \text{if } r \neq 0 \\ A_0 & \text{if } r = 0 \end{cases} \quad (3.22)$$

When $r \neq 0, \pm 1$, eigenvalue equation (3.11) is satisfied if

$$E = -4t \cos(K/2) \cos(k/2). \quad (3.23)$$

We require that the equation be satisfied also at $r = 0$ and at $r = \pm 1$. We get the following system of equations

$$\begin{cases} -4t \cos\left(\frac{K}{2}\right) (A_1 e^{-ik/2} + A_2 e^{ik/2}) + (U - E)A_0 = 0 \\ -2t \cos\left(\frac{K}{2}\right) (A_1 e^{-ik} + A_2 e^{ik} + A_0) + (V - E) \{A_1 e^{-ik/2} + A_2 e^{ik/2}\} = 0 \end{cases} \quad (3.24)$$

From the first equation we get

$$A_0 = \frac{2J_K (A_1 e^{-ik/2} + A_2 e^{ik/2})}{U + 2J_K \cos(k/2)} \quad (3.25)$$

where $J_K = 2t \cos(K/2)$. Inserting it into the second equation, we get

$$\begin{aligned} e^{-ik/2} \left(e^{ik/2} - \frac{2J_K}{U + 2J_K \cos(k/2)} + \frac{V}{J_K} \right) A_1 + \\ e^{ik/2} \left(e^{-ik/2} - \frac{2J_K}{U + 2J_K \cos(k/2)} + \frac{V}{J_K} \right) A_2 = 0. \end{aligned} \quad (3.26)$$

Separating real part and imaginary part in the factors that multiply A_1 and A_2 , we get

$$\frac{A_2}{A_1} = -\frac{x - iy}{x + iy} = e^{i2\delta} \quad (3.27)$$

with

$$x = 1 - \frac{2J_K \cos(k/2)}{U + 2J_K \cos(k/2)} + \frac{V \cos(k/2)}{J_K} \quad (3.28)$$

$$y = \left(-\frac{2J_K}{U + 2J_K \cos(k/2)} + \frac{V}{J_K} \right) \sin(k/2). \quad (3.29)$$

We observe that A_2/A_1 is a phase factor, since it is the ratio between a number and its complex conjugate. We can define the phase shift δ through

$$\tan \delta = \sqrt{\frac{1 - \cos(2\delta)}{1 + \cos(2\delta)}} = \frac{x}{y} = \frac{J_K U + (2J_K \cos(k/2) + U)V \cos(k/2)}{[UV - 2J_K(J_K - V \cos(k/2))] \sin(k/2)} \quad (3.30)$$

If we also define the phase shift δ_0 for $V = 0$

$$\tan \delta_0 = -\frac{U}{2J_K \sin(k/2)}, \quad (3.31)$$

we can write

$$A_0 = \cos \delta_0 \frac{\cos(k + \delta)}{\cos(k + \delta_0)}. \quad (3.32)$$

So the wave function is

$$\chi^S(R, r) = C e^{iKR} \begin{cases} \cos\left(\frac{kr}{2} + \delta\right) & \text{if } r \neq 0 \\ \frac{\cos \delta_0}{\cos(k/2 + \delta)} \cos\left(\frac{k}{2} + \delta_0\right) & \text{if } r = 0 \end{cases} \quad (3.33)$$

We observe that this result is the same obtained by Valiente and Petrosyan for the bosonic case [38], while the wave function of the triplet state is the same obtained for spinless fermions.

3.1.1 Periodic boundary conditions

We impose periodic boundary conditions on the wave function:

$$\chi\left(\frac{x_2}{2}, -x_2\right) = \chi\left(\frac{L+x_2}{2}, L-x_2\right); \quad \chi\left(\frac{x_2+1}{2}, 1-x_2\right) = \chi\left(\frac{L+1+x_2}{2}, L+1-x_2\right) \quad (3.34)$$

$$\chi\left(\frac{x_1}{2}, x_1\right) = \chi\left(\frac{L+x_1}{2}, x_1-L\right); \quad \chi\left(\frac{x_1+1}{2}, x_1-1\right) = \chi\left(\frac{x_1+L+1}{2}, x_2-L-1\right) \quad (3.35)$$

Because of the symmetry or the antisymmetry it is sufficient to consider one pair of equations. We consider equations (3.34). Both of them give the same result. So we apply only the first condition.

Triplet state In the case of the triplet state, the first equation (3.34) gives

$$e^{iKx_2/2} \left\{ \left([21, 21] + e^{i(K-k)L/2} [12, 21] \right) e^{ikx_2/2} + \left([12, 21] + e^{i(K+k)L/2} [21, 21] \right) e^{-ikx_2/2} \right\} = 0 \quad (3.36)$$

from which we get

$$-[12, 21] = e^{i(K+k)L/2} [21, 21] \quad (3.37)$$

$$-[21, 21] = e^{i(K-k)L/2} [12, 21] \quad (3.38)$$

and hence

$$\frac{[21, 21]}{[12, 21]} = -e^{-i(K+k)L/2} = -e^{i(K-k)L/2} = -\frac{2t \cos(K/2) + V e^{-ik/2}}{2t \cos(K/2) + V e^{ik/2}}. \quad (3.39)$$

The second equivalence gives a quantization condition on the centre of mass momentum: $K = \frac{2\pi n}{L}$. For each value of K , the third equivalence is an equation whose solutions give all possible values of the relative momentum k .

Singlet state In this case we have

$$e^{iKx_2/2} \left\{ (A_2 - e^{i(K-k)L/2} A_1) e^{ikx_2/2} + (A_1 - e^{i(K+k)L/2} A_2) e^{-ikx_2/2} \right\} = 0 \quad (3.40)$$

from which we get

$$\frac{A_2}{A_1} = e^{-i(K+k)L/2} = e^{i(K-k)L/2} = e^{i2\delta}. \quad (3.41)$$

So the quantization rule on K is the same as in triplet state. We can verify that this is also the required condition when the two particles are on the same site at the edge of the chain.

3.2 Second-neighbor interaction

We generalize further the problem with the addition of a second-neighbor interaction term to Hamiltonian (3.1). So it takes the form

$$H = -t \sum_i \sum_{\sigma} (c_{i\sigma}^{\dagger} c_{i+1\sigma} + c_{i+1\sigma}^{\dagger} c_{i\sigma}) + U \sum_i (n_{i\uparrow} n_{i\downarrow}) + V_1 \sum_i n_i n_{i+1} + V_2 \sum_i n_i n_{i+2}. \quad (3.42)$$

The procedure we apply is the same as before, but we need an ansatz with a great number of coefficients, because now we have an additional condition to be satisfied. It is the eigenvalue equation at $r = \pm 2$.

The two-particle state is the (3.3). Applying the Hamiltonian (3.42) to it, we get the eigenvalue equation (3.11), with an extra term. For the symmetric χ^S and antisymmetric χ^A wave functions, it is

$$\begin{aligned} & -t \left[\chi^{\alpha} \left(R + \frac{1}{2}, r + 1 \right) + \chi^{\alpha} \left(R - \frac{1}{2}, r - 1 \right) + \chi^{\alpha} \left(R + \frac{1}{2}, r - 1 \right) + \right. \\ & \left. \chi^{\alpha} \left(R - \frac{1}{2}, r + 1 \right) \right] + [U \delta_{r,0} + V_1 (\delta_{r,-1} + \delta_{r,1}) + V_2 (\delta_{r,-2} + \delta_{r,2}) - E] \chi^{\alpha}(R, r) = 0 \end{aligned} \quad (3.43)$$

with $\alpha = S, A$.

Let us consider the antisymmetric wave function, that is to say the triplet state. We need to add a coefficient to the ansatz (3.18). So we make the following ansatz

$$\chi^A(R, r) = e^{iKR} \underbrace{\text{sgn}(r) \{A_1 e^{-ik|r|/2} + A_2 e^{ik|r|/2} + C(|r|)\}}_{\chi^A(r)} \quad (3.44)$$

with

$$C(|r|) = \begin{cases} A_3 & \text{for } |r| = 1 \\ 0 & \text{otherwise} \end{cases} \quad (3.45)$$

Inserting it into eigenvalue equation, it reduces to

$$-J_K[\chi^A(r+1) + \chi^A(r-1)] + [V_1(\delta_{r,1} + \delta_{r,-1}) + V_2(\delta_{r,2} + \delta_{r,-2}) - E]\chi^A(r) = 0. \quad (3.46)$$

This equation, calculated at $r = \pm 1, \pm 2$, is verified with $E = -2J_K \cos(k/2)$. The request that it is satisfied at $r = \pm 1$ and $r = \pm 2$, gives the following system of equations

$$\begin{cases} (J_K + V_1 e^{-ik/2}) A_1 + (J_K + V_1 e^{ik/2}) A_2 + (2J_K \cos(k/2) + V_1) A_3 = 0 \\ -J_K A_3 + V_2 (A_1 e^{-ik} + A_2 e^{ik}) = 0 \end{cases} \quad (3.47)$$

from which we get

$$\frac{A_2}{A_1} = -\frac{J_K + V_1 e^{-ik/2} + V_2 e^{-ik/2} (1 + e^{-ik}) + \frac{V_1 V_2}{J_K} e^{-ik}}{J_K + V_1 e^{ik/2} + V_2 e^{ik/2} (1 + e^{ik}) + \frac{V_1 V_2}{J_K} e^{ik}} \quad (3.48)$$

and

$$\frac{A_3}{A_1} = \frac{V_2}{J_K} e^{-ik} \left\{ 1 - \frac{J_K e^{ik} + V_1 e^{ik/2} + 2V_2 \cos(k/2) + V_1 V_2 / J_K}{J_K e^{-ik} + V_1 e^{-ik/2} + 2V_2 \cos(k/2) + V_1 V_2 / J_K} \right\} \quad (3.49)$$

We observe that A_2/A_1 is the ratio between a complex number and its conjugate. Thus it is a phase factor. We can verify that for $V_2 = 0$ we recover the form (3.20).

For the singlet state we add a coefficient to the ansatz (3.22):

$$\chi^S(R, r) = e^{iKR} \underbrace{\{A_1 e^{-ik|r|/2} + A_2 e^{ik|r|/2} + C(|r|)\}}_{\chi^S(r)} \quad (3.50)$$

with

$$C(|r|) = \begin{cases} A_3 & \text{for } |r| = 1 \\ A_0 - A_1 - A_2 & \text{for } r = 0 \\ 0 & \text{otherwise} \end{cases} \quad (3.51)$$

Thus eigenvalue equation is

$$-J_K[\chi^A(r+1) + \chi^A(r-1)] + [U\delta_{r,0} + V_1(\delta_{r,1} + \delta_{r,-1}) + V_2(\delta_{r,2} + \delta_{r,-2}) - E]\chi^A(r) = 0 \quad (3.52)$$

and is always verified if $|r| \neq 0, 1, 2$ and $E = -2J_K \cos(k/2)$. Requiring the equation to be satisfied at $r = 0, \pm 1, \pm 2$, we get the following system

$$\begin{cases} -2J_K(A_1e^{-ik/2} + A_2e^{ik/2} + A_3) + (U + 2J_K \cos(k/2))A_0 = 0 \\ V_1(A_1e^{-ik/2} + A_2e^{ik/2} + A_3) + J_K(A_1 + A_2 - A_0 + 2A_3 \cos(k/2)) = 0 \\ -J_K A_3 + V_2(A_1e^{-ik} + A_2e^{ik}) = 0 \end{cases} \quad (3.53)$$

from which we get the relations between the coefficients. Once again, the ratio A_2/A_1 is a phase factor:

$$\frac{A_2}{A_1} = -\frac{f(k)}{f(-k)} \quad (3.54)$$

with

$$f(k) = J_K + V_1e^{-ik/2} + V_2e^{-ik/2}(1 + e^{-ik}) + \frac{V_1V_2}{J_K}e^{-ik} - \frac{2J_K^2e^{-ik/2} + 2V_2J_Ke^{-ik}}{U + 2J_K \cos(k/2)} \quad (3.55)$$

and it reduces to (3.27) if $V_2 = 0$. It can be easily verified from equation (3.26).

If we impose the periodic boundary conditions (3.34) and (3.35) on the wave function, we get the usual equation:

$$\mp \frac{A_2}{A_1} = e^{-i(K+k)L/2} = e^{i(K-k)L/2} \quad (3.56)$$

where the minus sign is valid for the triplet state and the plus sign is valid for the singlet state. In both cases they give the following quantization rule on the center of mass momentum

$$K = \frac{2\pi n}{L} \quad n = 1, 2, \dots, L \quad (3.57)$$

whereas the equation for the relative momentum k are explicitly written as

$$e^{i(\pi n+kL/2)} \frac{J_n + V_1 e^{-ik/2} + V_2 e^{-ik/2} (1 + e^{-ik}) + \frac{V_1 V_2}{J_n} e^{-ik}}{J_n + V_1 e^{ik/2} + V_2 e^{ik/2} (1 + e^{ik}) + \frac{V_1 V_2}{J_n} e^{ik}} - 1 = 0 \quad (3.58)$$

and

$$e^{i(\pi n+kL/2)} \frac{J_n + V_1 e^{-ik/2} + V_2 e^{-ik/2} (1 + e^{-ik}) + \frac{V_1 V_2}{J_n} e^{-ik} - \frac{2J_n^2 e^{-ik/2} + 2V_2 J_n e^{-ik}}{U + 2J_n \cos(k/2)}}{J_n + V_1 e^{ik/2} + V_2 e^{ik/2} (1 + e^{ik}) + \frac{V_1 V_2}{J_n} e^{ik} - \frac{2J_n^2 e^{ik/2} + 2V_2 J_n e^{ik}}{U + 2J_n \cos(k/2)}} + 1 = 0 \quad (3.59)$$

respectively, with $J_n = 2t \cos(\pi n/L)$ and $n = 1, 2, \dots, L$.

3.3 Bound states in the thermodynamic limit

Now we discuss the thermodynamic limit for the extended Hubbard model. We examine directly the case with the second-neighbour interaction, since the case with the first-neighbour interaction only can be obtained from it setting $V_2 = 0$.

For the triplet state, the boundary condition on the wave functions yields equation (3.58) which, for a bound state, is

$$\frac{J_K \pm V_1 e^{-\alpha} \pm V_2 e^{-\alpha} (1 + e^{-2\alpha}) + V_1 V_2 e^{-2\alpha} / J_K}{J_K \pm V_1 e^{\alpha} \pm V_2 e^{\alpha} (1 + e^{2\alpha}) + V_1 V_2 e^{2\alpha} / J_K} = \pm e^{i\pi n} e^{-\alpha L} \xrightarrow{L \rightarrow \infty} 0. \quad (3.60)$$

Hence, in the thermodynamic limit we find a cubic equation

$$\pm V_2 e^{-3\alpha} + \frac{V_1 V_2}{J_K} e^{-2\alpha} \pm (V_1 + V_2) e^{-\alpha} + J_K = 0 \quad (3.61)$$

whose roots give us the expression for $\pm e^{-\alpha}$. If $V_2 = 0$, it is

$$\pm e^{-\alpha} = -\frac{J_K}{V_1} \quad (3.62)$$

and the corresponding wave function is

$$\chi^A(r) = C \operatorname{sgn}(r) \left(-\frac{J_K}{V_1} \right)^{|r|}. \quad (3.63)$$

If $|V_1| > |J_K|$, it represent a bound state with energy

$$E = -J_K (\pm e^{\alpha} \pm e^{-\alpha}) = V_1 + \frac{J_K^2}{V_1}. \quad (3.64)$$

The third coefficient is given by

$$\frac{A_3}{A_1} = \frac{V_2}{J_K} e^{-2\alpha}. \quad (3.65)$$

For the singlet state, we must consider equation (3.59). For imaginary $k/2 = -i\alpha$ or $k/2 = \pm\pi - i\alpha$ and $L \rightarrow \infty$, it takes the form

$$J_K \pm V_1 e^{-\alpha} \pm V_2 e^{-\alpha} \pm V_2 e^{-3\alpha} + \frac{V_1 V_2}{J_K} e^{-2\alpha} - \frac{\pm 2J_K^2 e^{-\alpha} + 2V_2 J_K e^{-2\alpha}}{U \pm J_K(e^{-\alpha} + e^\alpha)} = 0. \quad (3.66)$$

It is a fifth degree equation

$$\begin{aligned} V_2 J_K \alpha_K^5 + (U + V_1) V_2 \alpha_K^4 + V_1 \left(J_K + \frac{UV_2}{J_K} \right) \alpha_K^3 + (UV_1 + UV_2 + V_1 V_2 - J_K^2) \alpha_K^2 \\ + (U + V_1 + V_2) J_K \alpha_K + J_K^2 = 0, \quad \alpha_K = \pm e^{-\alpha} \end{aligned} \quad (3.67)$$

that reduces to a cubic equation for $V_2 = 0$

$$V_1 J_K \alpha_K^3 + (UV_1 - J_K^2) \alpha_K^2 + (U + V_1) J_K \alpha_K + J_K^2 = 0. \quad (3.68)$$

We observe that for $V_1 = 0$ we recover equation (2.61), as expected; while for $V_1 \neq 0$ and $|U| \rightarrow \infty$ we get (3.62) and the energy is the same as into (3.64). This is indeed the result for the triplet state and is the same that we would obtain for spinless fermions or hard-core bosons [39]. Hence the infinitely on-site interaction makes the behaviour of two fermions in a singlet state similar to that of spinless fermions, by preventing them from staying on the same site. In fact

$$A_0 = 0 \implies \chi(r = 0) = 0. \quad (3.69)$$

However, there is another solution of equation (3.68), $\alpha_K = 0$, which represents an infinitely bound pair with energy $E = U$.

Chapter 4

Scattering resonances

In this chapter we describe the resonance phenomenon that occurs in our model when the energy of a bound state matches the energy of a state in the scattering band.

The idea of resonance scattering in atomic and molecular systems has been around since the earliest days of quantum physics. A conventional *resonance* occurs when the phase shift changes rapidly by $\approx \pi$ over a relatively narrow range of energy, due to the presence of a bound level of the system that is coupled to the scattering state of the colliding atoms.

Before illustrate our results for the extended Hubbard model (next chapter), we recall some basic concept of the scattering theory [40] and introduce some important parameter such as the *scattering length* which characterizes low-energy interactions between a pair of particles [41, Chap. 5].

4.1 Basic scattering theory

The problem of an elastic collision, like any two-body problem, amounts to a problem of the scattering of a single particle, with the reduced mass, in the field $U(r)$ of a fixed centre of force. This simplification is effected by changing to a system of coordinates in which the centre of mass of two particles is at rest. Let us consider the scattering of two-particles with no internal degrees of freedom, and masses m_1 and m_2 . The reduced mass is

$$\mu = \frac{m_1 m_2}{m_1 + m_2}. \quad (4.1)$$

The wave function for the centre-of-mass motion is a plane wave, while that for the relative motion satisfies a Schrödinger equation with the mass equal to μ . We assume the centre of mass is at rest. Hence we consider the wave

function for the relative motion only. It is the sum of an incoming plane wave and a scattered wave, which at great distance is an outgoing spherical wave. If the relative velocity in the incoming wave is in the z -direction, the wave function for large r is thus

$$\psi \approx e^{ikz} + f(\theta, k) \frac{e^{ikr}}{r} \quad (4.2)$$

where θ is the scattering angle, $k = (k_1 - k_2)/2$ is the scaled relative momentum and $f(\theta, k)$ is the scattering amplitude, which is related to the scattering cross section $\sigma(k)$ by

$$\sigma(k) = 2\pi \int_0^\pi |f(\theta, k)|^2 \sin \theta d\theta. \quad (4.3)$$

We notice that in the previous chapters the relative momentum didn't contain the $1/2$ factor. Here we use the scaled relative momentum to be consistent with the notation in literature.

Since we are assuming the potential to be spherically symmetric, the solution of the Schrödinger equation has axial symmetry with respect to the direction of the incident particle. Consequently, the wave function and the amplitude scattering can be expanded in terms of Legendre polynomials $P_\ell(\cos \theta)$

$$f(\theta, k) = \frac{1}{2ik} \sum_{\ell=0}^{\infty} (2\ell + 1) (e^{i2\delta_\ell} - 1) P_\ell(\cos \theta) \quad (4.4)$$

where δ_ℓ are the *phase shifts*, which in general depend on k .

At low energies, the s -wave scattering dominates and only the term for $\ell = 0$ survives in the preceding sum. Thus we have

$$f(k) = \frac{1}{2ik} (e^{2i\delta_0(k)} - 1) = \frac{1}{k \cot \delta_0(k) - ik} \quad (4.5)$$

and

$$\sigma(k) = 4\pi |f(k)|^2 = \frac{4\pi}{k^2} \sin^2 \delta_0(k). \quad (4.6)$$

We can finally define the *scattering length* a_s through the scattering amplitude in the limit $k \rightarrow 0$

$$f(k) \approx \frac{-1}{1/a_s + ik}. \quad (4.7)$$

From the comparison between this relation and the (4.5), we get

$$\delta_0(k \rightarrow 0) = -\arctan(ka_s) \quad (4.8)$$

from which we infer that the behaviour of the s -wave scattering phase shift is completely determined by the scattering length. From equation (4.8) we can also derive an alternative definition for the scattering length, which will be useful in the following

$$a_s = -\lim_{k \rightarrow 0} \frac{\partial \delta_0(k)}{\partial k}. \quad (4.9)$$

Finally we give the expression for the cross section in this limit

$$\sigma(k) = \frac{4\pi}{(1/a_s)^2 + k^2} \quad (4.10)$$

from which we deduce that the cross section diverges when the scattering length $a_s \rightarrow \infty$, for $k \rightarrow 0$. This large increase of the cross section occurs when a resonance appears, due to the energy of the scattering particle matching that of a discrete level.

4.1.1 Identical particles

When two identical particles collide, the wave function that describes the scattering must be symmetrised or antisymmetrised with respect to the particle permutations in order to account for the exchange interaction between them.

An interchange of the particles is equivalent to reversing the direction of the radius vector joining them. In the coordinate system in which the centre of mass is at rest, this means that r remains unchanged, while the angle θ is replaced by $\pi - \theta$ (and so $z = r \cos \theta$ becomes $-z$). Hence, instead of the asymptotic expression (4.2) for the wave function, we have

$$\psi = e^{ikz} \pm e^{-ikz} + [f(\theta, k) \pm f(\pi - \theta, k)] \frac{e^{ikr}}{r}. \quad (4.11)$$

At low energies, where the scattering is dominated by s -waves ($\ell = 0$), the scattering amplitude does not depend on the angle θ and so the wave function. Thus the antisymmetric scattered wave function is zero and the scattering wave function is simply the sum of two equal incident plane waves propagating in opposite directions

$$\psi = e^{ikz} - e^{-ikz} \quad (4.12)$$

while the symmetric wave function is

$$\psi = e^{ikz} + e^{-ikz} + 2f(k) \frac{e^{ikr}}{r}. \quad (4.13)$$

If we are dealing with a one-dimensional scattering, the antisymmetric scattering wave function can be written as (4.12), while the symmetric one takes the form

$$\psi = e^{ikz} + e^{-ikz} + 2f(k)e^{ikz} \quad (4.14)$$

with

$$f(k) = \frac{1}{2}(e^{ik\delta_0(k)} - 1). \quad (4.15)$$

Thus it is

$$\psi = e^{-ikz} + e^{2i\delta_0(k)}e^{ikz}. \quad (4.16)$$

4.2 Scattering process on a lattice

Our problem of two particles on a one-dimensional lattice with a contact interaction can be regarded as a scattering problem.

Concepts illustrated before, such as *phase shift* and *scattering length* can be generalized to describe two-particle scattering in an optical lattice represented by the Hubbard Hamiltonian or its extensions.

In this case, the periodic potential leads to a structured continuum with scattering states grouped in energy bands separated by band gaps. In the previous chapters we have concentrated on the lowest band and we will continue to ignore the upper bands in the following. The band structure implies that the continuum band has both a lower and an upper edge. As we will see, this has fundamental implications for both the bound states and the scattering states of the system. A counter-intuitive effect of the lattice is the existence of repulsively bound pairs of atoms, which are stable if the repulsive interaction is strong enough to lift the two-particle bound state out of the continuum and into the band gap, thereby preventing the pair from dissociating [42]. In one dimension repulsively bound pairs exist for an arbitrary small repulsion.

We can easily generalize the concept of *scattering amplitude* and *scattering length* to suit this case. From the comparison between equations (2.57) and (4.16), making attention to the scaling $k/2 \rightarrow k$ and taking $|r| = z$, we identify the ratio A_2/A_1 in our previous calculations with the phase factor $e^{2i\delta_0}$. Hence, using equations (2.58) and (4.15) and the scaled form for the momentum $k = (k_1 - k_2)/2$, we get

$$f(k) = \frac{-1}{1 - ik2|J_K|/U}, \quad \text{with } k \rightarrow 0 \quad (4.17)$$

Analogously, we can define an amplitude scattering at the other edge of the band $k = \pi$. Thus, we can write the following form for the amplitude scattering which incorporate either the two limiting cases

$$f(k) = \frac{-1}{1 - i\kappa 2|J_K|/U}, \quad \text{with } \kappa \rightarrow 0 \quad (4.18)$$

where, if we refer to the first Brillouin zone ($K \in [-\pi, \pi]$), $\kappa = k$ at the bottom of the band ($k = 0$) and $\kappa = \pi - k$ at the top of the band ($k = \pi$). Finally, from the comparison with equation (4.7), we get a natural definition of a generalized one-dimensional scattering length [43] in the lattice

$$a_s^{lattice} = -\frac{2|J_K|}{U}. \quad (4.19)$$

An equivalent definition is obtained from the generalization of definition (4.9) [44, 45]

$$a_s^{lattice} = -\lim_{\kappa \rightarrow 0} \frac{\partial \delta_0(k, K)}{\partial \kappa}. \quad (4.20)$$

We notice that in the lattice the phase shift depends on K in addition to k . This implies that the scattering length depends on the centre-of-mass motion of the pair, which is a crucial feature in the lattice.

For an attractive interaction ($U < 0$) a bound state is situated below the continuum, making $a_s^{lattice}$ positive. In this case, the pole of (4.18) lies along the positive imaginary axis

$$k = \frac{iU}{2|J_K|}. \quad (4.21)$$

When k approaches this value the plane wave becomes a dying exponential which represents the bound state. Conversely, for a repulsive interaction ($U > 0$), the bound state lies above the continuum and the scattering length is negative. The pole of the scattering amplitude is then at

$$k = \pi + \frac{iU}{2|J_K|}. \quad (4.22)$$

Hence in this case the wave function is a dying exponential with the addition of a phase factor $e^{i\pi|z|}$ which alternates between 1 and -1 from one lattice site to the next.

As $|U| \rightarrow 0$ the scattering length diverges and the bound state approaches the edge of the continuum. This is the only case in which $a_s^{lattice}$ diverges; hence only for vanishing U we observe a scattering resonance in the one-dimensional Hubbard model. As we will see in the following, when an adding non-contact interaction is present in the model, a scattering resonance appears also for finite interaction strength.

Chapter 5

Our results

In this chapter we illustrate some explicit results of our calculations, showing the emergence of scattering resonances in our model.

In this discussion we take into account the more general model with second-neighbor interaction. Hence we consider the Hamiltonian (3.42)

$$H = -t \sum_i \sum_{\sigma} (c_{i\sigma}^{\dagger} c_{i+1\sigma} + c_{i+1\sigma}^{\dagger} c_{i\sigma}) + U \sum_i (n_{i\uparrow} n_{i\downarrow}) + V_1 \sum_i n_i n_{i+1} + V_2 \sum_i n_i n_{i+2} \quad (5.1)$$

and equations obtained for it in section 3.2. Then we consider the particular cases of $V_2 = 0$ and $V_1 = 0$.

5.1 Scattering states and bound states

Solving equations (3.58) and (3.59) gives the permitted values of the relative momentum k for the triplet state and the singlet state, respectively. From now on to the end of this study we will refer to the scaled relative momentum $q = k/2$ rather than $k = k_1 - k_2$. We study the energy band structure in order to have some information about the physical behaviour of the particle pair on the lattice. For each permitted (q, K) couple there is a state of energy $E = -2J_K \cos q$. All relative momenta qs can be grouped into two families

1. $\Im m(q) = 0$
2. $|\Im m(q)| > 0 \quad \& \quad |\Re e(q)| = 0, \pi$

The first family corresponds to the scattering states, which have a real relative momentum ; the second one corresponds to the bound states, which have a relative momentum with a non-vanishing imaginary part. However

their real part is always 0 or π , so that the energy remains a real number. We start the analysis of results from the simpler cases. If $V_1 = V_2 = 0$, our model reduces to the Hubbard model, in which the triplet state has no bound states, while the singlet state has them, as mentioned in chapter 2 (see figure 2.2). In figure 5.1 a similar graph is plotted, in which the discrete energy levels are depicted for both an attractive and a repulsive interaction. The graph includes only the first Brillouin zone $K \in [-\pi, \pi]$. In this region, the upper band edge corresponds to $q = \pm\pi$ and the lower band edge corresponds to $q = 0$. The red dots represent the bound states that appear for a repulsive interaction with strength $U/t = 2.5$, while the brown dots represent the bound states that appear for an attractive interaction with the same strength. Blue and green dots are the scattering states for the first and the second case, respectively. We observe that the band scattering is not the same if U is reversed or, in general, if U is varied. This is a lattice effect, which disappears in the thermodynamic limit, when the band becomes a continuum and the graphic is perfectly symmetric. We observe that if the

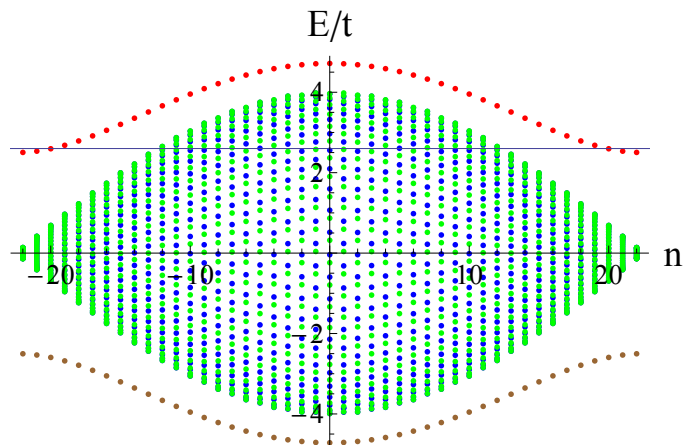


Figure 5.1: Energy band structure for a singlet state in the Hubbard model, with $U/t = 2.5$ (blue and red points) and $U/t = -2.5$ (green and brown points). The number of lattice sites is $L = 45$.

interaction strength is sufficiently low, as in this case, there are some bound states with the same energy of some states in the scattering band. However states with the same energy never have the same centre-of-mass momentum. Hence, two particles cannot bound together as a result of a scattering process, since the conservation of the centre-of-mass momentum would be violated. As the interaction strength $|U|$ is enhanced, the discrete levels repel from the scattering band. In the opposite limit, when $|U| \rightarrow 0$, the bound state level collapses onto the band.

Let us consider the case $V_2 = 0$, $V_1 \neq 0$. We analyse first the triplet state,

which is less complicated, since the contact interaction U has no physical effect. Thus the only tunable parameter in addition to the number of lattice sites is $V_1 \equiv V$. The band structure is similar to that of the singlet state in the Hubbard model with the on-site interaction only but the form of the curve produced by the bound states is different, as we can easily see by comparing equations (2.64) and (3.64). In both cases the number of bound states in an interval of width 2π in K equals the number of lattice size. However these bound states don't appear for each value of the interaction strength, depending on the chain length. Thus this is an effect of the finite size of lattice and the consequently discreteness of the energy levels. The number of bound states grows from 0 to L as the potential $|V|$ is enhanced. Once L bound states have appeared, their number doesn't grow anymore: there is at most a bound state for a fixed centre-of-mass momentum. In figure 5.2 the number of bound states versus V is indicated, for lattice size 7 and 15, respectively. We notice that the number of bound states grows more rapidly

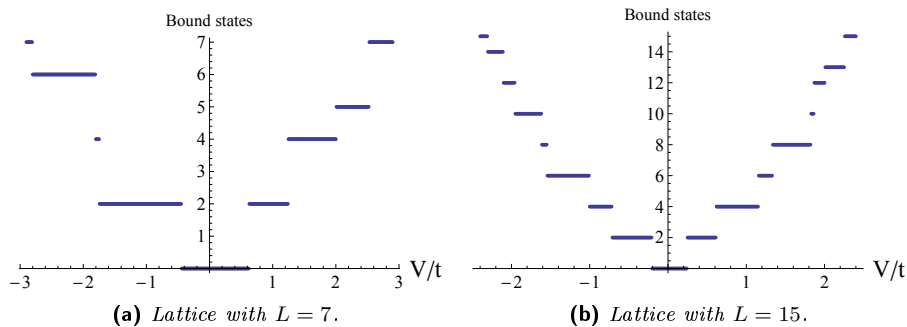


Figure 5.2: Number of bound states as a function of V/t , for lattices with $L = 7$ and $L = 15$ sites, respectively.

for a longer chain. Another counter-intuitive feature is that the appearance of bound states is not symmetric as the potential is reversed. However the asymmetry is weak and it reduces as the lattice size approaches the thermodynamic limit. Finally we observe that the energy is symmetric with respect to the centre of the Brillouin zone. Hence, the bound states appear always in pairs (obviously except that for $K = 0$). These two bound states have relative momenta with the same imaginary part and real part that is 0 and π , respectively¹.

In figure 5.3 the energy band structure has been plotted for a lattice length $L = 15$ and for a lattice length approaching the thermodynamic limit. We ob-

¹We notice that in each case the total number of states is fixed (if a bound state appears, a scattering state disappears) and the Bethe ansatz allows to find all of them. We refer the reader to appendix A for their counting.

serve that in the first case only 8 bound states appear at the edge of the Brillouin zone if the repulsive potential V/t is reduced from 3 to 1.5; in the second case 52 bound states appear. In figure 5.4 wave functions for both attractive

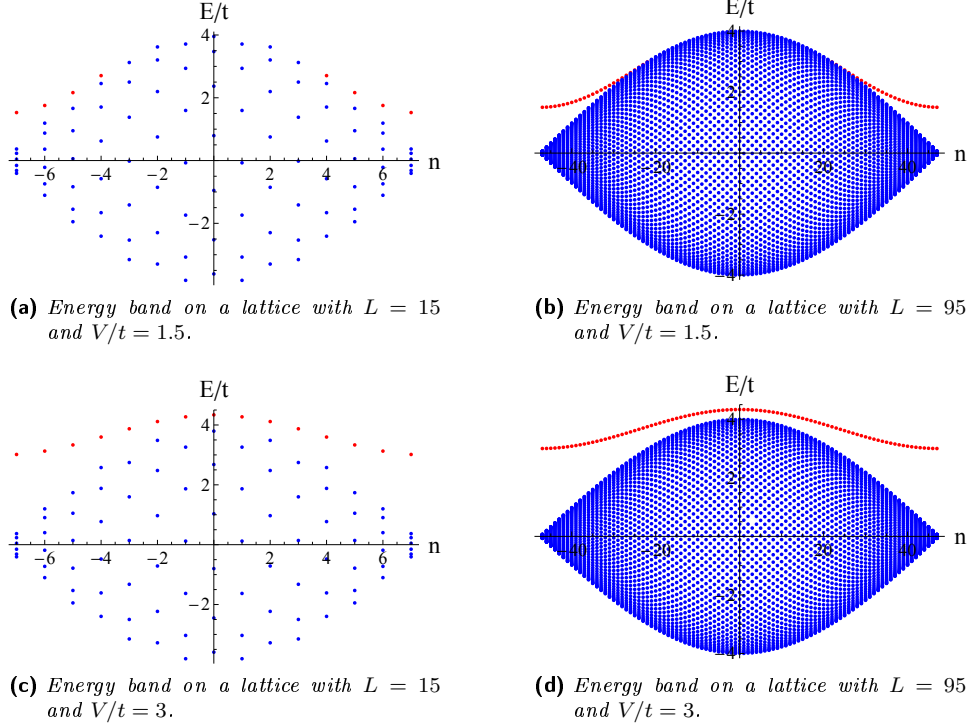
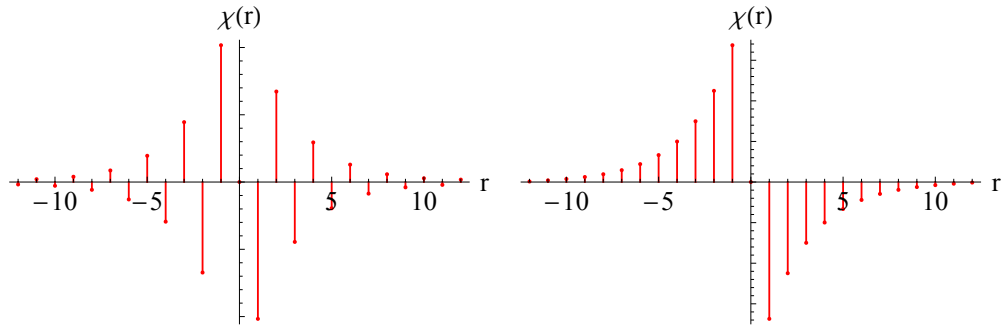


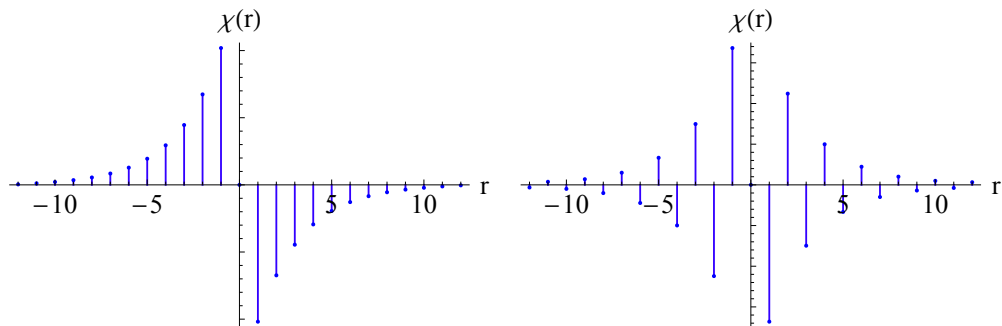
Figure 5.3: Energy band for the triplet state in the extended Hubbard model with the (repulsive) first-nearest-neighbor interaction only.

and repulsive potentials have been plotted. The form of the wave function depends on the centre-of-mass momentum K . Let us consider, for example, an odd lattice. If we refer to the range $K \in [2\pi/L, 2\pi]$, the wave function for a repulsive potential in the first semi-band ($K \in [2\pi/L, \pi(1 - 1/L)]$) is always positive or always negative when $r > 0$ and reverses its sign when $r < 0$; whereas in the other semi-band ($K \in [\pi(1 - 1/L), 2\pi]$), it alternates its sign. For an attractive potential it is the opposite. We also notice that in both cases the wave function reaches its maximum value at $r = 1$ and decreases with increasing r . This means that the two bound particles are more probably located at nearest-neighbor sites. Obviously the wave function vanishes at $r = 0$, since the Pauli principle prevents double occupancy. Finally, one can easily verify that the wave functions with alternating sign corresponds to the bound states with $\Re(q) = \pm\pi$, while the wave functions that reverse their sign only with a change in the sign of r correspond to the bound states with $\Re(q) = 0$.



(a) Wave function for a repulsively bound pair with $K = 2\pi/L$ in the triplet state.

(b) Wave function for a repulsively bound pair with $K = 2\pi$ in the triplet state.



(c) Wave function for an attractively bound pair with $K = 2\pi/L$ in the triplet state.

(d) Wave function for an attractively bound pair with $K = 2\pi$ in the triplet state.

Figure 5.4: Wave functions for a bound pair in the triplet state on a lattice with $L = 25$ sites. Red figures have been obtained for a repulsive potential with strength $V = 3$, whereas blue figures have been obtained for an attractive potential with strength $V = -3$.

When $V_2 \neq 0$ and $V_1 = 0$, the energy band is similar to that in the preceding case: there is at most one bound state for each permitted value of K and it is located above or below the scattering band depending on whether V_2 is positive or negative. When both V_1 and V_2 have non-vanishing values, a second bound state could appear for a fixed K . Let us examine some special cases. Consider first $V_1 = V_2 \equiv V$ (referring to a chain with 15 sites). In this case all bound states lie above the scattering band if $V > 0$ and below if $V < 0$. When $|V/t|$ is sufficiently small ($\lesssim 0.5$), there exists at most one bound state for each K . As increasing $|V|$, a second bound state appears at some points of the Brillouin zone, also if the first bound state has not appeared everywhere. As $|V|$ is enhanced, both the two family of bound states repel from the scattering band and new bound states appear where the discrete levels separate from the continuum band. When $|V/t| \sim 1$ the first set of bound state is complete and when $|V/t|$ reaches the value ~ 6 , also the second set is. In figure 5.5, the energy is plotted for three different values of V , for a chain with $L = 45$ sites.

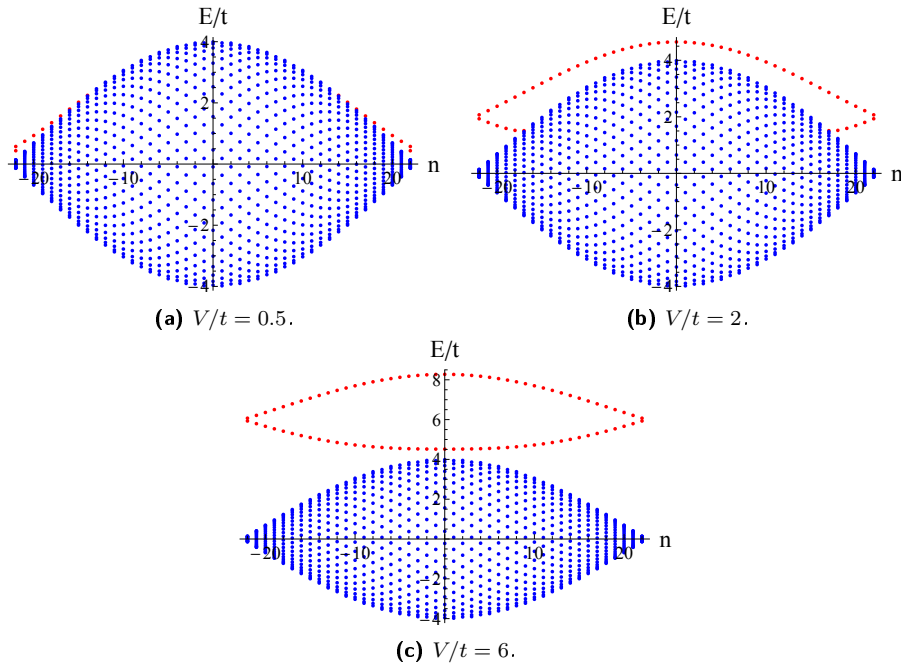


Figure 5.5: Energy band for the triplet state on a lattice with $L = 45$ sites and $V_1 = V_2 \equiv V$ for increasing potentials.

As one of the two interaction is varied respect to the other, the two discrete levels separate (fig. 5.6).

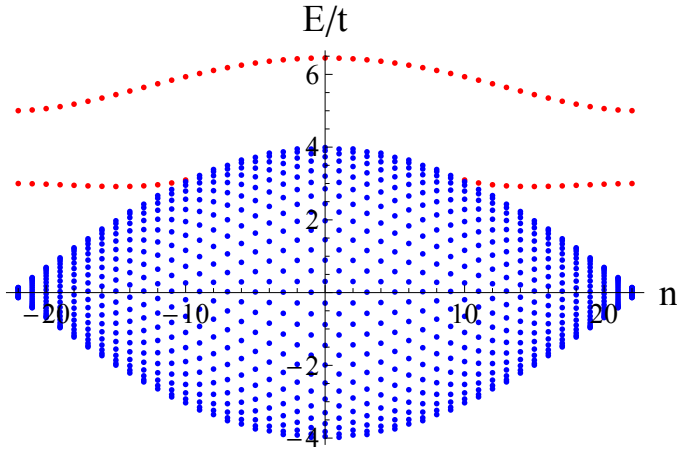


Figure 5.6: Energy band structure for a triplet state in the extended Hubbard model, with $V_1/t = 5$ and $V_2/t = 3$. The number of lattice sites is $L = 45$.

When the two interactions have different signs, the set of bound states associated with the positive interaction is located above the band and that associated with the negative interaction is located below it (fig. 5.7).

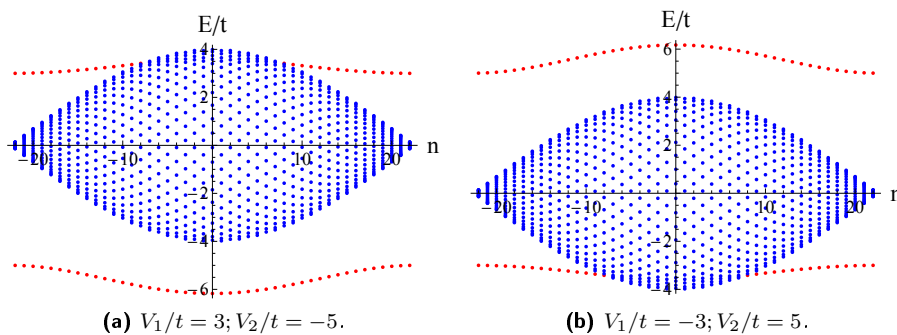
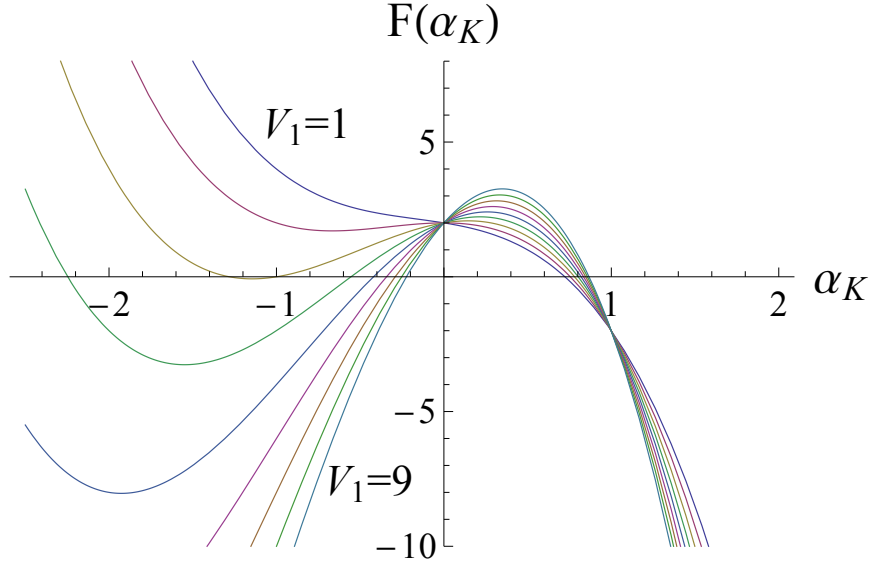


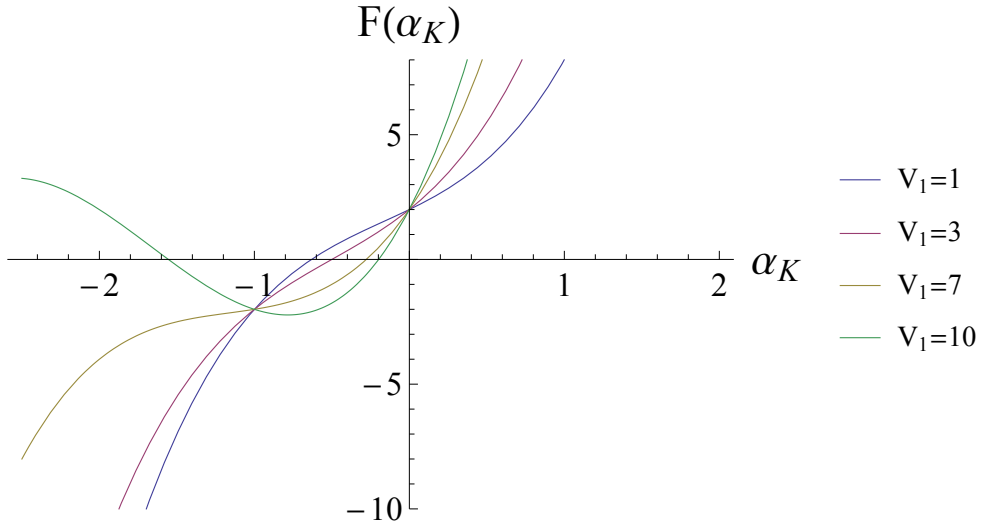
Figure 5.7: Energy band for the triplet state on a lattice with $L = 45$ sites and V_1 and V_2 having opposite signs.

In the thermodynamic limit, the number of bound states is the number of roots of equation (3.61). In figures 5.8 and 5.9 this cubic function has been plotted for different values of the interaction parameters. The bound states are given by the zeros of the function, in the range $|\alpha_K| < 1$ (because we have chosen $\alpha > 0$). Thus, we can see that one or two solutions are possible.

A similar scenario arises for the singlet state when one of the three interactions is zero.



(a) Cubic function for the triplet state with $V_2/t = -2$ and V_1/t varying from 1 to 9. Different curves refer to different values of V_1 (setting $t = 1$). In the range $\alpha_K < 0$, the curve is lowered as the potential is enhanced.



(b) Cubic function for the triplet state with $V_2/t = 2$ and V_1/t varying in a positive range. Different curves refer to different values of V_1 . In the range $\alpha_K > 0$, the curve is lowered as the potential decreases.

Figure 5.8: Cubic function for the triplet state in the thermodynamic limit, which determines the bound state solutions. The function has been evaluated at the centre of the first Brillouin zone ($K = 0$), with $t = 1$.

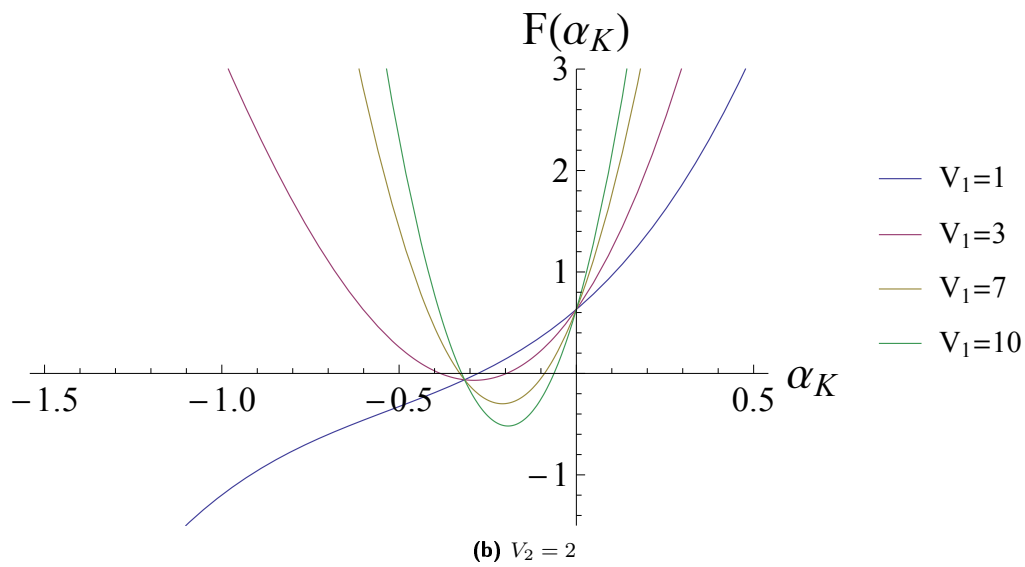
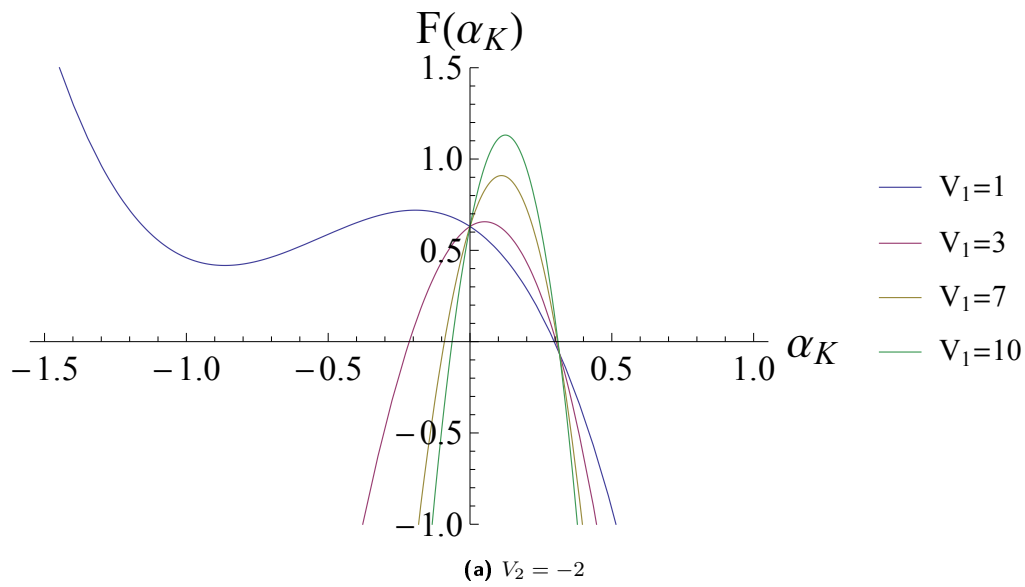


Figure 5.9: Cubic function for the triplet state in the thermodynamic limit, which determines the bound state solutions. The function has been evaluated at $K = 2.5$, with $t = 1$ and $V_2 = \pm 2$.

If all interactions are non-vanishing, a third set of bound states could appear. When they are all positive, all bound states lie above the scattering band; if they are all negative, all bound states lie below the scattering band. If an interaction reverses its sign, a set of bound states is overturned. In figure 5.10 some examples are given. An interesting outcome is the scattering states thickening around the ideal prosecution of bound state levels.

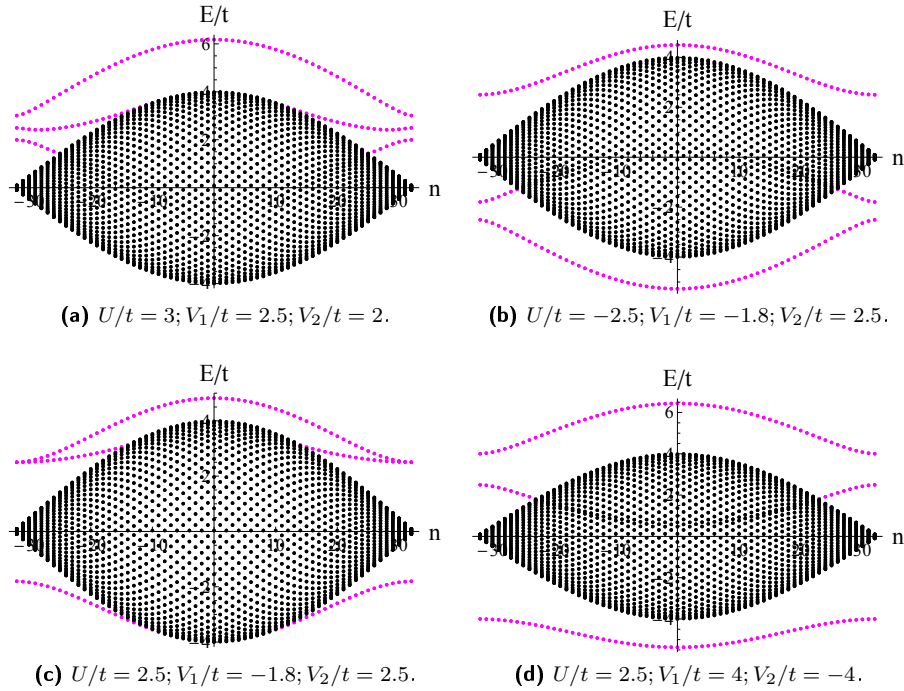


Figure 5.10: Energy band for the singlet state on a lattice with $L = 65$. Different picture refer to different values of the interaction parameters U, V_1, V_2 .

The number of bound states for the singlet state is equal to the number of roots of equation (3.67). In figure 5.11 the function has been plotted for a case in which the maximum number of bound states appear.

5.2 Resonances

From our preceding results we observe that both in the triplet and in the singlet state, the bound state level can merge into the scattering band. In the thermodynamic limit, the two closest bound states to the scattering band become degenerate with the scattering states and a resonance occurs. As in Chapter 4, we can define a generalized scattering phase shift δ and a generalized scattering length $a_s^{lattice}$. As in the Hubbard model, the phase shift depend on both the centre-of-mass and relative momenta and can be

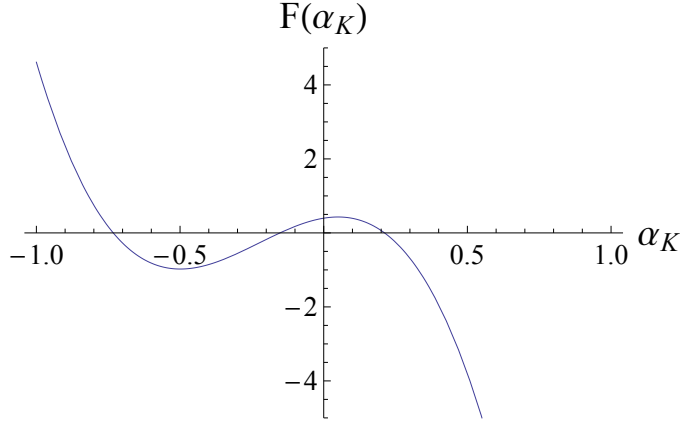


Figure 5.11: Function (3.67) for $U = -3$, $V_1 = 4$, $V_2 = 1$, $K = 2.5$. The zeros of the function in the range $\alpha_K \in [-1, 1]$ give the bound states solutions.

defined through the phase factor $e^{i2\delta}$, which is given by the ratio between the coefficients of the (generalized) Bethe ansatz

$$e^{i2\delta(K,q)} = \frac{A_2}{A_1}. \quad (5.2)$$

Since A_2/A_1 is the ratio between two complex conjugate numbers, it can be written as

$$\frac{A_2}{A_1} = -\frac{x - iy}{x + iy} \quad (5.3)$$

from which we get the phase shift

$$\delta(K, q) = \arctan \frac{x}{y}. \quad (5.4)$$

Then we define the scattering length at the edges of the continuum band in the usual way

$$a_s = -\lim_{q \rightarrow 0, \pi} \frac{\partial \delta(K, q)}{\partial q}. \quad (5.5)$$

Using equations (3.48) and (3.54) for the triplet state and the singlet state, respectively, we get the following expressions

$$a_s^A = \frac{2V_1V_2 \pm J_K(V_1 + 4V_2)}{V_1V_2 \pm J_K(V_1 + 2V_2 \pm J_K)} \quad (5.6)$$

$$a_s^S = \frac{2V_1V_2 \pm J_K(V_1 + 4V_2) - 2J_K^2 \frac{2V_2 \pm J_K}{U \pm 2J_K}}{V_1V_2 \pm J_K(V_1 + 2V_2 \pm J_K) - 2J_K^2 \frac{V_2 \pm J_K}{U \pm 2J_K}} \quad (5.7)$$

where we have labelled the triplet state with A (*antisymmetric*) and the singlet state with S (*symmetric*), since we are referring to spatial wave functions. The upper sign corresponds to the limit $q \rightarrow 0$ and the lower sign to $q \rightarrow \pi$. A resonance occurs when the scattering length diverges. Hence, imposing the denominator in (5.6) or in (5.7) to vanish, we get an equation whose solution determines the centre-of-mass momentum at which the bound state crosses the scattering band. For the triplet state it is a quadratic equation

$$J_K^2 \pm (V_1 + 2V_2)J_K + V_1V_2 = 0 \quad (5.8)$$

which reduces to

$$J_K = \mp gV_g, \quad g = 1, 2 \quad (5.9)$$

if one of the two interactions is zero. This yields

$$K_R = 2 \arccos \left(\mp \frac{gV_g}{2t} \right). \quad (5.10)$$

Also for the singlet state we have a quadratic equation

$$[U + 2(V_1 + V_2)]J_K^2 \pm (V_1U + 2V_2U + 2V_1V_2)J_K + V_1V_2U = 0 \quad (5.11)$$

which reduces to

$$J_K = \mp gW_g \quad \text{with } W_g = \frac{UV_g}{U + 2V_g}, \quad g = 1, 2 \quad (5.12)$$

if V_1 or V_2 vanishes; and the resonance occurs at

$$K_R = 2 \arccos \left(\mp \frac{gW_g}{2t} \right); \quad (5.13)$$

whereas, if $U = 0$, we have

$$J_K = \mp W_0 \quad \text{with } W_0 = \frac{V_1V_2}{V_1 + V_2} \quad (5.14)$$

and

$$K_R = 2 \arccos \left(\mp \frac{W_0}{2t} \right). \quad (5.15)$$

We observe that in the discrete case, the resonant bound state is not degenerate with a scattering state. Instead, since the number of states is unchanged, we could suggest that a scattering state transforms into a bound one which has an energy close to the edge scattering band but not equal.

In the thermodynamic limit, the energy of the bound state approaches that of a scattering state and the scattering length diverges. However, from equations (3.63) and (5.9) we see that the wave function for a resonant bound state - in the simpler case of a triplet state with $V_2 = 0$ - has the following form

$$\chi^A(r)_{res} = C \operatorname{sgn}(r)(\pm 1)^{|r|}. \quad (5.16)$$

It is no longer a decaying function, indicating that the pair is actually unbound.

Thus we have an ambiguity, since this phenomenon can be regarded as a resonance because the scattering length diverges, but indeed it is not a resonance because there aren't two degenerate energy levels. Hence we could more appropriately define it as a *quasi*-resonance.

Chapter 6

The role of resonances and future perspectives

In this chapter we want to investigate the role of bound states and scattering resonances in our model and their possible implications for both theoretical and experimental physics. Thus, we provide an overview on recent activities about ultra-cold atoms [1] and discuss the fundamental role that bound states and resonances play in this field. Then we try to give our work the right collocation into this context.

In recent times the search for the existence of a bound state not only for attractive interactions but also for repulsive interactions has drawn a lot of attention in both theoretical and experimental fields. The Hubbard model admits repulsively bound pairs of particles also in one dimension. Current studies in low dimensions are focusing on expansion dynamics of dimers of two bosons [46, 8], which are simpler to deal with both theoretically (since they don't obey the Pauli exclusion principle) and experimentally (since they are generally easier to cool than fermions). However much progress is being made in handling fermionic atoms and the existence of stable fermionic bound states [47] is really interesting since it is at the origin of the BCS-BEC crossover [41, 48]. In particular, in one and also in two dimensions, the existence of a *s*-wave bound state in the two-particle problem is a necessary and sufficient condition for the instability of the non-interacting ground state (filled Fermi sea) in the many-particle problem [49], [48, Chap. 14]. Hence, the study of the two-particle case, which is analytically soluble, allows to get some hint about the non-integrable many-particle case.

6.1 3D Feshbach resonance and BCS-BEC crossover

An important feature of cold atomic vapour is that they can reach very low densities. Consequently, the two-body interaction between atoms dominates, and three- and higher-body interaction are negligible. Moreover, since the atoms have low velocities, the scattering in these systems can be described in terms of s -waves, as in our preceding discussion, and the only relevant parameter is the scattering length.

In typical experiments with fermionic atoms, two species of fermions are used. They are actually two hyperfine states, but are often identified as *up spin* and *down spin*. One of the most important goal achieved with ultracold atomic gases is the possibility to tune the interaction between the two species of fermions. This can be obtained through the so-called *Feshbach resonances* [50]. This phenomenon is based on the existence of internal states for the scattering particles, described by a set of quantum numbers which generally changes after the collision. A possible choice of quantum numbers is usually referred to as a *channel*. At the temperature of interest for Bose-Einstein condensation or superfluidity, the only relevant internal states are the hyperfine states, since atoms are in their electronic ground states. Feshbach resonances arise from coupling between channels: elastic scattering in one channel can be altered dramatically if there is a low-energy bound state in a second channel which is forbidden by some conservation rules and is called “closed”. Feshbach resonances occur when the total energy of the two scattering particle in an open channel matches the energy of a bound state in a closed channel, causing a dramatic increase in the collision cross-section. In the closed channel there are, by definition, no continuum states. However, the two colliding particles can scatter to an intermediate state in a closed channel, which subsequently decays in another open channel.

Feshbach resonances have become an important tool in investigations that use cold atoms, because they can be controlled by an external magnetic field B thanks to the difference in the magnetic moments in the closed and open channels. In fact the scattering length depends on the energy E of the two particles and on the magnetic field in the following way [41]

$$a_s^{3D} \sim \frac{C}{E - E_{res}} \sim 1 - \frac{\Delta B}{B - B_0} \quad (6.1)$$

where E_{res} is the energy of the bound state in the closed channel. Hence, since the effective potential is proportional to the scattering length, one finds that coupling between channel gives rise to a repulsive interaction if $E > E_{res}$ and

an attractive one if $E < E_{res}$. The condition $E = E_{res}$, which determines the scattering length divergence, can be obtained by setting the external magnetic field B to B_0 . This is the threshold for bound state formation. Then it exists in whole range $a_s^{3D} > 0$, which means $B < B_0$ (see figure 6.1), where the scattering length has the simple physical interpretation as the size of the bound state, whose energy is given by

$$E_b = -\frac{1}{m(a_s^{3D})^2}. \quad (6.2)$$

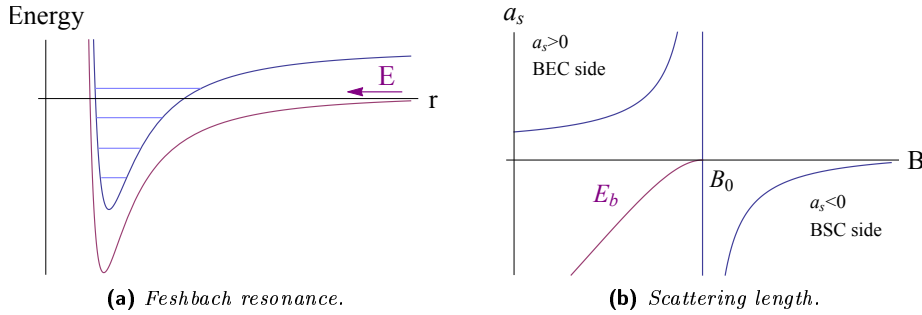


Figure 6.1: In the left panel Feshbach resonance mechanism is described: when the energy E of the two scattering particles in the open channel (violet line) matches that of a bound state in a closed channel (blue line), a resonance occurs. The distance between the two curves can be altered by a change in the external field B . In right panel the scattering length versus the magnetic field is plotted (blue line); the violet curve represents the energy of the bound state.

This scattering length is related to scattering amplitude and to phase shift through equations of the form (4.7) and (4.8), with $a_s \equiv a_s^{3D}$. At the threshold for bound state formation $|a_s^{3D}| \rightarrow \infty$, the phase shift $\delta_0(k=0) = \pi/2$ and the scattering amplitude $f(k) \approx -1/ik$ takes its maximum value.

An important implication of Feshbach resonance is that it can be used to produce molecules consisting of two bound fermions and observe a crossover between BCS and BEC states of the system. In the experiments to produce molecules, one starts with a mixture of two species of fermions, in a magnetic field of such a strength that the molecular state has an energy higher than that of two atoms at rest in the open channel. Under these conditions, the effective low-energy interaction between atoms is attractive and, away from the resonance ($E_{res} \gg E$), the attraction is weak. At sufficiently low temperatures, this system undergoes a transition to the BCS paired state, in which pairs of atoms are correlated in space over distances large compared with the

interatomic spacing. As the strength of the magnetic field is enhanced, the energy of the molecular state is lowered and the interaction becomes more attractive until a bound state forms. Then the scattering length changes its sign and the interaction becomes repulsive. Hence the system behaves like a gas of weakly interacting bosonic molecules that can undergo a Bose-Einstein condensation [41, 4].

6.2 Two-particle scattering and confinement-induced resonances in *quasi*-1D systems

One dimensional systems can be experimentally realized by introducing tight confinement via optical lattices that remove two spatial degrees of freedom [2]. Free-space scattering theory is no longer valid in such systems. This led to the development of quantum scattering theory in low dimensions, in which one assumes that atoms occupy only the ground state of the transverse confining potential and the result is a one-dimensional free motion. This assumption is justified by the fact that for a sufficiently dilute gas under strong confinement, both the chemical potential and the thermal energy are less than the transverse level spacing. However the presence of the additional structure of discrete levels provided by the confining waveguide modifies scattering processes via a mechanism similar to the 3D Feshbach resonance. Indeed the direction of the free motion (say the z -axis) plays the role of the open channel; whereas the transverse excited states can be considered as the closed channels. When the total energy of two scattering particles along the z -direction equals that of a transverse discrete level, a resonance occurs - the so-called CIR (*confinement-induced resonance*) - and a bound state is formed.

Typically, to describe this phenomenon, the waveguide is modelled through an axially symmetric 2D harmonic potential of a frequency ω_{\perp} in the $x - y$ plane and interaction between atoms is chosen to be the Huang's pseudopotential [51, 52]

$$V(r) = g\delta(\mathbf{r})\frac{\partial}{\partial r}(r\cdot), \quad g = \frac{2\pi\hbar^2 a_s^{3D}}{\mu}, \quad (6.3)$$

with μ the reduced mass, but also other choices among finite-range interaction potentials are possible, such as the screened Coulomb potential [53], Lennard-Jones potential or spherical square well [52]. Thus the Hamiltonian for the two-body problem is

$$H = H_z + H_{\perp} + V \quad (6.4)$$

where

$$\begin{aligned} H_z &= -\frac{\hbar^2}{2\mu} \frac{\partial^2}{\partial z^2} \\ H_\perp &= -\frac{\hbar^2}{2\mu} \left(\frac{\partial^2}{\partial \rho^2} + \frac{1}{\rho} \frac{\partial}{\partial \rho} \right) + \frac{\mu}{2} \omega_\perp^2 \rho^2 \end{aligned} \quad (6.5)$$

with $\rho^2 = x^2 + y^2$.

Using the pseudopotential, one can see that the 3D two-body scattering problem in such a waveguide always exhibits one and only one bound state [51]. Apart from it, all the scattering properties can be described by an effective 1D delta potential $g_{1D}\delta(z)$, with

$$g_{1D} = \frac{2\hbar^2 a_s^{3D}}{\mu a_\perp^2} \frac{1}{1 - C a_s^{3D}/a_\perp} = -\frac{\hbar^2}{\mu a_s^{1D}} \quad (6.6)$$

where $a_\perp = \sqrt{\hbar/\mu\omega_\perp}$ is the waveguide parameter and a_s^{1D} is a generalized one-dimensional scattering length

$$a_s^{1D} = -\frac{a_\perp^2}{2a_s^{3D}} \left(1 - C \frac{a_s^{3D}}{a_\perp} \right) \quad (6.7)$$

defined through equation (4.9) [51]. Hence the condition for a CIR to appear is $a_\perp \approx C a_s^{3D}$, with $C = 1.4603\dots$ (see also [54, 55, 56, 57]).

If H_g is the projection of the total 3D Hamiltonian on the ground state of H_\perp and H_e is the projection on the excited states, the CIR condition can be expressed as $E_{b,e} = E_{c,g}$, where $E_{c,g} = \hbar\omega_\perp$ is the threshold energy for H_g to have a continuum spectrum and $E_{b,e}$ is the energy of the bound state of H_e , which exists for all values of a_s^{3D} (see figure 6.2). In conclusion, by changing the waveguide parameter a_\perp , experimentalists can lead the system through a resonance and observe the appearance of a two-particle bound state.

In a many-body picture, the system can be modelled by the Gaudin-Yang Hamiltonian

$$H = -\frac{\hbar^2}{2m} \sum_{i=1}^N \frac{\partial^2}{\partial z_i^2} + g_{1D} \sum_{i<j} \delta(z_i - z_j) \quad (6.8)$$

remembering to take into account the existence of a bound state which influences the scattering. This Hamiltonian contains all information one needs to describe the BCS-BEC crossover in one dimension [58]. However, we underline that the presence of the confining potential is crucial to observe a bound state with a repulsive interaction $g_{1D} > 0$, since the two-body delta potential $g_{1D}\delta(z)$ supports a bound state only if $g_{1D} < 0$.

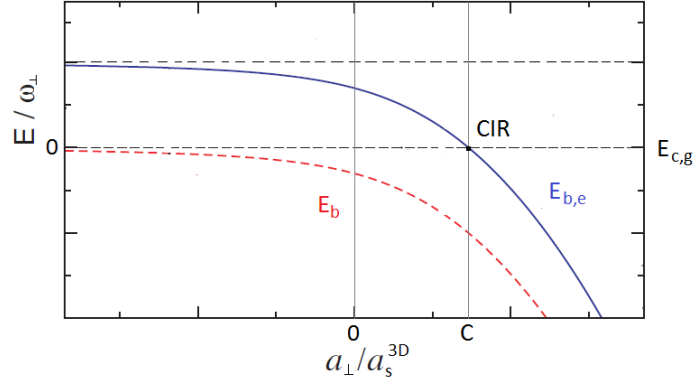


Figure 6.2: CIR: a resonance occurs when the energy $E_{b,e}$ (blue curve) of the transversally excited molecular bound state becomes degenerate with the energy $E_{c,g}$ of particles in the incoming scattering channel. The red curve is the bound state energy of the full Hamiltonian.

6.3 One-channel and two-channel Feshbach physics on a 1D lattice

The Hubbard model can be viewed as the lattice version of the continuum Gaudin-Yang model. As we have already seen, here a bound state appears for both positive and negative interactions and its existence can be directly attributed to the discreteness of the lattice. Quite generally, lattice models have a richer physics than the continuum model they contains as limiting case [5]. So the Hubbard Hamiltonian (1.21) reduces to the Gaudin-Yang Hamiltonian (6.8) when the distance a between adjacent sites approaches zero, for a fixed particle number N and system length L , i.e. $n = Na/L \ll 1$. In this limit, we have the following relations between the parameters of the two models [59]

$$m = \frac{\hbar^2}{2ta^2}, \quad g_{1D} = Ua, \quad \gamma = -\frac{U}{2tn}. \quad (6.9)$$

Thus the one-dimensional Hubbard model may be a possible candidate to better understand the physics of the BCS-BEC crossover. Indeed its parameter U/t includes the periodic potential of the optical lattice. Consequently it can be directly tuned by varying, for example, the intensity of the field generated by the counter-propagating laser beams that produce the lattice [3, 60, 61].

In our work, the first- and the second-neighbor interactions have been added to the contact potential, providing a more complete description of the atom-atom scattering.

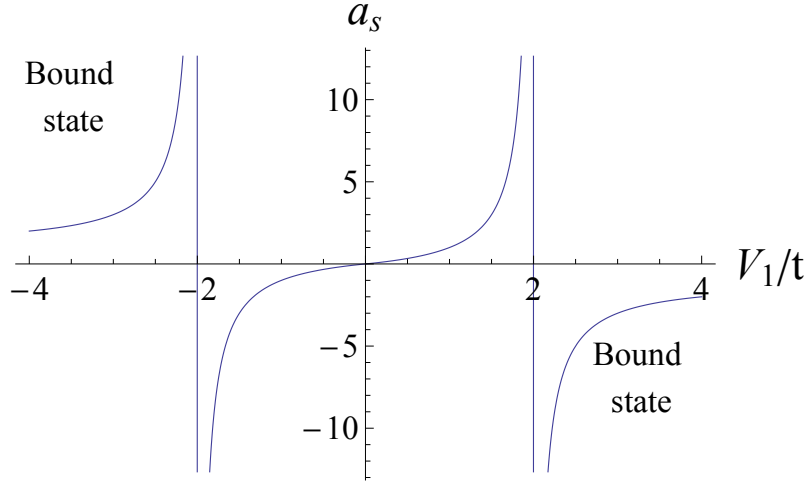


Figure 6.3: Scattering length of the triplet state with $V_2 = 0$ versus V_1/t . A resonance occurs when $V_1 = \pm J_K$ and a bound state forms. For the plot, $K = 0$ has been set, so that $J_K = 2t$.

Hence, our model is suitable to depict scattering processes and bound state formation in optical lattices.

In the 3D Feshbach resonance one tunes the external magnetic field to bring the system through a resonance. In the CIR, one tunes the waveguide parameter a_{\perp} . In our model, one directly tunes the interaction parameters U/t , V_1/t and V_2/t , by manipulating intensity and frequency of the laser beams. In figure (6.3) the scattering length is plotted in the simpler case of a triplet state with $V_2 = 0$ (see equation (5.6)). In the range $V/t < 0$ a resonance occurs when the relative momentum q approaches the lower edge of the scattering band in the K first Brillouin zone, i.e. $q \rightarrow 0$; in the range $V/t > 0$ a resonance occurs when q approaches the upper edge of the band, i.e. $q \rightarrow \pm\pi$. Thus, a bound state doesn't exist for small $|V/t|$. When $|V/t| > 2 \cos(K/2)$, a bound state appears. If the potential is further enhanced, the bound state repels from the band and becomes stable since it lies in the energy gap between two bands and is prevented from dissociation.

But, how are these phenomena related to Feshbach resonance and CIR?

To answer this question, consider atoms with mass m in a cubic optical lattice potential

$$V(\mathbf{x}) = V_0^{\perp} E_R \left(\sin^2\left(\frac{\pi x}{a}\right) + \sin^2\left(\frac{\pi y}{a}\right) \right) + V_0^{\parallel} E_R \sin^2\left(\frac{\pi z}{a}\right) \quad (6.10)$$

created by off-resonant laser light. If we indicate with λ_L the laser wavelength, the lattice period is $a = \lambda_L/2$ and $E_R = \hbar^2/2m\lambda_L^2$. For cubic lattices the motion separates along the three spatial directions and the single-particle

Hamiltonian

$$h = -\frac{\hbar^2}{2m}\nabla^2 + V(\mathbf{x}) \quad (6.11)$$

can be identified with that of equation (1.8). It is diagonalized by products of three Bloch functions. The energy eigenstates form a band structure, with band gaps growing and band widths decreasing as the laser intensity is increased. If the Fermi surface lies within a single conduction band, we can ignore the coupling with the others. Moreover, if the lattice depth along the transverse directions, V_0^\perp , is much larger than the depth along the longitudinal direction, V_0^\parallel , we can assume that particles don't have enough energy to exceed the transverse level splitting and the motion is indeed one-dimensional. If we use a second-quantized representation, the lattice potential is included into the one-body operator. Hence the parameter of the laser enters the hopping parameter t . A two-body operator is needed to describe atom-atom interaction. Usually a contact interaction is chosen and the system is described by the Hubbard model. In our work we have taken into account also longer range interactions. Since we use a discrete lattice model, a bound state always exists and we don't need a CIR. However, since the one-dimensional system is obtained through a confinement, a CIR occurs if $a_\perp/a_s^{3D} = 1.4603\dots$, where a_\perp is related to transverse lattice depth through the following relation

$$a_\perp = \frac{\sqrt{2}a}{\pi(V_0^\perp)^{1/4}}. \quad (6.12)$$

Nevertheless this resonance may be avoided by not choosing the transverse confinement too tight.

In a Feshbach resonance scheme, our model can be considered as a one-channel model, in which only the entrance open channel is considered. But a two channel picture is also possible. In this case, the Feshbach resonance can be included by adding a coupling \tilde{V} between the open channel and an energetically closed channel. Thus we obtain two coupled equations for the relative motion of an atom pair

$$\begin{aligned} H^{op}|\Psi^{op}\rangle + \tilde{V}|\Psi^{cl}\rangle &= E|\Psi^{op}\rangle \\ H^{cl}|\Psi^{cl}\rangle + \tilde{V}|\Psi^{op}\rangle &= E|\Psi^{cl}\rangle \end{aligned} \quad (6.13)$$

where H^{op} is the Hamiltonian in the open channel, which coincides with the Hamiltonian of our model, and H^{cl} is the Hamiltonian in the closed channel [43].

Conclusions and outlooks

In this work, the one dimensional extended Hubbard model, with first- and second-neighbor interactions has been studied, concentrating on the two-particle problem, for which an exact analytical solution is possible. The analysis has been conducted through the Bethe ansatz, which allows to obtain all the eigenvalues and eigenfunctions of the Hamiltonian. This is of fundamental importance for the study of expansion dynamics of bound states, which is of great interest in current physics. In our model, much attention has been devoted to bound states and to resonances from which they arise. Indeed the existence of stable two-body bound states plays a key role in a many-body picture, such as in the BCS-BEC crossover. Since we have dealt with fermionic particles, the spin internal degrees of freedom must have been taken into account. Triplet state, with total spin $S = 1$, and singlet state, with $S = 0$, have been decoupled and the problem has been studied separately for the two cases. In the first case, two families of bound states have been observed, for both attractive and repulsive interaction. In the second case, also a third family of bound states appears. For some particular values of the interactions parameters, these bound states can merge into the scattering band. When this happens, a resonance occurs.

Our results could be experimentally verified in optical lattices, where the interaction parameters can be tuned.

Finally we would propose a further extent of this work. We observe that the exact solution of the Hubbard model shows that fermions can bind in pairs, but N -body bound state with $N > 2$ are generally forbidden [62]. However, it has recently been shown that, if the two species of fermions have unequal masses (and consequently unequal hopping parameters t_σ), three-body bound states exist and can have considerable effects on the many-body picture [48, Chap. 14], [63, 64]. Hence, an interesting extent of this work may be the introduction of a third particle in the extended Hubbard model to see under what conditions a three-body bound state appears.

Appendix A

Number of states

In each of the studied cases, the Bethe ansatz (or the modified Bethe ansatz) allows to find all the solutions of the problem. To calculate this number, we consider all possible configurations for two particles on L sites. Two particles can be sorted on L distinct sites in

$$\binom{L}{2} = \frac{L!}{(L-2)!2!} = \frac{L(L-1)}{2} \quad (\text{A.1})$$

different combinations. Each particle has two spin degrees of freedom. Hence each pair has four possible spin states, which are

$$(\uparrow, \uparrow) \quad (\uparrow, \downarrow) \quad (\downarrow, \uparrow) \quad (\downarrow, \downarrow) \quad (\text{A.2})$$

or, equivalently, in terms of (S, S^z)

$$(0, 0) \quad (1, -1) \quad (1, 0) \quad (1, 1). \quad (\text{A.3})$$

Consequently, the total number of states is

$$4 \binom{L}{2} + L = 2L^2 - L \quad (\text{A.4})$$

where the adding L states take into account for the possibility that particles lie on the same site with opposite spins. Among all states,

$$3 \binom{L}{2} = \frac{L(L-1)}{2} \quad (\text{A.5})$$

are triplet states ($S = 1$) and

$$\binom{L}{2} + L = \frac{L(L+1)}{2} \quad (\text{A.6})$$

are singlet states ($S = 0$).

Bibliography

- [1] S. Giorgini, L. P. Pitaevskii, and S. Stringari. Theory of ultracold atomic Fermi gases. *Review of Modern Physics*, 80, 2008.
- [2] I. Bloch, J. Dalibard, and W. Zwerger. Many-Body Physics with Ultracold Gases. *Rev. Mod. Phys.*, 80:885, 2008.
- [3] I. Bloch. Ultracold quantum gases in optical lattices. *Nature Physics*, 1, 2005.
- [4] M. Randeria and E. Taylor. BCS-BEC Crossover and the Unitary Fermi Gas. *arXiv*, (1306.5785v2 [cond-mat.quant-gas]), 2013.
- [5] F. H. L. Essler, H. Frahm, Göhmann, A. Klümper, and E. Korepin. *The One-Dimensional Hubbard Model*. Cambridge University Press, 2005.
- [6] A. Montorsi. *The Hubbard Model: A Reprint Volume*. World Scientific Pub. Co. Pte. Ltd, 1992.
- [7] B. Sutherland. *Beautiful Models: 70 Years of Exactly Solved Quantum Many-Body Problems*. World Scientific Pub. Co. Pte. Ltd., 2004.
- [8] C. Degli Esposti Boschi, E. Ercolessi, L. Ferrari, P. Naldesi, F. Ortolani, and L. Taddia. Bound states and expansion dynamics of bosons on a one-dimensional lattice. *arXiv*, (1407.2105v1 [cond-mat.quant-gas]), 2014.
- [9] A. Auerbach. *Interacting Electrons and Quantum Magnetism*. Springer-Verlag, 1994.
- [10] J. Hubbard. Electron Correlations in Narrow Energy Bands. *Proc. R. Soc. (London) A*, 276:238, 1963.
- [11] J. Hubbard. Electron Correlations in Narrow Energy Bands. II. The Degenerate Band Case. *Proc. R. Soc. (London) A*, 277:237, 1964.

-
- [12] J. Hubbard. Electron Correlations in Narrow Energy Bands. III. An Improved Solution. *Proc. R. Soc. (London) A*, 281:401, 1964.
- [13] J. Hubbard. Electron Correlations in Narrow Energy Bands. IV. The Atomic Representation. *Proc. R. Soc. (London) A*, 285:542, 1965.
- [14] J. Hubbard. Electron Correlations in Narrow Energy Bands. V. A Perturbation Expansion About the Atomic Limit. *Proc. R. Soc. (London) A*, 296:82, 1967.
- [15] J. Hubbard. Electron Correlations in Narrow Energy Bands. VI. The Connexion with Many-Body Perturbation Theory. *Proc. R. Soc. (London) A*, 296:100, 1967.
- [16] Neil W Ashcroft and N. David Mermin. *Solid State Physics*. Harcourt College Publisher, 1976.
- [17] O. J. Heilmann and E. H. Lieb. Violation of noncrossing - rule Hubbard Hamiltonian for benzene. *Ann. N.Y. Acad. Sci.*, 172:584, 1971.
- [18] M.C. Gutzwiller. Effect of correlation on the ferromagnetism of transition metals. *Physical Review Letters*, 10:159–162, 1963.
- [19] F. Gebhard. *The Mott Metal-Insulator transition*. Springer Verlag, 1997.
- [20] J. E. Hirsch. Two-dimensional Hubbard model: Numerical simulation study. *Physical Review B*, 31(7):4403, 1985.
- [21] M. Cyrot. Theory of Mott transition: application to transition metal oxides. *Le journal de physique*, 33:125, 1971.
- [22] M. Greiner, O. Mandel, T. Esslinger, T. W. Hänsch, and I. Bloch. Quantum phase transition from a superfluid to a Mott insulator in a gas of ultracold atoms. *Nature*, 415:39–44, 2002.
- [23] G. G. Batrouni, V. G. Rousseau, R. T. Scalettar, and B. Grémaud. Competing phases, phase separation and co-existence in the extended one-dimensional bosonic hubbard model. *arXiv*, (1405.5382v2 [cond-mat.quant-gas]), 2014.
- [24] L. De Leo, J. S. Bernier, C. Kollath, A. Georges, and V. W. Scarola. Thermodynamics of the three-dimensional Hubbard model: Implications for cooling cold atomic gases in optical lattices. *Physical Review A*, 83(023606), 2011.

-
- [25] S. Fuchs, E. Gull, L. Pollet, E. Burovski, E. Kozik, T. Pruschke, and M. Troyer. Thermodynamics of the 3D Hubbard Model on Approaching the Néel Transition. *Physical Review Letters*, 106(030401), 2011.
- [26] E. H. Lieb and W. Liniger. Exact analysis of an interacting Bose gas I. The general solution and the ground state. *Phys. Rep.*, 130:1605, 1963.
- [27] E. H. Lieb. Exact solution of the F model of an antiferroelectric. *Phys. Rev. Lett.*, 18:1046, 1967.
- [28] E. H. Lieb. Exact solution of the two-dimensional Slater KDP model of a ferroelectric. *Phys. Rev. Lett.*, 18:108, 1967.
- [29] E. H. Lieb. Residual entropy of square ice. *Phys. Rev.*, 162:162, 1967.
- [30] C. N. Yang. Some exact results for the many-body problem in one dimension with repulsive delta-function interaction. *Phys. Rev. Lett.*, 19(23):1312, 1967.
- [31] M. Gaudin. Un système à une dimension de fermions en interaction. *Phys. Lett.*, 24A:55, 1967.
- [32] Michael Karbach and Gerhard Müller. Introduction to the Bethe Ansatz I. *Computers in Physics*, 11:36–43, 1997.
- [33] Michael Karbach, Kun Hu, and Gerhard Müller. Introduction to the Bethe Ansatz II. *Computers in Physics*, 12:565–573, 1998.
- [34] Michael Karbach, Kun Hu, and Gerhard Müller. Introduction to the Bethe Ansatz III. *cond-mat/0008018*, 2000.
- [35] E. H. Lieb and F. H. Wu. Absence of Mott transition in an exact solution of the short-range, one-band model in one dimension. *Phys. Rev. Lett.*, 20:1445–1448, 1968. Erratum: *Phys. Rev. Lett.* 21 (1968) 192.
- [36] M. Takahashi. *Thermodynamics of One-Dimensional Solvable Models*. Cambridge University Press, 1999.
- [37] M. Valiente and D. Petrosyan. Two-particle states in the Hubbard model. *J. Phys. B: At. Mol. Opt. Phys.*, 41:161002, 2008.
- [38] M. Valiente and D. Petrosyan. Scattering resonances and two-particle bound states of the extended hubbard model. *J. Phys. B: At. Mol. Opt. Phys.*, 42:121001, 2009.

-
- [39] M. Girardeau. Relationship between Systems of Impenetrable Bosons and Fermions in One Dimension. *Journal of Mathematical Physics*, 1(6):516, 1960.
- [40] L. D. Landau and E. M. Lifshitz. *Quantum Mechanics*. Pergamon Press, 2 edition, 1965.
- [41] C. J. Pethick and H. Smith. *Bose-Einstein Condensation in Dilute Gases*. Cambridge University Press, 2 edition, 2008.
- [42] K. Winkler, G. Thalhammer, F. Lang, R. Grimm, J. Hecker Denschlag, A. J. Daley, A. Kantian, H. P. Büchler, and P. Zoller. Repulsively bound atom pairs in an optical lattice. *Nature*, 441(04918):853, 2006.
- [43] N. Nygaard, R. Piil, and K. Mølmer. Two-channel Feshbach physics in a structured continuum. *Physical Review A*, 78(023617), 2008.
- [44] P. Naidon, E. Tiesinga, F. Mitchell, and P. S. Julienne. Effective-range description of a Bose gas under strong one- or two-dimensional confinement. *New journal of Physics*, 9(19), 2007.
- [45] R. Piil and K. Mølmer. Tunneling couplings in discrete, single-particle band structure, and eigenstates of interacting atom pairs. *Physical Review A*, 76(023607), 2007.
- [46] J. Javanainen, O. Odong, and J. C. Sanders. Dimer of two bosons in a one-dimensional optical lattice. *Physical Review A*, 81(043609), 2010.
- [47] H. Moritz, T. Stöferle, K. Günter, M. Köhl, and T. Esslinger. Confinement Induced Molecules in a 1d Fermi Gas. *Physical Review Letters*, 94, 2005.
- [48] W. Zwerger. *The BCS-BEC Crossover and the Unitary Fermi Gas*. Springer, 2012.
- [49] M. Randeria, J.-M. Duan, and L. Y. Shieh. Bound States, Cooper Pairing, and Bose Condensation in Two Dimensions. *Physical Review Letters*, 62(9), 1989.
- [50] W. C. Stwalley. Stability of Spin-Aligned Hydrogen at Low Temperatures and High Magnetic Fields: New Field-Dependent Scattering Resonances and Predissociations. *Physical Review Letters*, 37(24), 1976.

- [51] M. Olshanii. Atomic Scattering in the Presence of an External Confinement and a Gas of Impenetrable Bosons. *Phys. Rev. Lett.*, 81(5), 1998.
- [52] T. Bergeman, M. G. Moore, and M. Olshanii. Atom-Atom Scattering Under Cylindrical Harmonic Confinement: Numerical and Analytic Studies of the Confinement Induced Resonance. *Phys. Rev. Lett.*, 91(16), 2003.
- [53] S. Saeidian, V. S. Melezhik, and P. Schmelcher. Multichannel atomic scattering and confinement-induced resonances in waveguides. *Phys. Rev. A*, 77(042721), 2008.
- [54] G. E. Astrakharchik, D. Blume, S. Giorgini, and L. P. Pitaevskii. Interacting Fermions in Highly Elongated Harmonic Traps. *Phys. Rev. Lett.*, 93(5), 2004.
- [55] V. Peano, M. Thorwart, C. Mora, and R. Egger. Confinement-induced resonances for a two-component ultracold atom gas in arbitrary quasi-one-dimensional traps. *New Journal of Physics*, 7(192), 2005.
- [56] S. G. Peng, S. S. Bohloul, X. J. Liu, H. Hu, and P. D. Drummond. Confinement-induced resonance in quasi-one-dimensional systems under transversely anisotropic confinement. *Phys. Rev. A*, 82(063633), 2010.
- [57] E. Haller, M. J. Mark, R. Hart, I. Danzl, J. G. aand Reichsöllner, V. Melezhik, P. Schmelcher, and H.-C. Nägerl. Confinement-Induced Resonances in Low-Dimensional Quantum Systems. *Phys. Rev. Lett.*, 104(153203), 2010.
- [58] J. N. Fuchs, A. Recati, and W. Zwerger. Exactly Solvable Model of the BCS-BEC Crossover. *Phys. Rev. A*, 77(042721), 2008.
- [59] E. Zhao and V. Liu. Theory of quasi-one-dimensional imbalanced Fermi gas. *Phys. Rev. A*, 78(063605), 2008.
- [60] Z. Yan and A. Zong. Optical lattice and its application in strongly correlated condensed matter system. <http://web.stanford.edu/~alfredz/cgi-bin/doc/opticallattice.pdf>, 2014.
- [61] P. B. Blakie and C. W. Clark. Wannier states and Bose-Hubbard parameters for 2d optical lattices. *Journal of Physics B: Atomic, Molecular and Optical Physics*, 37(7), 2004.

-
- [62] D. C. Mattis. The few-body problem on a lattice. *Reviews of Modern Physics*, 58(2), 1986.
- [63] E. Burovski, G. Orso, and T. Jolicoeur. Multiparticle Composites in Density-Imbalanced Quantum Fluids. *Phys. Rev. Lett.*, 103(215301), 2009.
- [64] E. Burovski, G. Orso, and T. Jolicoeur. Luttinger Liquid of Trimers in Fermi Gases with Unequal Masses. *Phys. Rev. Lett.*, 104(065301), 2010.